Characterization of cortico-subthalamic networks during deep brain stimulation surgery in Parkinson's disease

Dissertation

zur Erlangung des Grades eines
Doktors der Naturwissenschaften

der Mathematisch-Naturwissenschaftlichen Fakultät
und
der Medizinischen Fakultät
der Eberhard-Karls-Universität Tübingen

vorgelegt
von

Ramin Azodi Avval
aus Mashhad, Iran

September - 2016

Tag der mündlichen Prüfung: Dezember 20, 2016.

Dekan der Math.-Nat. Fakultät: Prof. Dr. W. Rosenstiel

Dekan der Medizinischen Fakultät: Prof. Dr. I. B. Autenrieth

1. Berichterstatter: Prof. Dr. Alireza Gharabaghi

2. Berichterstatter: Prof. Dr. Christoph Braun

1. Prüfungskommission: Prof. Dr. Ulf Ziemann

2. Prüfungskommission: Prof. Dr. Ingo Hertrich

Declaration:

*I hereby declare that I have produced the work entitled "*Characterization of cortico-subthalamic networks during deep brain stimulation surgery in Parkinson's disease*", submitted for the award of a doctorate, on my own (without external help), have used only the sources and aids indicated and have marked passages included from other works, whether verbatim or in content, as such. I swear upon oath that these statements are true and that I have not concealed anything. I am aware that making a false declaration under oath is punishable by a term of imprisonment of up to three years or by a fine.*

Tübingen, den 01.09.2016
Date Signature

Contents

List of Abbreviations

BO	Beta Oscillations
DBS	Deep Brain Stimulation
DTI	Diffusion Tensor Imaging
dWPLI	debiased Weighted Phase Lag Index
EEG	Electroencephalogram
fMRI	Functional Magnetic Resonance Imaging
GPi	Globus Pallidus internus
GPe	Globus Pallidus externus
HFO	High Frequency Oscillations
LFP	Local field potential
MEG	Magnetoencephalography
MER	Microelectrode Recording
PD	Parkinson's disease
PRC	Phase Response Curve
sEPs	Subcortical Evoked Potentials
SNc	Substantia Nigra pars compacta
STN	Subthalamic Nucleus

Abstract

Deep brain stimulation (DBS) of the subthalamic nucleus (STN) is a well-established symptomatic treatment for Parkinson's diseases (PD). However, knowledge on local electrophysiological biomarkers within the STN and their cortical connectivity profile is still scarce. Such information would be necessary for optimal positioning of the DBS leads based on PD network pathophysiology.

This thesis describes the introduction and exploration of a novel technique for electrophysiological measurements during DBS surgery. Combined electroencephalography (EEG) with stepwise local field potentials recordings during insertion of the DBS lead was performed intraoperatively, thereby, allowing to capture local STN and cortico-subthalamic physiology with high speactral and spatial specificity. Our results revealed that strong beta oscillatory activity in the STN was located more dorsally than the STN-ipsilateral motor network phase coupling; the respective frequency bands were in the low and high beta-band, respectively. Moreover, the spot within the STN, where this STN-cortical phase coupling occurred, correlated highly with the STN spot where the phase of beta oscillations modulated the amplitude of high-frequency oscillations. This STN location was furthermore, characterized by information flowed from the ipsilateral motor cortex to the STN in the high beta-band suggesting a pathologically synchronized network with a direct STN-motor cortex connection via the hyperdirect pathway. Interestingly, the very same STN spot showed a resonance like responses to electrical stimulation suggesting a decoupling of pathologically synchronized STN-motor cortex connectivity during therapeutic DBS.

In conclusion, this PhD thesis provides first evidence that macroelectrode recordings with the chronic electrode concurrent with EEG recordings are a reliable method for STN localization during DBS surgery. Additionally, combining LFP and EEG recordings during mapping of STN offered a new way of DBS targeting on the basis of pathological local biomarkers and network activity.

1. Introduction

Any morphological and/or neurochemical disturbance in the brain might lead to dysfunctions in cognitive and/or motor performance. Parkinson's disease (Jankovic, 2008; Lang and Lozano 1998), dystonia (Breakefield et al., 2008; Tarsy and Simon 2006), major depression (Brunoni et al., 2008; Gold et al., 1988), and obsessive-compulsive disorder (Abramowitz et al.; Kuelz et al., 2004) are examples of such disorders. There is a considerable amount of research reporting the changes in functional and effective connectivity in various cortical and subcortical areas that are responsible for clinical symptoms and functional abnormalities in these diseases (Anand et al., 2005; Colosimo et al., 2005; Fernández-Seara et al., 2015; Menzies et al., 2008; Nicoletti et al., 2010; Szeszko et al., 2005; Whitwell et al., 2011); however, specific electrophysiological changes or signatures of local (e.g., subcortical or cortical site) and long-range cortico-subcortical communication have received little attention.

For instance, the dopamine depletion in Parkinson's disease (PD) patients is believed to directly modulate the normal state of the cortico-basal ganglia loop (Fig. 1), which could cause functional changes in various brain regions (Bergman et al., 1998; Bernheimer et al., 1973; Levy et al., 2002; Obeso et al., 2004; Obeso et al., 2000). Indeed, the loss of dopaminergic neurons, which project from substantia nigra pars compacta (SNc) to the dorsal striatum, not only disturbs the local balance but also affects ongoing brain rhythms in large-scale areas of the brain (Bergman et al., 1998; Brown, 2003; Obeso et al., 2008; Terman et al., 2002; Utter and Basso, 2008). Electrophysiological data has suggested that enhanced beta oscillations (BO) at the level of the subthalamic nucleus (STN), globus pallidus pars interna (GPi), and motor cortical area are responsible for motor impairment in PD, typically inducing resting tremor and rigidity in humans (Brittain and Brown, 2014; Deffains et al., 2014; Hammond et al., 2007; Little and Brown, 2014; Novak et al., 2011; Ray et al., 2008; Silberstein et al., 2003; Steigerwald et al., 2008; Weinberger et al., 2012; Zaidel et al., 2010). The origins of these pathological BO remain controversial. One theory argues that abnormal BO could be generated in the STN-GPe (globus pallidus externus) network. It suggests that the reduction in dopamine results in a stronger coupling strength in the STN-GPe loop (Plenz and Kital, 1999). As a

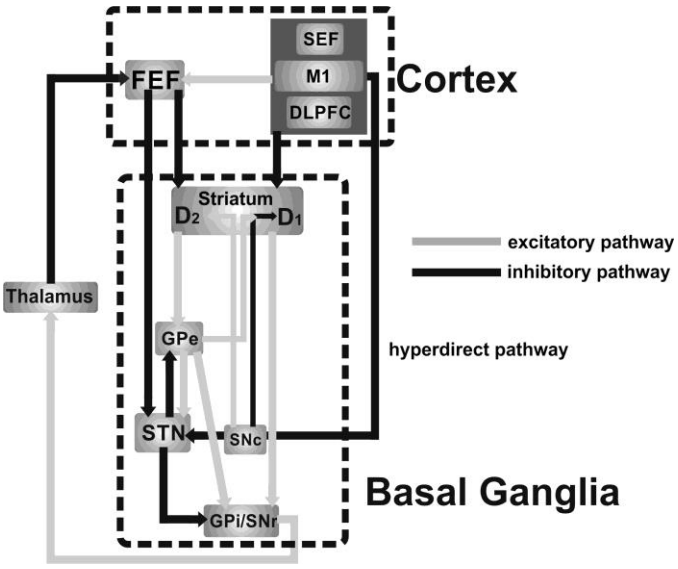

Figure 1: Basal ganglia loop. The basal ganglia are a group of heavily coupled subcortical nuclei. The striatum is the primary receptive nucleus of the basal ganglia receiving afferent projections from cortical areas including: the dorsolateral prefrontal cortex (DLPFC), the supplementary eye field (SEF), the frontal eye fields (FEF), primary motor cortex (M1) and also from dopaminergic neurons of the substantia nigra pars compacta (SNc). Medium spiny neurons (MSNs) in striatum are connected to the basal ganlia output structures through D1-receptors (direct pathway) and D2-receptors (indirect pathway). D1-type MSNs project to the Globus pallidus internus (Gpi) and the substantia nigra pars reticulata (SNr) facilitating movement, whereas the D2-type MSNs, decrease movement, projects to the Globus pallidus externus (GPe) and the subthalamic nucleus (STN) (Belujon and Grace, 2011; Hikosaka et al., 2000; Little and Brown, 2014). The direct connection from the motor area to STN, the so-called hyperdirect pathway, plays an important role in PD and therapeutic interventions.

consequence, intermittent synchronized oscillations are produced in the beta oscillatory band; a state different from complete synchronization (Park et al., 2010). Moreover, a recent study suggested that changes in the striatum network dynamics are able to generate beta synchronization as well (McCarthy et al., 2011).

Apparently, compensation for the loss of dopamine, for example, by levodopa medication, might be a possible treatment approach to reduce symptoms in PD (Lloyd et al., 1975); however, resistance to medication and side effects in the long run are serious limitations of this intervention (Rascol et al., 2003). Neuromodulation by deep brain stimulation (DBS) is a possible alternative which has shown promising results in alleviating PD symptoms (Deuschl et al., 2013; Okun, 2012; Schuepbach et al., 2013).

1.1 Subcortical localization during surgery

STN DBS is the most typical surgical procedure to treat Parkinson's disease (Krack and Hariz, 2013; Lozano and Lipsman, 2013; Odekerken et al., 2013; Schuepbach et al., 2013). Optimal positioning of the implanted DBS lead plays a critical role in the effectiveness of this PD treatment modality and long-term quality of patients (Deuschl et al., 2006; Guo et al., 2013; Maks et al., 2009; Voges et al., 2002; Witt et al., 2013)**.** In clinical practice, microelectrode recording (MER) of single cell activity is a well-established technique for delineating STN boundaries in PD (Hutchison et al., 1998; Seifried et al., 2012); it is commonly used to target

other subcortical structures as well (Gaze et al., 1964; Hutchison et al., 1994; Starr et al., 2000). Although such spike activity recording is a reliable and robust method, it suffers from a number of drawbacks related to DBS implantation during surgery and inherent electrophysiological problems. One of the major issues with MER through microrecording electrodes with multiple trajectories is the increased risk of surgical complications related to injured blood vessels (i.e., hemorrhages) (Park et al., 2011; Zrinzo et al., 2012). One large study (Ludvic Zrinzo et al., 2012) compared two groups of patients, one undergoing pure image-guided DBS lead placement without MER and another one on the basis of MER recordings. The researchers concluded that the approach without MER had a significantly lower risk of hemorrhage than the other approach. However, macroelectrode LFP recordings might provide additional advantages in comparison to pure image-guided approaches without the risks related to MER; this might be particularly important for novel therapeutic approaches and for increasing targeting specificity while decreasing surgery-related risks (Chen et al., 2006; Telkes et al., 2016). Furthermore, very recent findings indicate that LFP could be employed as a biomarker for more efficient and effective closed-loop DBS application (Arlotti et al., 2016; Little and Brown, 2012; Little et al., 2013; Rosin et al.; Rossi et al., 2007; Tass et al., 2012). Moreover, from a signal processing and engineering perspective, LFP recordings could offer greater longevity, that is, they may be more robust over time compared to spike recordings where amplitudes change significantly from day to day (Cynthia et al., 2011; Nurmikko et al., 2010). Additionally, macroelectrode recordings can be performed with much lower bandwidth compared to single cell recordings, which in turn require much higher sampling rates. For chronic closed-loop DBS applications, higher bandwidth necessitates higher power requirements and thus leads to an increase in the heat and size of chronically implanted devices (Polikov et al., 2005). Recording LFPs instead offers the capability of acquiring physiological information for targeting while using the standard DBS electrodes, which are used for chronic implantation anyway and which pose a smaller complication risk by design. Given network neuromodulation of DBS (Alhourani et al., 2015), advanced physiological biomarkers based on connectivity measures between distal brain regions can only be determined with LFP (Litvak et al., 2011; Oswal et al., 2016) but not with spike activity.

1.2 Network and local biomarkers in Parkinson patients

PD is a neurodegenerative disease characterized by resting tremor, bradykinesia, rigidity, posture instability, speech problems, and, in the progressive state, cognitive impairment as well (Hughes et al., 1992; Jankovic, 2008). Neuroimaging techniques such as functional magnetic resonance imaging (fMRI), diffusion tensor imaging (DTI), and positron emission tomography provide valuable insights into various functional, structural, and morphological changes of PD (Lenka et al., 2015; Politis, 2014). fMRI studies in PD suggest that during medication OFF state, increased cortico-subcortical functional connectivity takes place between the cortical areas involved in motor processes and the STN compared to healthy control subjects (Fernández-Seara et al., 2015). Increased connectivity between the motor area and cerebellum occurs as well (Wu and Hallett, 2013). On the other hand, during dopamine administration (medication ON), functional connectivity was enhanced between the mesial premotor loop and cortico-striatal interactions with amelioration of bradykinesia (Michely et al., 2015). In this line of research, using probabilistic tractography with DTI, clinical effectiveness of activated DBS contacts was shown to positively correlate with as cortical network connectivity to the STN (Accolla et al., 2016) involving the superior frontal gyrus and the thalamus (Vanegas-Arroyave et al., 2016). These advanced imaging methods provide considerable spatial resolution, but miss a fine temporal resolution of spontaneous brain activity. Electrophysiological signals enable researchers to investigate functional and/or causal interactions between different brain regions and brain network dynamics with high temporal resolutions (Buzsáki et al., 2012; Marcel van et al., 2009). Moreover, in recent years, closed-loop DBS by real-time modulation of pathological oscillations has shown promising results in pilot trials when compared to conventional open-loop DBS (Arlotti et al., 2016; Little et al., 2013; Rossi et al., 2007). Therefore, neurophysiological recordings have received greater attention in recent years as a valuable measure to monitor disease state and understand PD pathophysiology (Little and Brown, 2012).

There is increasing evidence that enhanced BO in both the cortical and subcortical regions correlate with the clinical features and pathophysiology of PD (Brittain and Brown, 2014; Brown, 2003; Brown, 2007; Little and Brown, 2014; Marreiros et al., 2013; Stein and Bar-Gad, 2013). Enhanced BO (14-35 Hz) have been detected in the dorso-lateral part of the STN

(Deffains et al., 2014; Kühn et al., 2009; Novak et al., 2011; Ray et al., 2008; Steigerwald et al., 2008); moreover, the normalized power in the beta range is shown to correlate with postoperative improvement (Zaidel et al., 2010). At the cortical level, the rigidity of patients with PD can be predicted by the relative spectral power of beta and gamma oscillations in bilateral frontal areas (Cao et al., 2015). Nonlinear complex interactions of different frequency bands, referred to as cross-frequency coupling, have been observed in the primary motor cortex and also in the dorso-lateral part of the STN in PD. More specifically, the phase of subthalamic BO modulates the amplitude of HFO (B-HFO) in the STN (López-Azcárate et al., 2010; Özkurt et al., 2011; Yang et al., 2014), while the phase of cortical BO modulates broadband gamma oscillations in the cortex (de Hemptinne et al., 2013a; Qasim et al., 2016). Furthermore, high-frequency oscillations (HFO, >150 Hz) have been shown to be associated with PD symptoms via an inverse correlation with akinesia (Wang et al., 2014). Both pharmacological treatment with L-dopa (Barbeau, 1969) and neurostimulation by DBS (Schuepbach et al., 2013) have shown changes in functional connectivity of the cortico-STN area in comparison to pathological states, i.e. when no medication or neurostimulation was applied. A magnetoencephalography (MEG) study (Litvak et al., 2011; van Wijk et al.) in which simultaneous resting state recordings of subcortical-LFP and cortical-MEG were performed in the OFF medication state showed that STN-motor cortex coherence in the high beta band changed due to L-dopa medication. In a recent MEG study (Oswal et al., 2016), cortical-STN connectivity was investigated during therapeutic DBS. This study provided evidence for reduced functional connectivity in high beta band, specifically between the STN and the ipsilateral motor area. It is not clear, however, how the electrophysiological signatures within the STN are related to the pathological network activity, and how this interaction is modulated by therapeutic interventions.

1.3 Hypotheses and aims

(i) Simultaneous EEG and LFP recordings across the STN during DBS surgery allow detecting subthalamic biomarkers for direct cortico-subcortical connectivity in PD patients (Study 1).

(ii) Beta oscillations in the STN and cortico-subthalamic connectivity can be disentangled during DBS surgery in PD (Study 2).

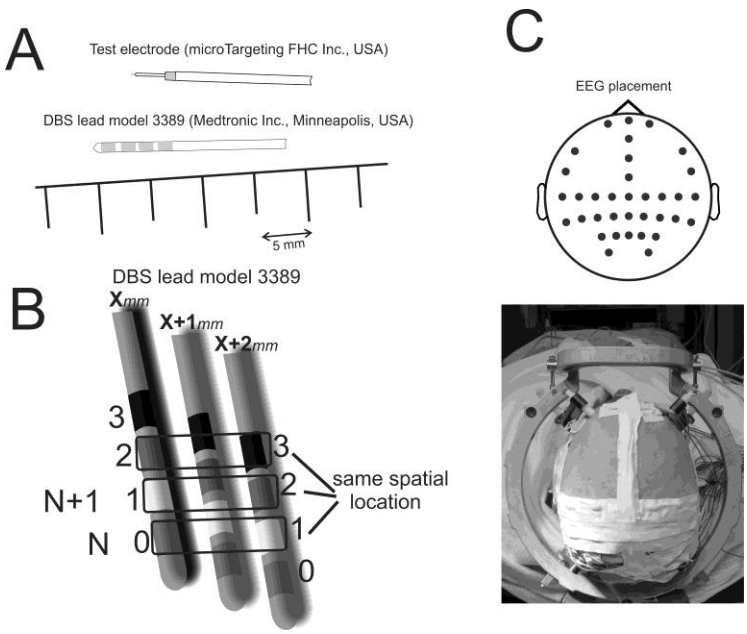

Figure 2, Electrophysiology during the DBS surgery. (A) Chronic DBS electrode (here: Medtronic Inc) for therapeutic stimulation and capable of LFP recordings and test electrode capable of MER and LFP recordings (here: microtargeting FHC Inc) (B) Pictogram shows the subcortical mapping procedure while inserting the chronic DBS lead millimeter by millimeter. Due to the physical characteristics of the electrode (four 1.5 mm macroelectrode contacts, separated by 0.5 mm; contact 0 and 3 are the lowest and highest contacts), every 2 mm the contact N+1 will be located in the same spatial position that was previously occupied by N. (C) Topography and experimental set-up of EEG electrode placement during DBS surgery.

(iii) Resonance characteristics in the STN area are related to STN-motor network connectivity and predict clinical effects of DBS in PD (Study 3).

(iv) Delivering stimulation on specific phases of the detected oscillations maximizes the disruption of the pathological activity (Study 4).

These hypotheses necessitate methodological innovations, which are specified in the following paragraphs: while image-based localization combined with MER (tip of the test electrode Fig. 2A, upper figure) is the gold standard method for optimally targeting the STN (Hutchison et al., 1998; Seifried et al., 2012), there are some concerns with employing MER recordings with test electrodes during DBS surgery:

(a) increased surgery-related risk factors, (b) misplacement of the chronic DBS electrode when replacing the MER test electrodes, and (c) different DBS effects induces by the test electrodes used for MER and the chronic electrodes due to distinct physical characteristics (Fig. 2A), (d) implications of novel neuromodulation interventions, such as closed-loop DBS or connectivity based localization (Little and Brown, 2012; McClelland, 2011; Paffi et al., 2015; Park et al., 2011; Telkes et al., 2016; Zrinzo et al., 2012). Implementing macroelectrode recordings with the chronic electrode would address these issues. The lack of such an approach in the past might be related to the limited capabilities of real-time recording hardware and software for analysis of multidimensional neural activity at the time when neurophysiological monitoring

was introduced to DBS surgery. Thanks to advanced data acquisition systems, high-level computer language, and high-speed data processing tools capable of on-line monitoring of brain oscillations, researchers are now able to search for various electrophysiological biomarkers during DBS surgery for refining the targeting. One of the aims of this PhD thesis was therefore to implement and explore the chronic DBS electrodes for identifying the STN boundaries by applying macroelectrode LFP recordings simultaneous to EEG recordings. Since MER spike activity in the dorsal part of STN has been shown to be highly correlated with LFP beta oscillation, previous studies have already attempted to delineate the STN entry based on electrophysiological features captured with macroelectrode recordings (Chen et al., 2006; Telkes et al., 2016; Winestone et al., 2012). However, it remains unknown how robust and reliable these LFP features are during STN mapping. This thesis proposes a novel technique to address this issue.

Higher neuronal discharge rates (Deffains et al., 2014), synchronization in the beta frequency range (Priori et al., 2004; Weinberger et al., 2013; Ray et al., 2004), HFO (Hirschmann et al., 2016; Wang et al., 2014), and beta-coupled HFO have been detected in the dorsolateral motor part of STN (Yang et al., 2014) and have been shown to correlate with the severity of the disease (Neumann et al., 2016; Özkurt et al., 2011; Sharott et al., 2014). Recent evidence suggests that DBS of the STN mediates the effects on PD symptoms by modulating cortical motor activity, presumably via a direct cortico-subthalamic connection (de Hemptinne et al., 2013b; Kuriakose et al., 2010; Li et al., 2012; Walker et al., 2012; Weiss et al., 2015). However, little is known about the spatio-temporal interaction between the cortico-subcortical interaction and local STN markers in the basal ganglia loop. BO, HFO, beta-coupled HFO and STN-cortical motor coupling which lie in close proximity to each other in the dorsal STN, cannot be disentangled using standard postoperative measurements with DBS electrodes, since their positions are fixed (Fogelson et al., 2006; Gilbertson et al., 2005; Kato et al., 2015; Lalo et al., 2008; Litvak et al., 2010; Oswal et al., 2016; Whitmer et al., 2012; Williams et al., 2002). By contrast, intraoperative electrophysiological recordings during DBS surgery could help to compile a highly precise mapping of the STN region in a stepwise manner on a millimeter scale, but they are limited with regard to simultaneous cortical recordings. In the few studies in which cortical activity was recorded during DBS implantation in the STN to unravel cortico-subcortical connectivity (de Hemptinne et al., 2013a; Shimamoto et al., 2013; Whitmer et al.,

2012) it was performed with implanted electrode grids which covered the inspilateral sensorimotor cortex and not with the spatially more extended bilateral EEG recordings applied in our approach.

We hypothesized that the ongoing oscillations recorded by EEG (Fig. 2B) simultaneous to macroelectode recordings in the STN during implantation of DBS electrodes would unravel different oscillatory regions and connectivity profiles of the STN to the cortex. Moreover, we expected electrical stimulation in different subcortical depths across the STN to provide a complementary measure of connectivity to verify the functional relevance of the detected subthalamic biomarkers. Furthermore, delivering electrical stimulation at various subcortical depths in the STN might reveal different evoked response components reflecting particular pathological sub-regions and cortico-subcortical hubs. Finally, the thesis explored on the basis of the spatial specificity achieved by the previous studies, whether improving the temporal specificity of stimulation, i.e. delivering stimulation on specific phases of the previously detected oscillations, would maximize the disruption of the pathological activity; for this purpose, a simulation study on the basis of intraoperative physiological data was conducted.

2. Included studies

2.1 Subthalamic cross-frequency coupling mediates direct cortico-subcortical connectivity in Parkinson's disease

In the first study, combined EEG and stepwise LFP recordings in the STN of 12 PD patients during implantation of DBS electrodes was introduced as a novel approach to investigating cortio-subthalamic connectivity and relevant bio-markers within the STN. For subcortical invasive recordings, we did not perform the analysis based on the micro tip of the test electrode (Fig. 2A, upper figure) for our intraoperative measurements, which is common for most MER studies. Instead, the non-insulated macro tip of the cannula, which is also known as the mactroelectrode (and which has physical characteristics similar to the chronic DBS electrode), was applied. This technique was combined with simultaneous scalp EEG (non-sterile EEG electrodes were placed before surgery) with surface electrodes (Ag/AgCl electrodes, MedCaT GmbH, Netherlands) covering the head around the burr holes (Fig. 2C) in accordance with the international 10–20 EEG system (Alpha-Omega, Nazareth, Israel). These simultaneous

recordings enabled us to unravel local electrophysiology in the STN and to probe simultaneously the respective connectivity to the cortical area.

In the same vein, recent research indicates that DBS of the STN in PD mediates its clinical effects by modulating cortical oscillations, presumably via a direct STN-motor cortex connection (hyperdirect pathway) (Brittain and Brown, 2014; Chiken and Nambu, 2015; Little and Brown, 2014). However, a subthalamic electrophysiological marker for this cortico-subcortical pathway has not yet been found. Enhanced BO and, more recently, beta-coupled HFO have both been linked to the pathophysiology of Parkinson's disease and, as such, may serve as candidate markers (de Hemptinne et al., 2015; Hirschmann et al., 2016; Özkurt et al., 2011; Wang et al., 2014). In this study, maximum BO and beta-coupled high-frequency oscillations were separated in the dorsal subthalamic nucleus both spatially and spectrally, with peaks in the lower (13-20 Hz) and upper (21-35 Hz) beta-frequency range, respectively. The spot of maximum beta-coupled HFO, but not the more dorsally located spot of peak BO, correlated highly with cortico-subthalamic phase coupling calculated by the debised Weighted Phase Lag Index (dWPLI), which was most pronounced in the ispilateral medial motor cortex. This cortical area also displayed the highest long-range beta-coupled high-frequency oscillations between cortical BO in the ipsilateral motor cortex and HFO in the STN, which matched the spot of maximum local beta-coupled HFO. In this coherent loop, the STN activity was led by activity in the motor area. In the same line of evidence, low frequency electrical stimulation - when applied at the different sites of the dorsal STN - revealed the highest short-latency cortical-evoked potentials projecting to the ipsilateral motor area at the spot of highest beta-coupled HFO in the STN as well. Furthermore, the subthalamic-motor area phase coupling correlated significantly with the severity of motor symptoms in the medication OFF state. These converging evidences suggest that subthalamic beta-coupled HFO represent a node in segregated functional loops and may serve as local markers of the hyperdirect pathway between the motor area and STN for refined targeting of deep brain stimulation in Parkinson's disease.

2.2 Spatial specificity of beta oscillation and cortico-subthalamic connectivity in Parkinson's disease

In the second study, simultaneous cortical-EEG and subcortical-LFP was acquired during the DBS surgery with the same approach as applied in the first study. However, the quadripolar final DBS electrode (model 3389: four 1.5 mm macroelectrode contacts, separated by 0.5 mm, Medtronic Inc., Minneapolis, USA) was used during STN localization, instead of the test electrode. We recorded 32 to 38 cortical EEG sensors covering the frontal, central, temporal, parietal, and midline regions, which was a larger cortical region than recorded in the first study. For the subcortical-LFP mapping the quadripolar DBS electrode was passing through the STN region in steps of 1 mm. Due to the physical characteristics of the chronic DBS electrodes, each area in the STN is recorded several times; i.e. first by the lowest electrode contact, then (after inserting the electrode lead 2 mm) by the next contact etc (Fig. 2B). This technique allows us to check the reliability of the recording and determine the oscillatory region with high accuracy during DBS implantation. In comparison with the first study, the coverage of the cortical area with EEG electrodes that could uncover different STN-cortical connections was considerably higher. This study included recordings in 21 PD patients during DBS surgery. We could identify spatially and spectrally distinct beta oscillatory regions in the STN, which were robustly detectable at different time points by several DBS electrode contacts during STN mapping. At the same time, cortico-subthalamic phase coupling was calculated with dWPLI at each depth. This measurement is more robust and efficient in detecting true phase interaction between the cortex and subcortical area than common phase measurements such as the imaginary part of coherence (Nolte et al., 2004). We found the site in the STN that had the most significant phase coherence to the ispilateral medial motor cortex, a finding which was also reproducible across different DBS electrode contacts during STN mapping. Thereby, cortico-subthalamic coupling could be separated in the dorsal STN both spatially and spectrally. The site of cortico-subthalamic coupling which projected to the ispilateral medial motor cortex but not the beta oscillatory region was highly correlated with the clinical severity of PD (motor score assessed by UPDRS III). These findings suggest that STN-motor cortex coupling and the beta oscillatory region might be detected and disentangled in a reliable manner intraoperatively and may serve as markers during DBS surgery.

2.3 Resonance characteristics in the subcortical area predict clinical effects of deep brain stimulation and subthalamic-motor network connectivity in Parkinson's disease

In the first two studies, we proposed and tested a novel technique to target the STN with macroelectrode LFP measurements instead of performing single-cell recording with a microelectrode. The findings differentiated two oscillatory regions in the dorso-lateral motor STN: the first one, which was located more dorsally, exhibited pronounced beta activity, whereas the second more ventral site had the highest phase-coupling to an ipsilateral cortico-subcortical motor network. This leads to the question how these oscillatory regions respond to DBS and which relevance they have for the therapeutic intervention.

In order to address how oscillatory regions change in response to external perturbation, low frequency electrical stimulation (1 Hz and 5 Hz electrical stimulation), delivered at various depths, was applied during simultaneous LFP recordings at adjacent contacts in 13 PD patients. Before DBS was applied, the resting state STN spectral characteristics and the functional phase-coupling between STN and cortical areas were captured as well. The subcortical evoked potentials (sEPs) after DBS showed a distinct spatial and temporal pattern in the STN. This stimulation response was prominent in the dorsal part of the STN and was highly correlated with the region in the STN where resting motor-subthalamic coherence and HFO reached their highest values; there was no correlation found between the spatial location of the highest STN-motor coupling and the beta oscillatory region. During low frequency DBS, the amplitude of the recorded sEPs underwent several oscillations before neutralized by the inherent subcortical resistance. Here, this energy dissipation property of the brain region under electrical stimulation is referred to as damping. An oscillation model was used to establish the damping characteristics of different subcortical sites in response to electrical stimulation. The results demonstrated that the most prominent sEPs site in the dorsal STN was also less resistant (i.e. low damping) to DBS and that maximum energy absorption occurred in this area. This novel approach might bring new insights about the way DBS affects oscillatory brain regions. Interestingly, the damping of the system increased (decrease in sEP amplitude) during therapeutic high-frequency stimulation, thus, reflecting a resonance inhibiting effect on the system; notably, the clinicaly effective electrode contact matched with the electrode contact position with the most prominent sEPs response. These findings suggest that this node in the

STN might facilitate the electrical responses to decouple pathological cortico-subcortical connectivity during high-frequency DBS.

2.4 Phase-dependent modulation as a novel approach to therapeutic brain stimulation

In the last study, we were interested in triggering DBS pulses on the basis of the pathological oscillatory activity rather than applying traditional open-loop DBS. Closed-loop DBS interventions could provide us with the opportunity to optimize stimulation protocols for perturbation of pathological oscillatory activity in PD patients.

Here, a data-driven model was explored in two PD patients to reveal phase specificity of pathalogical oscillations to external stimulation. By delivering stimulation pulses relative to the ongoing oscillation phase, an alternative approach, namely, the targeted perturbation of pathological rhythms might be obtained. In this study, the phase sensitivity of a pathological oscillation was investigated using the phase model approach (Pikovsky et al., 2002) to reconstruct the phase response curve (PRC) of the LFP signals recorded in the STN. However, due to hardware limitations (e.g., latency), the optimal and precise DBS timing was not applied in real-time; instead the PRC was derived off-line on the basis of LFP recorded from the motor part of the STN. In order to measure PRC empirically, we determined specific electrode contact that displayed pronounced oscillatory activity in the beta-band, which is a known pathophysiological marker of motor area in the STN (Priori et al., 2004; Weinberger et al., 2006); the PRC was obtained by the method proposed by Rosenblum and Pikovsky (Rosenblum and Pikovsky, 2001). Similar PRCs were identified for both PD patients, indicating the phase specificity of pathological beta oscillations in the STN.

On the basis of these findings, phase-specific interventions appear to be the most straightforward approach for disrupting the beta synchronization in the STN. Also, phase locked stimulation in relation to the BO might induce plastic changes of the pathological oscillations by inducing long-term potentiation/depotentiation-like effects (Huerta and Lisman, 1995).

3. Discussion

In this PhD thesis, the synchronized oscillatory activity within and between the STN and cortical regions was studied in PD patients when at rest and in the medication OFF state during

the implantation of DBS electrodes. Here, novel subcortical and cortical recording methods were proposed and tested: cortical activity was captured by intraoperative EEG, while macroelectrode recordings were performed in the STN. Moreover, the response of oscillatory regions to electrical stimulation were investigated during low-frequency and therapeutic high-frequency DBS.

3.1 Biomarkers in the subthalamic nucleus and cortico-subcortical connectivity

Enhanced beta oscillations, HFO, and their coupling, namely, B-HFO, in basal ganglia loops are shown to be correlated with the state of PD and with changes in response to pharmacological and/or neurostimulation interventions (Brittain and Brown, 2014; Little and Brown, 2014). A recent study, in which cortical and subcortical oscillatory activities were recorded with a chronic device suggested that dyskinesia corresponded to strong oscillation in the STN, motor cortex, and to their phase coherence coupling in the same band (Swann et al., 2016). These electrophysiological biomarkers and their connection to the cortex at the same time have rarely received attention. In this PhD thesis, considerable evidence is provided for delineating the spatial and spectral specificities of physiological biomarkers both within the STN and the cortex, particularly as it pertains to cortico-subthalamic functional and effective connectivity.

Several features of STN-LFP, such as excessive beta oscillatory activity or coupling of the beta phase to the amplitude of HFO (B-HFO) have been reported as potential biomarkers in PD, and have recently shown the potential to be used as feedback signals for closed-loop DBS (de Hemptinne et al., 2015; Little and Brown, 2012; Little et al., 2013). Although, both BO and B-HFO were identified in the motor territory of the STN, their role and mechanism in the STN is still unclear. Here, we showed that the maximum BO and beta-coupled HFO were separated in the dorsal STN spectrally, with peaks in the low and high frequency-beta band, respectively. BO in the low-frequency beta band may serve a rather, local, i.e. subcortical function, while high-frequency beta oscillations may serve the distal communication to the cortex (Friston et al., 2015; Oswal et al., 2016). Low beta oscillation might be generated from the reciprocal connectivity between the subcortical structures STN and GPi (Plenz and Kital, 1999). This interpretation may be supported by the recent MEG study of Oswal and colleagues (Oswal et al., 2016). They have suggested the hyperdirect pathway to be characterized by high

beta band oscillations and low beta band activity to mediate local subcortical function. Here, confirm this hypothesis by demonstrating in all studies that the STN-motor network synchronization was strongest in the upper beta-range as well. Furthermore, the peak beta frequency within the STN was always in the low beta range in our recordings.

The results of the presented intraoperative studies match with the postoperative studies using simultaneous MEG and STN-LFP recordings in DBS patients. These previous studies suggest that the frequency of cortico-STN coherence with the ipsilateral M1 lies in the upper beta band (~25 Hz) (Litvak et al., 2011; van Wijk et al., 2016). However, the spatial specificity of the spot in the STN which connected to the cortical motor network remained unknown since these post-operative measurements did not allow to move the electrode, i.e. map the across the STN. The novel method implemented in this work employed millimeter by millimeter measurements of cortico-subcortical phase coherence during DBS surgery and revealed the spatial specificity of the STN-motor network. The most prominent STN-motor network was located ventral to the beta oscillatory region, but was still within the dorsolateral motor part of the STN.

Previous studies applied bipolar LFP recordings in the STN region to cancel out artifacts (e.g. related to movements) or to address the same referencing issue (Bastos and Schoffelen, 2016); however, this method decreases the spatial specificity of the recordings considerably. To best our knowledge, this work showed for the first time that the power spectrum of monopolar recordings is robust and reliable for detecting the oscillatory regions in the STN. On the basis of the repeated recording technique that calculated the power spectrum of the same spatial location at different time points, it could be demonstrated that the findings were reproducible and could be applied in an operation environment.

In summary, a novel technique for electrophysiological recordings during DBS surgery has been introduced, which is capable of detecting the spot of STN-motor cortex coupling. This spot may serve as a marker of the hyperdirect pathway and could potentially facilitate intraoperative, connectivity-based targeting during DBS surgery in PD. Furthermore, the STN localization with the chronic electrode may reduce the surgery-related risk, a proposal that needs to be verified in future studies.

3.2 How does deep brain stimulation influence subcortical oscillatory activity?

There are several lines of evidence suggesting a reduction of low beta power in the STN (Eusebio et al., 2012) and reduced phase coherence connectivity between the STN and mesial premotor regions in the high beta band (Oswal et al., 2016) during therapeutic DBS. However, most of these studies did not provide proper spatial specificity or a direct oscillatory response to DBS. Furthermore, in most of studies artefact-rejection methods were employed to recover the brain signals from DBS related artefacts during electrical stimulation. However, it remains unclear how these methods could fully reject the stimulation artefact from genuine induced DBS oscillations due to the nonlinear nature of artefacts (Noury et al.). In this PhD thesis, a novel strategy is proposed to record neural responses during STN DBS.

To examine the neural response to STN DBS during different stimulation conditions, the LFPs were acquired with a very high sampling rate providing high temporal resolution of the evoked activities during mapping the STN area millimeter by millimeter. This high temporal and spatial resolution revealed a distinct sEP pattern, which had a significant correlation with STN-motor cortex connectivity. The spatial co-location of prominent sEPs with strong STN-motor coupling and with HFO might explain the emergence of a short latency evoked response in the STN. At the same time, no correlation was found between the spatial location of the beta oscillatory region and the STN-motor network coherence. It can, therefore, be speculated that an information flow from the cortical motor area to the STN through a hyperdirect pathway may jam the synchronized pathological activity of beta range oscillations to produce high frequency rhythms in the STN. Two recent studies support this speculation by providing neurophysiological evidence for the relevance of HFO as a functional marker of the motor state in PD (Hirschmann et al., 2016; Wang et al., 2014). Furthermore, increases of the HFO power have been shown within the STN at movement onset, indicating that HFO in the STN plays a prominent role in the motor circuit (López-Azcárate et al., 2010; Özkurt et al., 2011).

One possible approach to probe the neural oscillatory characteristics is to directly perturb the system with external stimulation. The resulting neural activity response may reveal valuable information about the properties of the system. Intrinsic dynamical properties of cortical sites were revealed by transcranial magnetic stimulation (Harquel et al., 2016; Rosanova et al., 2009). In parallel to this approach, cortical evoked potentials were recorded

during various DBS frequencies (between 5 and 30 Hz) in the STN of PD patients (Eusebio et al., 2009). Eusebio and colleagues showed that the amplitude of cEP in the ipsilateral sensorimotor cortex increased significantly at as timulation frequency of 20 Hz as compared to 5 Hz stimulation, thereby, suggesting that the basal ganglia–cortical network involving the STN has a tendency to resonate at 20 Hz in PD. They also pointed out that under L-dopa administration damping was increased in the basal ganglia- cortical network, thereby, potentially limiting this loop to resonance at 20 Hz oscillation. However, to the best of our knowledge, no study up to now has investigated the dynamical properties of different subcortical sites across the STN in response to DBS. The present results are thus in line with the study performed by Eusebio and colleagues. While this previous study applied dopamine to reduce the resonance effect, this work applied electrical stimulation for the same purpose. In fact, the reduction of sEPs during high-frequency stimulation indicated that the damping of the stimulated subcortical site increased during the intervention and that the pathologically increased resonance state of the system was reduced. Since the sEPs dynamically changed with respect to the neural activity, these results could offer a practical and reliable marker for closed-loop stimulation.

3.3 Future outlook

DBS is used for many years in PD patients achieving considerable clinical effects (Schuepbach et al., 2013). The underlying electrophysiological mechanisms of this intervention are, however, still not completely clear. The present work provides novel methods for electrophysiologically-driven DBS implantation and new insights into the neurophysiological manifestations of PD. The studies showed the feasibility and reliability of monopolar macroelectrode recordings through the chronic electrode (DBS lead model 3389) to locate the STN boundaries during surgery in a relatively large group of PD patients (more than 35 patients). The STN mapping was reproducible under real intraoperative conditions. This method has potentially important surgical implications by providing an alternative to the common practice of inserting microelectrode test electrodes prior to the implantation of the chronic electrode. It may, thereby, reduce surgical complications and avoid lead misplacement, which has to be demonstrated in future studies. Moreover, recording cortical activity as an additional neural information source provided a new biomarker for targeting the pathological

PD network, and will, thereby, facilitate network based DBS implantations. In this regard, antidromic cortical activation has been shown to play a key role during STN DBS in the suppression of pathological cortical and subcortical oscillations in human and animal studies (Gradinaru et al., 2009; Kahan et al., 2014; Li et al., 2012; Li et al., 2007; Walker et al., 2012). This underlines the importance of the M1-STN direct connection (hyperdicret pathway) in PD. Based on this evidence, the present work suggested a new intraoperative technique for the detection of the hyperdirect pathway to facilitate network based DBS lead placement; an approach that will help to maximize the perturbation of the pathological brain network in PD.

Continues high-frequency DBS has been shown therapeutically effective in reducing PD motor symptom and disrupting ongoing pathological oscillations; adaptive intervals of stimulation might potentially increases both the therapeutic effect and efficacy of stimulation (Little et al., 2013). However, maximal perturbation of the pathological beta activity could be reached by our proposed targeted perturbation method. Delivering DBS based on specific phases of the ongoing beta oscillation may not only optimize the pathological disruption, but could also induce plastic changes (Cagnan et al., 2015). A recent computational model of PD confirmed our approach to target specific phases of the beta oscillatory cycle (Holt et al., 2016).

The spatial specificity of the STN-motor network connection and prominent sEPs at distinct STN sites were demonstrated at a resolution of about 1 mm. With the current design of DBS leads (DBS lead model 3389; 1.5 mm contact height, 1.27 mm diameter, cylindrical design with a surface area of about 22 mm^2) a spatially precise targeting based on these electrophysiological markers seems less feasible. However, recent advances in high density DBS lead technology may provide a tool for directional steering of the stimulation with a higher spatial resolution in the submillimeter range (contact surface area of about 100 μm^2) (Connolly et al., 2016; Contarino et al., 2014; Pollo et al., 2014). Such increased spatial precision of stimulation and recording would enable us to specifically target the spot of B-HFO/maximum M1-STN coherence.

In conclusion, this work provides sufficient evidence that macroelectrode recordings with the chronic electrode (DBS lead model 3389, Medtronic Inc., Minneapolis, USA) are a safe and robust method for targeting the STN during DBS surgery. Additionally, combining LFP and EEG recordings in the surgical environment offered a new way of DBS targeting on the

basis of pathological network activity. Applying these techniques, the correlation between various electrophysiological markers in PD could be revealed for the first time.

4. References

Abramowitz, J.S., Taylor, S., and McKay, D. Obsessive-compulsive disorder. The Lancet 374, 491-499.

Accolla, E.A., Herrojo Ruiz, M., Horn, A., Schneider, G.-H., Schmitz-Hübsch, T., Draganski, B., and Kühn, A.A. (2016). Brain networks modulated by subthalamic nucleus deep brain stimulation. Brain.

Alhourani, A., McDowell, M.M., Randazzo, M., Wozny, T., Kondylis, E., Lipski, W.J., Beck, S., Karp, J.F., Ghuman, A.S., and Richardson, R.M. (2015). Network Effects of Deep Brain Stimulation. Journal of Neurophysiology.

Anand, A., Li, Y., Wang, Y., Wu, J., Gao, S., Bukhari, L., Mathews, V.P., Kalnin, A., and Lowe, M.J. (2005). Activity and Connectivity of Brain Mood Regulating Circuit in Depression: A Functional Magnetic Resonance Study. Biological Psychiatry 57, 1079-1088.

Arlotti, M., Rossi, L., Rosa, M., Marceglia, S., and Priori, A. (2016). An external portable device for adaptive deep brain stimulation (aDBS) clinical research in advanced Parkinson's Disease. Medical Engineering & Physics 38, 498-505.

Barbeau, A. (1969). L-Dopa Therapy in Parkinson's Disease: A Critical Review of Nine Years' Experience. Canadian Medical Association Journal 101, 59-68.

Bastos, A.M., and Schoffelen, J.-M. (2016). A Tutorial Review of Functional Connectivity Analysis Methods and Their Interpretational Pitfalls. Frontiers in Systems Neuroscience 9.

Belujon, P., and Grace, A.A. (2011). Reorganization of striatal inhibitory microcircuits leads to pathological synchrony in the basal ganglia. Neuron 71, 766-768.

Bergman, H., Feingold, A., Nini, A., Raz, A., Slovin, H., Abeles, M., and Vaadia, E. (1998). Physiological aspects of information processing in the basal ganglia of normal and parkinsonian primates. Trends in Neurosciences 21, 32-38.

Bernheimer, H., Birkmayer, W., Hornykiewicz, O., Jellinger, K., and Seitelberger, F. (1973). Brain dopamine and the syndromes of Parkinson and Huntington Clinical, morphological and neurochemical correlations. Journal of the Neurological Sciences 20, 415-455.

Breakefield, X.O., Blood, A.J., Li, Y., Hallett, M., Hanson, P.I., and Standaert, D.G. (2008). The pathophysiological basis of dystonias. Nat Rev Neurosci 9, 222-234.

Brittain, J.-S., and Brown, P. (2014). Oscillations and the basal ganglia: Motor control and beyond. NeuroImage 85, Part 2, 637-647.

Brown, P. (2003). Oscillatory nature of human basal ganglia activity: Relationship to the pathophysiology of Parkinson's disease. Movement Disorders 18, 357-363.

Brown, P. (2007). Abnormal oscillatory synchronisation in the motor system leads to impaired movement. Current Opinion in Neurobiology 17, 656-664.

Brunoni, A.R., Lopes, M., and Fregni, F. (2008). A systematic review and meta-analysis of clinical studies on major depression and BDNF levels: implications for the role of neuroplasticity in depression. International Journal of Neuropsychopharmacology 11, 1169-1180.

Buzsáki, G., Anastassiou, C.A., and Koch, C. (2012). The origin of extracellular fields and currents — EEG, ECoG, LFP and spikes. Nat Rev Neurosci 13, 407-420.

Cagnan, H., Brown, P., Bourget, D., and Denison, T. (2015). Inertial-based control system concepts for the treatment of movement disorders. In 2015 Transducers - 2015 18th International Conference on Solid-State Sensors, Actuators and Microsystems (TRANSDUCERS), pp. 70-73.

Cao, C., Li, D., Jiang, T., Ince, N.F., Zhan, S., Zhang, J., Sha, Z., and Sun, B. (2015). Resting state cortical oscillations of patients with Parkinson disease and with and without subthalamic deep brain stimulation: a magnetoencephalography study. Journal of clinical neurophysiology : official publication of the American Electroencephalographic Society 32, 109-118.

Chen, C.C., Pogosyan, A., Zrinzo, L.U., Tisch, S., Limousin, P., Ashkan, K., Yousry, T., Hariz, M.I., and Brown, P. (2006). Intra-operative recordings of local field potentials can help localize the subthalamic nucleus in Parkinson's disease surgery. Experimental Neurology 198, 214-221.

Chiken, S., and Nambu, A. (2015). Mechanism of Deep Brain Stimulation: Inhibition, Excitation, or Disruption? The Neuroscientist.

Colosimo, C., Pantano, P., Calistri, V., Totaro, P., Fabbrini, G., and Berardelli, A. (2005). Diffusion tensor imaging in primary cervical dystonia. Journal of Neurology, Neurosurgery & Psychiatry 76, 1591-1593.

Connolly, A.T., Vetter, R.J., Hetke, J.F., Teplitzky, B.A., Kipke, D.R., Pellinen, D.S., Anderson, D.J., Baker, K.B., Vitek, J.L., and Johnson, M.D. (2016). A Novel Lead Design for Modulation and Sensing of Deep Brain Structures. IEEE Transactions on Biomedical Engineering 63, 148-157.

Contarino, M.F., Bour, L.J., Verhagen, R., Lourens, M.A.J., de Bie, R.M.A., van den Munckhof, P., and Schuurman, P.R. (2014). Directional steering: A novel approach to deep brain stimulation. Neurology 83, 1163-1169.

Cynthia, A.C., Vikash, G., Paul, N., Justin, D.F., Joline, M.F., Matthew, T.K., Mark, M.C., Zuley, R.-A., John, P.C., Stephen, I.R., and Krishna, V.S. (2011). Long-term stability of neural prosthetic control signals from silicon cortical arrays in rhesus macaque motor cortex. Journal of Neural Engineering 8, 045005.

de Hemptinne, C., Ryapolova-Webb, E.S., Air, E.L., Garcia, P.A., Miller, K.J., Ojemann, J.G., Ostrem, J.L., Galifianakis, N.B., and Starr, P.A. (2013a). Exaggerated phase-amplitude coupling in the primary

motor cortex in Parkinson disease. Proceedings of the National Academy of Sciences of the United States of America 110, 4780-4785.

de Hemptinne, C., Ryapolova-Webb, E.S., Air, E.L., Garcia, P.A., Miller, K.J., Ojemann, J.G., Ostrem, J.L., Galifianakis, N.B., and Starr, P.A. (2013b). Exaggerated phase–amplitude coupling in the primary motor cortex in Parkinson disease. Proceedings of the National Academy of Sciences 110, 4780-4785.

de Hemptinne, C., Swann, N.C., Ostrem, J.L., Ryapolova-Webb, E.S., San Luciano, M., Galifianakis, N.B., and Starr, P.A. (2015). Therapeutic deep brain stimulation reduces cortical phase-amplitude coupling in Parkinson's disease. Nat Neurosci 18, 779-786.

Deffains, M., Holland, P., Moshel, S., de Noriega, F.R., Bergman, H., and Israel, Z. (2014). Higher neuronal discharge rate in the motor area of the subthalamic nucleus of Parkinsonian patients. Journal of Neurophysiology 112, 1409-1420.

Deuschl, G., Schade-Brittinger, C., Krack, P., Volkmann, J., Schäfer, H., Bötzel, K., Daniels, C., Deutschländer, A., Dillmann, U., Eisner, W., *et al.* (2006). A Randomized Trial of Deep-Brain Stimulation for Parkinson's Disease. New England Journal of Medicine 355, 896-908.

Deuschl, G., Schuepbach, M., Knudsen, K., Pinsker, M.O., Cornu, P., Rau, J., Agid, Y., and Schade-Brittinger, C. (2013). Stimulation of the subthalamic nucleus at an earlier disease stage of Parkinson's disease: Concept and standards of the EARLYSTIM-study. Parkinsonism & Related Disorders 19, 56-61.

Eusebio, A., Cagnan, H., and Brown, P. (2012). Does suppression of oscillatory synchronisation mediate some of the therapeutic effects of DBS in patients with Parkinson's disease? Frontiers in Integrative Neuroscience 6, 47.

Fernández-Seara, M.A., Mengual, E., Vidorreta, M., Castellanos, G., Irigoyen, J., Erro, E., and Pastor, M.A. (2015). Resting state functional connectivity of the subthalamic nucleus in Parkinson's disease assessed using arterial spin-labeled perfusion fMRI. Human Brain Mapping 36, 1937-1950.

Fogelson, N., Williams, D., Tijssen, M., van Bruggen, G., Speelman, H., and Brown, P. (2006). Different functional loops between cerebral cortex and the subthalmic area in Parkinson's disease. Cerebral Cortex 16, 64-75.

Friston, K.J., Bastos, A.M., Pinotsis, D., and Litvak, V. (2015). LFP and oscillations—what do they tell us? Current Opinion in Neurobiology 31, 1-6.

Gaze, R.M., Gillingham, F.J., Kalyanaraman, S., Porter, R.W., Donaldson, A.A., and Donaldson, I.M.L. (1964). MICROELECTRODE RECORDINGS FROM THE HUMAN THALAMUS. Brain 87, 691-706.

Gilbertson, T., Lalo, E., Doyle, L., Di Lazzaro, V., Cioni, B., and Brown, P. (2005). Existing motor state is favored at the expense of new movement during 13-35 Hz oscillatory synchrony in the human corticospinal system. Journal of Neuroscience 25, 7771-7779.

Gold , P.W., Goodwin , F.K., and Chrousos , G.P. (1988). Clinical and Biochemical Manifestations of Depression. New England Journal of Medicine 319, 348-353.

Gradinaru, V., Mogri, M., Thompson, K.R., Henderson, J.M., and Deisseroth, K. (2009). Optical Deconstruction of Parkinsonian Neural Circuitry. Science 324, 354-359.

Guo, S., Zhuang, P., Hallett, M., Zheng, Z., Zhang, Y., Li, J., and Li, Y. (2013). Subthalamic deep brain stimulation for Parkinson's disease: Correlation between locations of oscillatory activity and optimal site of stimulation. Parkinsonism & Related Disorders 19, 109-114.

Hammond, C., Bergman, H., and Brown, P. (2007). Pathological synchronization in Parkinson's disease: networks, models and treatments. Trends in Neurosciences 30, 357-364.

Harquel, S., Bacle, T., Beynel, L., Marendaz, C., Chauvin, A., and David, O. (2016). Mapping dynamical properties of cortical microcircuits using robotized TMS and EEG: Towards functional cytoarchitectonics. NeuroImage 135, 115-124.

Hikosaka, O., Takikawa, Y., and Kawagoe, R. (2000). Role of the Basal Ganglia in the Control of Purposive Saccadic Eye Movements. Physiological Reviews 80, 953.

Hirschmann, J., Butz, M., Hartmann, C.J., Hoogenboom, N., Özkurt, T.E., Vesper, J., Wojtecki, L., and Schnitzler, A. (2016). Parkinsonian Rest Tremor Is Associated With Modulations of Subthalamic High-Frequency Oscillations. Movement Disorders, n/a-n/a.

Holt, A.B., Wilson, D., Shinn, M., Moehlis, J., and Netoff, T.I. (2016). Phasic Burst Stimulation: A Closed-Loop Approach to Tuning Deep Brain Stimulation Parameters for Parkinson’s Disease. PLoS Comput Biol 12, e1005011.

Huerta, P.T., and Lisman, J.E. (1995). Bidirectional synaptic plasticity induced by a single burst during cholinergic theta oscillation in CA1 in vitro. Neuron 15, 1053-1063.

Hughes, A.J., Daniel, S.E., Kilford, L., and Lees, A.J. (1992). Accuracy of clinical diagnosis of idiopathic Parkinson's disease: a clinico-pathological study of 100 cases. Journal of Neurology, Neurosurgery & Psychiatry 55, 181-184.

Hutchison, W.D., Allan, R.J., Opitz, H., Levy, R., Dostrovsky, J.O., Lang, A.E., and Lozano, A.M. (1998). Neurophysiological identification of the subthalamic nucleus in surgery for Parkinson's disease. Annals of Neurology 44, 622-628.

Hutchison, W.D., Lozano, A.M., Davis, K.D., Saint-Cyr, J.A., Lang, A.E., and Dostrovsky, J.O. (1994). Differential neuronal activity in segments of globus pallidus in Parkinson's disease patients. NeuroReport 5.

Jankovic, J. (2008). Parkinson’s disease: clinical features and diagnosis. Journal of Neurology, Neurosurgery & Psychiatry 79, 368-376.

Kahan, J., Urner, M., Moran, R., Flandin, G., Marreiros, A., Mancini, L., White, M., Thornton, J., Yousry, T., Zrinzo, L., *et al.* (2014). Resting state functional MRI in Parkinson’s disease: the impact of deep brain stimulation on ‘effective’ connectivity. Brain.

Kato, K., Yokochi, F., Taniguchi, M., Okiyama, R., Kawasaki, T., Kimura, K., and Ushiba, J. (2015). Bilateral coherence between motor cortices and subthalamic nuclei in patients with Parkinson’s disease. Clinical Neurophysiology 126, 1941-1950.

Krack, P., and Hariz, M.I. (2013). Deep brain stimulation in Parkinson's disease: reconciliation of evidence-based medicine with clinical practice. Lancet Neurology 12, 25-26.

Kuelz, A.K., Hohagen, F., and Voderholzer, U. (2004). Neuropsychological performance in obsessive-compulsive disorder: a critical review. Biological Psychology 65, 185-236.

Kühn, A.A., Tsui, A., Aziz, T., Ray, N., Brücke, C., Kupsch, A., Schneider, G.-H., and Brown, P. (2009). Pathological synchronisation in the subthalamic nucleus of patients with Parkinson's disease relates to both bradykinesia and rigidity. Experimental Neurology 215, 380-387.

Kuriakose, R., Saha, U., Castillo, G., Udupa, K., Ni, Z., Gunraj, C., Mazzella, F., Hamani, C., Lang, A.E., Moro, E., *et al.* (2010). The Nature and Time Course of Cortical Activation Following Subthalamic Stimulation in Parkinson's Disease. Cerebral Cortex 20, 1926-1936.

Lalo, E., Thobois, S., Sharott, A., Polo, G., Mertens, P., Pogosyan, A., and Brown, P. (2008). Patterns of bidirectional communication between cortex and basal ganglia during movement in patients with Parkinson disease. Journal of Neuroscience 28, 3008-3016.

Lang , A.E., and Lozano , A.M. (1998). Parkinson's Disease. New England Journal of Medicine 339, 1044-1053.

Lenka, A., Jhunjhunwala, K.R., Saini, J., and Pal, P.K. (2015). Structural and functional neuroimaging in patients with Parkinson's disease and visual hallucinations: A critical review. Parkinsonism & Related Disorders 21, 683-691.

Levy, R., Ashby, P., Hutchison, W.D., Lang, A.E., Lozano, A.M., and Dostrovsky, J.O. (2002). Dependence of subthalamic nucleus oscillations on movement and dopamine in Parkinson’s disease. Brain 125, 1196-1209.

Li, Q., Ke, Y., Chan, D.C.W., Qian, Z.-M., Yung, K.K.L., Ko, H., Arbuthnott, G.W., and Yung, W.-H. (2012). Therapeutic Deep Brain Stimulation in Parkinsonian Rats Directly Influences Motor Cortex. Neuron 76, 1030-1041.

Li, S., Arbuthnott, G.W., Jutras, M.J., Goldberg, J.A., and Jaeger, D. (2007). Resonant antidromic cortical circuit activation as a consequence of high-frequency subthalamic deep-brain stimulation. Journal of Neurophysiology 98, 3525-3537.

Little, S., and Brown, P. (2012). What brain signals are suitable for feedback control of deep brain stimulation in Parkinson's disease? In Brain Stimulation in Neurology and Psychiatry, T.A. Pedley, S.H. Lisanby, H.S. Mayberg, and N.D. Schiff, eds., pp. 9-24.

Little, S., and Brown, P. (2014). Focusing Brain Therapeutic Interventions in Space and Time for Parkinson's Disease. Current Biology 24, R898-R909.

Little, S., Pogosyan, A., Neal, S., Zavala, B., Zrinzo, L., Hariz, M., Foltynie, T., Limousin, P., Ashkan, K., FitzGerald, J., *et al.* (2013). Adaptive Deep Brain Stimulation In Advanced Parkinson Disease. Annals of Neurology 74, 449-457.

Litvak, V., Eusebio, A., Jha, A., Oostenveld, R., Barnes, G.R., Penny, W.D., Zrinzo, L., Hariz, M.I., Limousin, P., Friston, K.J., and Brown, P. (2010). Optimized beamforming for simultaneous MEG and intracranial local field potential recordings in deep brain stimulation patients. Neuroimage 50, 1578-1588.

Litvak, V., Jha, A., Eusebio, A., Oostenveld, R., Foltynie, T., Limousin, P., Zrinzo, L., Hariz, M.I., Friston, K., and Brown, P. (2011). Resting oscillatory cortico-subthalamic connectivity in patients with Parkinson's disease. Brain 134, 359-374.

Lloyd, K.G., Davidson, L., and Hornykiewicz, O. (1975). The neurochemistry of Parkinson's disease: effect of L-dopa therapy. Journal of Pharmacology and Experimental Therapeutics 195, 453-464.

López-Azcárate, J., Tainta, M., Rodríguez-Oroz, M.C., Valencia, M., González, R., Guridi, J., Iriarte, J., Obeso, J.A., Artieda, J., and Alegre, M. (2010). Coupling between Beta and High-Frequency Activity in the Human Subthalamic Nucleus May Be a Pathophysiological Mechanism in Parkinson's Disease. The Journal of Neuroscience 30, 6667-6677.

Lozano, A.M., and Lipsman, N. (2013). Probing and Regulating Dysfunctional Circuits Using Deep Brain Stimulation. Neuron 77, 406-424.

Ludvic Zrinzo, Thomas Foltynie, Patricia Limousin, and Marwan I. Hariz (2012). Reducing hemorrhagic complications in functional neurosurgery: a large case series and systematic literature review. Journal of Neurosurgery 116, 84-94.

Maks, C.B., Butson, C.R., Walter, B.L., Vitek, J.L., and McIntyre, C.C. (2009). Deep brain stimulation activation volumes and their association with neurophysiological mapping and therapeutic outcomes. Journal of Neurology, Neurosurgery & Psychiatry 80, 659-666.

Marcel van, G., Jason, F., Rebecca, S., Rutger, V., Jeroen, G., Anton, N., Nick, R., Pim, H., Louis, V., Stan, G., and Peter, D. (2009). The brain–computer interface cycle. Journal of Neural Engineering 6, 041001.

Marreiros, A.C., Cagnan, H., Moran, R.J., Friston, K.J., and Brown, P. (2013). Basal ganglia-cortical interactions in Parkinsonian patients. Neuroimage 66, 301-310.

McCarthy, M.M., Moore-Kochlacs, C., Gu, X., Boyden, E.S., Han, X., and Kopell, N. (2011). Striatal origin of the pathologic beta oscillations in Parkinson's disease. Proceedings of the National Academy of Sciences of the United States of America 108, 11620-11625.

McClelland, S. (2011). A cost analysis of intraoperative microelectrode recording during subthalamic stimulation for Parkinson's disease. Movement Disorders 26, 1422-1427.

Menzies, L., Chamberlain, S.R., Laird, A.R., Thelen, S.M., Sahakian, B.J., and Bullmore, E.T. (2008). Integrating evidence from neuroimaging and neuropsychological studies of obsessive-compulsive disorder: The orbitofronto-striatal model revisited. Neuroscience & Biobehavioral Reviews 32, 525-549.

Michely, J., Volz, L.J., Barbe, M.T., Hoffstaedter, F., Viswanathan, S., Timmermann, L., Eickhoff, S.B., Fink, G.R., and Grefkes, C. (2015). Dopaminergic modulation of motor network dynamics in Parkinson’s disease. Brain 138, 664-678.

Neumann, W.-J., Degen, K., Schneider, G.-H., Brücke, C., Huebl, J., Brown, P., and Kühn, A.A. (2016). Subthalamic synchronized oscillatory activity correlates with motor impairment in patients with Parkinson's disease. Movement Disorders, n/a-n/a.

Nicoletti, G., Manners, D., Novellino, F., Condino, F., Malucelli, E., Barbiroli, B., Tonon, C., Arabia, G., Salsone, M., Giofre', L., *et al.* (2010). Diffusion tensor MRI changes in cerebellar structures of patients with familial essential tremor. Neurology 74, 988-994.

Nolte, G., Bai, O., Wheaton, L., Mari, Z., Vorbach, S., and Hallett, M. (2004). Identifying true brain interaction from EEG data using the imaginary part of coherency. Clinical Neurophysiology 115, 2292-2307.

Noury, N., Hipp, J.F., and Siegel, M. Physiological processes non-linearly affect electrophysiological recordings during transcranial electric stimulation. NeuroImage.

Novak, P., Przybyszewski, A.W., Barborica, A., Ravin, P., Margolin, L., and Pilitsis, J.G. (2011). Localization of the subthalamic nucleus in Parkinson disease using multiunit activity. Journal of the Neurological Sciences 310, 44-49.

Nurmikko, A.V., Donoghue, J.P., Hochberg, L.R., Patterson, W.R., Song, Y.-K., Bull, C.W., Borton, D.A., Laiwalla, F., Park, S., Ming, Y., and Aceros, J. (2010). Listening to Brain Microcircuits for Interfacing With External World—Progress in Wireless Implantable Microelectronic

Neuroengineering Devices: Experimental systems are described for electrical recording in the brain using multiple microelectrodes and short range implantable or wearable broadcasting units. Proceedings of the IEEE Institute of Electrical and Electronics Engineers 98, 375-388.

Obeso, J.A., Marin, C., Rodriguez-Oroz, C., Blesa, J., Benitez-Temiño, B., Mena-Segovia, J., Rodríguez, M., and Olanow, C.W. (2008). The basal ganglia in Parkinson's disease: Current concepts and unexplained observations. Annals of Neurology 64, S30-S46.

Obeso, J.A., Rodriguez-Oroz, M., Marin, C., Alonso, F., Zamarbide, I., Lanciego, J.L., and Rodriguez-Diaz, M. (2004). The origin of motor fluctuations in Parkinson's disease: Importance of dopaminergic innervation and basal ganglia circuits. Neurology 62, S17-S30.

Obeso, J.A., Rodriguez-Oroz, M.C., Rodriguez, M., Lanciego, J.L., Artieda, J., Gonzalo, N., and Olanow, C.W. (2000). Pathophysiology of the basal ganglia in Parkinson's disease. Trends in Neurosciences 23, Supplement 1, S8-S19.

Odekerken, V.J.J., van Laar, T., Staal, M.J., Mosch, A., Hoffmann, C.F.E., Nijssen, P.C.G., Beute, G.N., van Vugt, J.P.P., Lenders, M.W.P.M., Contarino, M.F., *et al.* (2013). Subthalamic nucleus versus globus pallidus bilateral deep brain stimulation for advanced Parkinson's disease (NSTAPS study): a randomised controlled trial. Lancet Neurology 12, 37-44.

Okun, M.S. (2012). Deep-Brain Stimulation for Parkinson's Disease. New England Journal of Medicine 367, 1529-1538.

Oswal, A., Beudel, M., Zrinzo, L., Limousin, P., Hariz, M., Foltynie, T., Litvak, V., and Brown, P. (2016). Deep brain stimulation modulates synchrony within spatially and spectrally distinct resting state networks in Parkinson's disease. Brain 139, 1482-1496.

Özkurt, T.E., Butz, M., Homburger, M., Elben, S., Vesper, J., Wojtecki, L., and Schnitzler, A. (2011). High frequency oscillations in the subthalamic nucleus: A neurophysiological marker of the motor state in Parkinson's disease. Experimental Neurology 229, 324-331.

Paffi, A., Camera, F., Apollonio, F., d'Inzeo, G., and Liberti, M. (2015). Numerical characterization of intraoperative and chronic electrodes in deep brain stimulation. Frontiers in Computational Neuroscience 9, 2.

Park, C., Worth, R.M., and Rubchinsky, L.L. (2010). Fine Temporal Structure of Beta Oscillations Synchronization in Subthalamic Nucleus in Parkinson's Disease. Journal of Neurophysiology 103, 2707-2716.

Park, J.H., Chung, S.J., Lee, C.S., and Jeon, S.R. (2011). Analysis of hemorrhagic risk factors during deep brain stimulation surgery for movement disorders: comparison of the circumferential paired and multiple electrode insertion methods. Acta Neurochirurgica 153, 1573-1578.

Pikovsky, A., Rosenblum, M., Kurths, J., and Hilborn, R.C. (2002). Synchronization: A Universal Concept in Nonlinear Science. American Journal of Physics 70, 655-655.

Plenz, D., and Kital, S.T. (1999). A basal ganglia pacemaker formed by the subthalamic nucleus and external globus pallidus. Nature 400, 677-682.

Polikov, V.S., Tresco, P.A., and Reichert, W.M. (2005). Response of brain tissue to chronically implanted neural electrodes. Journal of Neuroscience Methods 148, 1-18.

Politis, M. (2014). Neuroimaging in Parkinson disease: from research setting to clinical practice. Nat Rev Neurol 10, 708-722.

Pollo, C., Kaelin-Lang, A., Oertel, M.F., Stieglitz, L., Taub, E., Fuhr, P., Lozano, A.M., Raabe, A., and Schüpbach, M. (2014). Directional deep brain stimulation: an intraoperative double-blind pilot study. Brain 137, 2015-2026.

Priori, A., Foffani, G., Pesenti, A., Tamma, F., Bianchi, A.M., Pellegrini, M., Locatelli, M., Moxon, K.A., and Villani, R.M. (2004). Rhythm-specific pharmacological modulation of subthalamic activity in Parkinson's disease. Experimental Neurology 189, 369-379.

Qasim, S.E., de Hemptinne, C., Swann, N.C., Miocinovic, S., Ostrem, J.L., and Starr, P.A. (2016). Electrocorticography reveals beta desynchronization in the basal ganglia-cortical loop during rest tremor in Parkinson's disease. Neurobiology of Disease 86, 177-186.

Rascol, O., Payoux, P., Ory, F., Ferreira, J.J., Brefel-Courbon, C., and Montastruc, J.-L. (2003). Limitations of current Parkinson's disease therapy. Annals of Neurology 53, S3-S15.

Ray, N.J., Jenkinson, N., Wang, S., Holland, P., Brittain, J.S., Joint, C., Stein, J.F., and Aziz, T. (2008). Local field potential beta activity in the subthalamic nucleus of patients with Parkinson's disease is associated with improvements in bradykinesia after dopamine and deep brain stimulation. Experimental Neurology 213, 108-113.

Rosanova, M., Casali, A., Bellina, V., Resta, F., Mariotti, M., and Massimini, M. (2009). Natural Frequencies of Human Corticothalamic Circuits. The Journal of Neuroscience 29, 7679-7685.

Rosenblum, M.G., and Pikovsky, A.S. (2001). Detecting direction of coupling in interacting oscillators. Physical review E, Statistical, nonlinear, and soft matter physics 64, 045202.

Rosin, B., Slovik, M., Mitelman, R., Rivlin-Etzion, M., Haber, Suzanne N., Israel, Z., Vaadia, E., and Bergman, H. Closed-Loop Deep Brain Stimulation Is Superior in Ameliorating Parkinsonism. Neuron 72, 370-384.

Rossi, L., Foffani, G., Marceglia, S., Bracchi, F., Barbieri, S., and Priori, A. (2007). An electronic device for artefact suppression in human local field potential recordings during deep brain stimulation. Journal of Neural Engineering 4, 96-106.

Schuepbach, W.M.M., Rau, J., Knudsen, K., Volkmann, J., Krack, P., Timmermann, L., Haelbig, T.D., Hesekamp, H., Navarro, S.M., Meier, N., *et al.* (2013). Neurostimulation for Parkinson's Disease with Early Motor Complications. New England Journal of Medicine 368, 610-622.

Seifried, C., Weise, L., Hartmann, R., Gasser, T., Baudrexel, S., Szelenyi, A., van de Loo, S., Steinmetz, H., Seifert, V., Roeper, J., and Hilker, R. (2012). Intraoperative microelectrode recording for the delineation of subthalamic nucleus topography in Parkinson's disease. Brain Stimulation 5, 378-387.

Sharott, A., Gulberti, A., Zittel, S., Tudor Jones, A.A., Fickel, U., Münchau, A., Köppen, J.A., Gerloff, C., Westphal, M., Buhmann, C., *et al.* (2014). Activity Parameters of Subthalamic Nucleus Neurons Selectively Predict Motor Symptom Severity in Parkinson's Disease. The Journal of Neuroscience 34, 6273-6285.

Shimamoto, S.A., Ryapolova-Webb, E.S., Ostrem, J.L., Galifianakis, N.B., Miller, K.J., and Starr, P.A. (2013). Subthalamic Nucleus Neurons Are Synchronized to Primary Motor Cortex Local Field Potentials in Parkinson's Disease. The Journal of Neuroscience 33, 7220-7233.

Silberstein, P., Kühn, A.A., Kupsch, A., Trottenberg, T., Krauss, J.K., Wöhrle, J.C., Mazzone, P., Insola, A., Di Lazzaro, V., Oliviero, A., *et al.* (2003). Patterning of globus pallidus local field potentials differs between Parkinson’s disease and dystonia. Brain 126, 2597-2608.

Starr, P.A., Subramanian, T., Bakay, R.A.E., and Wichmann, T. (2000). Electrophysiological localization of the substantia nigra in the parkinsonian nonhuman primate. Journal of Neurosurgery 93, 704-710.

Steigerwald, F., Pötter, M., Herzog, J., Pinsker, M., Kopper, F., Mehdorn, H., Deuschl, G., and Volkmann, J. (2008). Neuronal Activity of the Human Subthalamic Nucleus in the Parkinsonian and Nonparkinsonian State. Journal of Neurophysiology 100, 2515-2524.

Stein, E., and Bar-Gad, I. (2013). Beta oscillations in the cortico-basal ganglia loop during parkinsonism. Experimental Neurology 245, 52-59.

Swann, N.C., de Hemptinne, C., Miocinovic, S., Qasim, S., Wang, S.S., Ziman, N., Ostrem, J.L., San Luciano, M., Galifianakis, N.B., and Starr, P.A. (2016). Gamma Oscillations in the Hyperkinetic State Detected with Chronic Human Brain Recordings in Parkinson's Disease. The Journal of Neuroscience 36, 6445-6458.

Szeszko, P.R., Ardekani, B.A., Ashtari, M., and et al. (2005). White matter abnormalities in obsessive-compulsive disorder: A diffusion tensor imaging study. Archives of General Psychiatry 62, 782-790.

Tarsy , D., and Simon , D.K. (2006). Dystonia. New England Journal of Medicine 355, 818-829.

Tass, P.A., Qin, L., Hauptmann, C., Dovero, S., Bezard, E., Boraud, T., and Meissner, W.G. (2012). Coordinated reset has sustained aftereffects in Parkinsonian monkeys. Annals of Neurology 72, 816-820.

Telkes, I., Jimenez-Shahed, J., Viswanathan, A., Abosch, A., and Ince, N.F. (2016). Prediction of STN-DBS Electrode Implantation Track in Parkinson's Disease by Using Local Field Potentials. Frontiers in Neuroscience 10, 198.

Terman, D., Rubin, J.E., Yew, A.C., and Wilson, C.J. (2002). Activity Patterns in a Model for the Subthalamopallidal Network of the Basal Ganglia. The Journal of Neuroscience 22, 2963-2976.

Utter, A.A., and Basso, M.A. (2008). The basal ganglia: An overview of circuits and function. Neuroscience & Biobehavioral Reviews 32, 333-342.

van Wijk, B.C.M., Beudel, M., Jha, A., Oswal, A., Foltynie, T., Hariz, M.I., Limousin, P., Zrinzo, L., Aziz, T.Z., Green, A.L., *et al.* Subthalamic nucleus phase-amplitude coupling correlates with motor impairment in Parkinson's disease. Clinical Neurophysiology.

van Wijk, B.C.M., Beudel, M., Jha, A., Oswal, A., Foltynie, T., Hariz, M.I., Limousin, P., Zrinzo, L., Aziz, T.Z., Green, A.L., *et al.* (2016). Subthalamic nucleus phase–amplitude coupling correlates with motor impairment in Parkinson's disease. Clinical Neurophysiology 127, 2010-2019.

Vanegas-Arroyave, N., Lauro, P.M., Huang, L., Hallett, M., Horovitz, S.G., Zaghloul, K.A., and Lungu, C. (2016). Tractography patterns of subthalamic nucleus deep brain stimulation. Brain.

Voges, J., Volkmann, J., Allert, N., Lehrke, R., Koulousakis, A., Freund, H.-J., and Sturm, V. (2002). Bilateral high-frequency stimulation in the subthalamic nucleus for the treatment of Parkinson disease: correlation of therapeutic effect with anatomical electrode position. Journal of Neurosurgery 96, 269-279.

Walker, H.C., Huang, H., Gonzalez, C.L., Bryant, J.E., Killen, J., Cutter, G.R., Knowlton, R.C., Montgomery, E.B., Guthrie, B.L., and Watts, R.L. (2012). Short latency activation of cortex during clinically effective subthalamic deep brain stimulation for Parkinson's disease. Movement Disorders 27, 864-873.

Wang, J., Hirschmann, J., Elben, S., Hartmann, C.J., Vesper, J., Wojtecki, L., and Schnitzler, A. (2014). High-frequency oscillations in Parkinson's disease: Spatial distribution and clinical relevance. Movement Disorders 29, 1265-1272.

Weinberger, M., Hutchison, W.D., Alavi, M., Hodaie, M., Lozano, A.M., Moro, E., and Dostrovsky, J.O. (2012). Oscillatory activity in the globus pallidus internus: Comparison between Parkinson's disease and dystonia. Clinical Neurophysiology 123, 358-368.

Weinberger, M., Mahant, N., Hutchison, W.D., Lozano, A.M., Moro, E., Hodaie, M., Lang, A.E., and Dostrovsky, J.O. (2006). Beta oscillatory activity in the subthalamic nucleus and its relation to dopaminergic response in Parkinson's disease. Journal of Neurophysiology 96, 3248-3256.

Weiss, D., Klotz, R., Govindan, R.B., Scholten, M., Naros, G., Ramos-Murguialday, A., Bunjes, F., Meisner, C., Plewnia, C., Krüger, R., and Gharabaghi, A. (2015). Subthalamic stimulation modulates cortical motor network activity and synchronization in Parkinson's disease. Brain 138, 679-693.

Whitmer, D., de Solages, C., Hill, B.C., Yu, H., Henderson, J.M., and Bronte-Stewart, H. (2012). High frequency deep brain stimulation attenuates subthalamic and cortical rhythms in Parkinson's disease. Frontiers in Human Neuroscience 6.

Whitwell, J.L., Avula, R., Master, A., Vemuri, P., Senjem, M.L., Jones, D.T., Jack Jr, C.R., and Josephs, K.A. (2011). Disrupted thalamocortical connectivity in PSP: A resting-state fMRI, DTI, and VBM study. Parkinsonism & Related Disorders 17, 599-605.

Williams, D., Tijssen, M., van Bruggen, G., Bosch, A., Insola, A., Di Lazzaro, V., Mazzone, P., Oliviero, A., Quartarone, A., Speelman, H., and Brown, P. (2002). Dopamine-dependent changes in the functional connectivity between basal ganglia and cerebral cortex in humans. Brain 125, 1558-1569.

Winestone, J.S., Zaidel, A., Bergman, H., and Israel, Z. (2012). The use of macroelectrodes in recording cellular spiking activity. Journal of Neuroscience Methods 206, 34-39.

Witt, K., Granert, O., Daniels, C., Volkmann, J., Falk, D., van Eimeren, T., and Deuschl, G. (2013). Relation of lead trajectory and electrode position to neuropsychological outcomes of subthalamic neurostimulation in Parkinson's disease: results from a randomized trial. Brain 136, 2109-2119.

Wu, T., and Hallett, M. (2013). The cerebellum in Parkinson's disease. Brain 136, 696-709.

Yang, A.I., Vanegas, N., Lungu, C., and Zaghloul, K.A. (2014). Beta-Coupled High-Frequency Activity and Beta-Locked Neuronal Spiking in the Subthalamic Nucleus of Parkinson's Disease. The Journal of Neuroscience 34, 12816-12827.

Zaidel, A., Spivak, A., Grieb, B., Bergman, H., and Israel, Z. (2010). Subthalamic span of β oscillations predicts deep brain stimulation efficacy for patients with Parkinson's disease. Brain 133, 2007-2021.

Zrinzo, L., Foltynie, T., Limousin, P., and Hariz, M. (2012). Image-verified deep brain stimulation reduces risk and cost with no apparent impact on efficacy. Movement Disorders 27, 1585-1586.

5. Acknowledgement

I would like to thank my PhD supervisor, Prof. Dr. Alireza Gharabaghi, who has supported me throughout my thesis. I would like to thank Dr. Florian Grimm, Dr. Georgios Naros, Simeon Knieling and Kousik Sarathy, S for their support with data acquisition in the operation room, and Dr. Robert Bauer for his valuable statistical advice. The author also wants to thank the members of the advisory committee, Prof. Dr. Christoph Braun and Prof. Dr. Ulf Ziemann for their helpful suggestions and, Dr. Paolo Belardinelli for his helpful comments.

Last but not the least, I would like to offer my sincerest gratitude to my partner and parents who continuously support me without question.

6. List of appended manuscripts and contributions

1. **Subthalamic cross-frequency coupling mediates direct cortico-subcortical connectivity in Parkinson's disease (Azodi-Avval, R., and Gharabaghi, A., pending submission)**

   Contributions:

   R. Azodi-Avval: Study design. Data acquisition including local field potentials and electroencephalogram. Data analysis: phase coherence, analysis of power spectrum and phase amplitude coupling, statistical analysis. Writing the methods and results parts.

   A. Gharabaghi: Idea and conceptualization of the study. Study design. Data acquisition: planning surgical trajectory, defining targeting region, surgical procedure, defining recording strategy. Writing the introduction and discussion.

2. **Spatial specificity of beta oscillations and cortico-subthalmic connectivity in Parkinson's disease (Azodi-Avval, R., and Gharabaghi, A., pending submission)**

   Contributions:

   Azodi-Avval: Study design. Data acquisition including local field potentials and electroencephalogram. Data analysis: phase coherence, analysis of power spectrum and phase amplitude coupling, statistical analysis, Matlab computer code for online power and phase coherence calculation during surgery. Writing the manuscript.

   Gharabaghi: Idea and conceptualization of the study. Study design. Data acquisition: planning surgical trajectory, defining targeting region, surgical procedure, defining recording strategy. Editing the manuscript.

3. **Subthalamic resonance properties predict cortico-subcortical motor network connectivity and deep brain stimulation effects in Parkinson's disease (Azodi-Avval, R., and Gharabaghi, A., pending submission)**

   Contributions:

   Azodi-Avval: Study design. Concept of the resonance. Data acquisition including local field potentials and electroencephalogram. Data analysis: phase coherence, analysis of power spectrum and phase amplitude coupling, statistical analysis, Matlab computer code for online power and phase coherence calculation during surgery. Writing the manuscript.

   Gharabaghi: Idea and conceptualization of the study. Study design. Data acquisition: planning surgical trajectory, defining targeting region, surgical procedure, defining recording strategy. Editing the manuscript.

4. **Phase-dependent modulation as a novel approach to therapeutic brain stimulation (Azodi-Avval, R., and Gharabaghi, A. (2015). Phase-dependent modulation as a novel approach for therapeutic brain stimulation. Frontiers in Computational Neuroscience 9)**

   Contributions:

   Azodi-Avval: Study design. Concept of the mathematical modelling. Data acquisition including local field potentials. Data analysis: phase coherence, analysis of power spectrum, statistical analysis. Writing the methods and results parts.

   Gharabaghi: Idea and conceptualization of the study. Study design. Data acquisition: planning surgical trajectory, defining targeting region, surgical procedure, defining recording strategy. Writing the introduction and discussion.

Subthalamic cross-frequency coupling mediates direct cortico-subcortical connectivity in Parkinson's disease

Ramin Azodi-Avval, Alireza Gharabaghi*

Division of Functional and Restorative Neurosurgery, and Centre for Integrative Neuroscience, Eberhard Karls University Tuebingen, Germany

* Correspondence: Prof. Dr. Alireza Gharabaghi, Division of Functional and Restorative Neurosurgery, Eberhard Karls University, Otfried-Mueller-Str.45, 72076 Tuebingen, Germany, Tel: +49 7071 29 83550, Fax: +49 7071 29 25104, E-Mail address: alireza.gharabaghi@uni-tuebingen.de

Running title: Biomarker for direct cortico-subcortical connectivity

Keywords: cortico-subcortical connectivity; hyperdirect pathway; phase-amplitude coupling; subthalamic nucleus; Parkinson's disease

Abstract

Deep brain stimulation (DBS) of the subthalamic nucleus (STN) in Parkinson's disease mediates its effects as a network-modulating therapy by influencing cortical oscillatory activity via cortico-subthalamic pathways. A STN marker for this hyperdirect pathway has not yet been found. Using a novel mapping technique, we demonstrated that the subthalamic spot of maximum beta-coupled high-frequency oscillations (B-HFO), but not the more dorsally located spot of peak beta oscillations, correlated with cortico-subthalamic phase coupling to the ipsilateral motor cortex. In a second line of evidence, focal electrical stimulation revealed that the highest short-latency cortical-evoked potentials projecting to the ipsilateral motor cortex could be induced at the spot of highest B-HFO in the STN as well. Moreover, the cortico-subthalamic synchronization correlated with the severity of motor symptoms. These converging findings suggest that B-HFO may serve as local markers of the hyperdirect pathway between motor cortex and STN.

Introduction

Subthalamic nucleus (STN) pathophysiology often correlates with the clinical outcome of deep brain stimulation (DBS) in Parkinson's disease (PD) (Kühn et al., 2008; Kühn et al., 2006; Kühn et al., 2009; Ray et al., 2008). Increased beta oscillations (BO, 13-35 Hz) have been detected in the dorsal part of the STN and the power in this frequency-band is known to correlate with postoperative improvement (Zaidel et al., 2010). More recently, high-frequency oscillations (HFO, >150 Hz) have been associated with PD symptoms, e.g. via an inverse correlation with akinesia (Wang et al., 2014), and were also shown to peak in the dorsal STN (Yang et al., 2014). These HFO might couple to lower frequency oscillations and reveal a statistical relationship between phase and amplitude in two different frequency bands (cross-frequency coupling). This phase amplitude coupling (PAC) may refer to different phenomena, i.e. when the phase of subthalamic BO modulates the amplitude of HFO (B-HFO) in the STN (López-Azcárate et al., 2010; Özkurt et al., 2011; Yang et al., 2014), or when the phase of cortical BO modulates broadband gamma oscillations in the cortex (de Hemptinne et al., 2013; Qasim et al., 2016). Although subthalamic B-HFO are found throughout the STN (López-Azcárate et al., 2010; Yang et al., 2014), they peak in the dorsal STN (Yang et al., 2014) like BO (Holdefer et al., 2010; Steigerwald et al., 2008).

One parallel line of research indicates that the dorsal STN not only hosts the local physiological markers BO and B-HFO, but also shows significant anatomical connectivity with the ipsilateral motor cortex (M1) via a direct connection. This connection, known as the hyperdirect pathway, is demonstrated in tracer studies in nonhuman primates (Haynes and Haber, 2013). These observations tally with postoperative physiological recordings using externalized DBS electrodes for simultaneous recordings of local field potentials (LFPs) and magnetoencephalography (MEG) in PD patients. In these LFP-MEG studies, the highest cortico-subthalamic coupling (CSC) was found in the beta band between the dorsal STN and the M1, suggesting that the hyperdirect pathway is involved (Hirschmann et al., 2011). This CSC was measured at a higher beta-frequency (21-35Hz)

(Litvak et al., 2011; Oswal et al., 2016; van Wijk et al., 2016) than the maximum subthalamic power (13-20 Hz) opening the possibility that they are involved in different cortico-basal ganglia loops.

Furthermore, recent evidence suggests that DBS of the STN in Parkinson's disease mediates its effects by modulating cortical oscillatory activity, presumably via a direct cortico-subthalamic connection (de Hemptinne et al., 2015; Kuriakose et al., 2010; Li et al., 2012). However, little is known about the spatio-temporal interaction between the local STN markers (BO and B-HFO) and their involvement in the coherent loops connected to the cortex (CSC). BO and B-HFO, which lie in close proximity to each other in the dorsal STN, cannot be disentangled using standard postoperative measurements with externalized DBS electrodes, since they provide poor spatial resolution and their positions are fixed (Fogelson et al., 2006; Hirschmann et al., 2011; Kato et al., 2015; Lalo et al., 2008; Litvak et al., 2011; Oswal et al., 2016; Whitmer et al., 2012; Williams et al., 2002). By contrast, intraoperative electrophysiological recordings during DBS surgery enable us to compile a highly precise mapping of the STN region in a stepwise manner on a sub-millimeter scale, but are limited with regard to simultaneous cortical recordings. In the few reports in which cortical physiology is evaluated during STN surgery (de Hemptinne et al., 2013; Shimamoto et al., 2013; Whitmer et al., 2012) it has not yet been combined with high-precision mapping of the STN to unravel the connectivity of different local STN markers to cortical areas. Our intention was to close this gap. We hypothesized that combined EEG and stepwise LFP recordings in the STN of PD patients during implantation of DBS electrodes unravels BO and B-HFO in the dorsal STN, thus enabling us to examine their spatial specificity as biomarkers for direct cortico-subcortical connectivity. Furthermore, we reasoned that lower and upper beta-frequency bands are differently involved in this cortico-subcortical connectivity. Moreover, when applied at the different levels of the dorsal STN during simultaneous recordings of cortical evoked potentials, we expected focal electrical stimulation to provide a complementary measure of connectivity to verify the functional relevance of the physiological biomarkers in the STN.

Results

The patients enrolled in this study were examined before surgery using the motor part of the Unified Parkinson's Disease Rating Scale (UPDRS III) and by applying an L-Dopa test (medication "ON" and "OFF"). The mean UPDRS III score was 25.5±6.15 and 40±8.49 in the ON state and OFF states, respectively. The clinical information, which was assessed on average 4.5±1.92 months before surgery, is summarized in Table 1. Intraoperative recordings during DBS surgery were performed in 15 subthalamic nuclei of 12 PD patients The calculation of the beta band showed a mean peak frequency of 19.93±3.59 Hz, with a different power distribution as a function of depth (Fig. 2A). Comparative analysis of all recordings of the dorsal and the ventral part revealed a significantly higher average of power ($p = 0.004$; Mann–Whitney U test) for the dorsal STN (Fig. 2B).

Phase-amplitude coupling in STN

A calculation of the cross-frequency coupling (i.e. PAC) between the phase of lower frequencies (10-40 Hz) and the amplitude of higher frequencies (100-350 Hz) across all STN depths showed spatial specificity with regard to the power spectrum, PAC and preferred coupling phase (Fig. 3A). On the group level, significant PAC was observed between the phase of 26.23±3.70 Hz and the amplitude of 260.92±41.05 Hz oscillations. These beta-coupled high-frequency oscillations (B-HFO) peaked in the dorsal part of the STN at 1.54±0.46 mm below the STN entry (Fig. 3B). Comparative analysis of all recordings of pre-STN, dorsal and ventral STN revealed a significantly higher average B-HFO in the dorsal STN than in the pre-STN and ventral STN, respectively (Fig. 3B). At the STN depth of maximum PAC, the high frequency amplitude oscillated consistently at a specific beta phase (Fig. 3C), i.e. the mean preferred coupling phase was at -38.468±16.484°.

Cortico-subcortical connectivity

Functional connectivity analysis with phase coherence showed significant CSC in the beta-band (25.07±3.64 Hz, Fig. 4A). This beta CSC revealed a specific spatial pattern at the cortical level, (electrodes projecting to the

medial motor cortex of the ipsilateral hemisphere, i.e. the C1/3 electrodes, Fig. 4B) as well as within the STN (peaking in the dorsal part of the STN 1.65±0.43 mm below the STN entry).

Effective connectivity analysis with PSI confirmed the ipsilateral medial motor area as the region with the highest cortico-subcortical coherence with the ipsilateral STN and also revealed an information flow from cortex to STN in the beta band. The ipsilateral PSI of the central cortical region was significantly higher than the corresponding contralateral PSI ($p = 0.01$; Mann–Whitney U test).

The effective connectivity was further characterized by electrical stimulation when passing through the dorsal STN in steps of 0.5 mm to detect (hyper)direct cortico-subcortical connectivity. The short latency cortical-evoked potential (CEP) was identified 2.54±0.73 ms after stimulation, indicating a direct pathway (Fig. 5A) with a specific spatial pattern at both subcortical and cortical level. The hyperdirect pathway peaked in the dorsal part of the STN and projected to central electrodes of the ipsilateral hemisphere (Fig. 5B). Group results with a total of 1,927 stimuli revealed topographic specificity of CEP on the cortical level, i.e. that CEP projected to C3 (Fig. 5C). In the STN, the sites that led to the highest CEP also revealed the strongest local PAC (i.e. B-HFO) and the highest connectivity (i.e. dWPLI) to the motor cortex (Fig. 5D).

Beta power, phase-amplitude coupling and phase coherence

The prominent BO within the STN (19.93±3.60 Hz) peaked at the STN entry and decreased gradually from the dorsal to the ventral border, whereas the average beta-coupled (26.23±3.70 Hz) HFO peaked at 1.54±0.46 mm below the STN entry. Statistical analysis revealed that the peak beta frequencies of both B-HFO (26.23±3.70 Hz) and CSC (25.07±3.64 Hz) differed significantly from those of BO ($P= 0.01$; Mann–Whitney U test and $P= 0.01$; Mann–Whitney U test, respectively), whereas the peak beta frequencies of B-HFO and CSC did not differ significantly from each other ($P= 0.9$; Mann–Whitney U test). In each patient, the site of maximum B-HFO ($r=0.76$; $P=0.003$; Spearman test) in the STN – but not the site of peak BO ($r=-0.44$; $P=0.14$; Spearman test) – correlated highly with the site of maximum cortico-subcortical phase coherence to the ispilateral M1 (Fig. 6B). On the group level, the site of maximum B-HFO (1.54±0.46 mm below STN entry) also differed significantly

from the site of peak BO (0.29±0.28 mm below STN entry; P= 0.001; Mann–Whitney U test). Table 2A summarizes the relationship between the different physiological markers. Notably, the cortico-subthalamic synchronization was the only physiological marker (Table 2B) that correlated significantly (r=0.72, P=0.014) with the severity of motor symptoms in the medication OFF state (Fig. 6).

Phase-amplitude coupling in the cortex and between cortex and STN

The maximum cortical PAC, i.e. the beta-coupled (19.92±0.20 Hz) broadband gamma oscillations (108.29±16.66), was located in M1. However, in 11 out of 12 patients, it was located more laterally than the cortico-subcortical connectivity measures, which projected to C1/3 (Fig. 4C). This cortical PAC showed a consistently preferred coupling phase at a mean of -12.36 ± 18.45°. Furthermore, effective connectivity analysis within the central cortical areas with PSI revealed an information flow from the lateral to the medial M1 in the beta band (25.17±2.79 Hz).

Notably, the highest long-range PAC, i.e. the B-HFO between ipsilateral cortical BO (27.22±4.07 Hz) and high-frequency STN activity, also projected to lateral M1 in 9 out of 12 patients (Fig. 4D, E). This long-range PAC showed a consistently preferred coupling phase at a mean of 5.49± 42.56°. Interestingly, the high-frequency activity of this cortico-subcortical PAC, i.e. of the long-range B-HFO, was located at the same site within the STN as the maximum PAC in the STN, i.e. local B-HFO.

Direct and indirect cortico-subcortical loops

In summary, the results indicate two connectivity patterns: (i) A direct connection between the medial M1 and STN (at the site of subthalamic PAC, i.e. local B-HFO) captured via phase coherence (dWPLI), phase-slope index (PSI) and short-latency cortical evoked potential (CEP). (ii) An indirect connection between M1 and STN, which is captured via long-range phase-amplitude coupling (PAC, i.e. long-range B-HFO) between cortex (at the site of cortical PAC, i.e. beta-coupled broadband gamma oscillations) and STN (at the site of

subthalamic PAC, i.e. local B-HFO) and which is – at least partly – mediated via information flow (PSI) from lateral to medial M1. Both of these loops converge on local B-HFO in the STN.

Discussion

Deep brain stimulation of the STN is an established therapy in movement disorders such as Parkinson's disease (Krack and Hariz, 2013; Lozano and Lipsman, 2013; Schuepbach et al., 2013). The mechanism of action has, however, still not been completely elucidated (Chiken and Nambu, 2015; Little and Brown, 2014). Previous findings in animals (Gradinaru et al., 2009; Li et al., 2012) suggest that antidromically activated responses in the motor cortex play an important role in mediating the beneficial effects of STN-DBS in PD. Human DBS studies measuring short-latency cortical evoked potentials following STN stimulation also indicate such a direct cortico-subcortical connection (Kuriakose et al., 2010; Walker et al., 2012). In this context, ex vivo tracing studies in animals revealed the hyperdirect pathway as the anatomical substrate for such a direct link between the STN and the motor cortex (Haynes and Haber, 2013). These observations were paralleled by imaging findings in humans, showing that these regions are also directly connected (Brunenberg et al., 2012; Kahan et al., 2014). However, specific knowledge about a physiological marker within the STN that reflects the functional substrate for this cortico-subcortical pathway is still somewhat limited. In this study, we provide converging evidence suggesting that cross-frequency coupling, i.e. B-HFO, in the STN is a physiological biomarker of the hyperdirect pathway.

Biomarkers in the subthalamic nucleus

Although different local STN markers, such as beta oscillations (Zaidel et al., 2010; Schlaier et al., 2013), high-frequency oscillations (López-Azcárate et al., 2010; Özkurt et al., 2011; Wang et al., 2014) and their coupling, i.e. B-HFO (de Hemptinne et al., 2013; de Hemptinne et al., 2015; López-Azcárate et al., 2010; Özkurt et al., 2011) are already known to be prominent in the dorsal part of the STN, their mutual relation is not yet known..

The B-HFO observed in the dorsal STN may be related to different PAC mechanisms. An increasing number of studies in PD patients show that low-frequency oscillations can modulate high-frequency oscillations by means of phase-amplitude coupling between local and distant sites of interconnected cortical-basal ganglia loops (de Hemptinne et al., 2015; Swann et al., 2015; Yang et al., 2014). Since a comparison of STN spike activity and local field potentials revealed that beta-locked STN neurons did not correlate with the B-HFO, the latter are probably not a purely "local" phenomenon (Yang et al., 2014).

In our study, the maximum BO and B-HFO were separated in the dorsal STN spectrally, with peaks in the lower (13-20 Hz) and upper (21-35 Hz) beta-frequency range, respectively. A spatial separation between BO and B-HFO in the STN was also apparent, with a more dorsal location of the former. These findings suggest that BO and B-HFO are involved in segregated basal-ganglia and cortico-subcortical loops; a hypothesis which might be supported by the observed differences in peak frequencies within these loops serving indirect and hyperdirect pathways (Oswal et al., 2016). These different cortico-subcortical loops allow for sequential information processing, i.e. only the selected motor program is initiated, executed and terminated at the selected timing (Deffains et al., 2016; Jahanshahi et al., 2015; Nambu et al., 2002).

Functional connectivity

We observed that the STN-M1 synchronization was strongest in the upper beta-range (25.07±3.64 Hz) and correlated with the beta-frequency range of both the *long-range* B-HFO and the *local* B-HFO, but not with the peak frequency within the STN (19.97±3.6 Hz). These findings tally with postoperative studies using simultaneous MEG and STN-LFP recordings in DBS patients (Hirschmann et al., 2011; Litvak et al., 2011; van Wijk et al., 2016). They suggest that the frequency of cortico-STN coherence with the medial and lateral ipsilateral (pre)motor cortex usually lies in the upper beta band (~25 Hz) and therefore differs from the average beta oscillation (~17 Hz) in the STN.

Reports evaluating the cortical physiology with electrocorticography during STN surgery confirmed this beta-CSC and revealed additional cortical-STN drive in the broad gamma band (de Hemptinne et al., 2013).

Interestingly, the latter study also revealed a PAC from the STN to the motor cortex, but not in the other direction, as was to be expected from the CSC findings of that particular study as well as of preceding studies. This might be related to the fact that the DBS electrodes used for these connectivity measurements were of poor spatial resolution, i.e. there was no specific spotting of the local B-HFO with high-precision STN mapping. This very technique enabled us to demonstrate that the locations of the B-HFO and the CSC in the dorsal STN are highly correlated, thus suggesting that the local PAC is a marker of the hyperdirect pathway connected to M1.

Effective connectivity

In a second line of evidence, while studying effective cortico-subcortical connectivity, i.e. the directionality of interaction (PSI), we detected an information flow from M1 to STN. This suggests that the B-HFO in the STN is driven by motor cortex activity rather than by basal-ganglia loops. Moreover, the topographical specificity of this connectivity in the motor cortex matches earlier MEG source localization of cortico-STN coherence well, indicating that precisely this cortical area is the origin of the hyperdirect pathway (Hirschmann et al., 2011).

Finally, when focal electrical stimulation was applied at the spot of maximum B-HFO in the dorsal STN, which was also the spot with the maximum cortico-subcortical connectivity, the induced cortical-evoked potentials showed the same cortical topography in the ipsilateral medial M1 as the other connectivity measures. When stimulating across the dorsal STN in steps of 0.5 mm, this spot of maximum B-HFO and CSC also revealed the highest amplitudes of cortical-evoked potentials projecting to the cortex at a short latency, which is suggestive of a (hyper)direct connection. The simultaneous activation of prefrontal regions is possibly related to the spread of stimulation current to those associative and limbic regions of the STN that have connections with prefrontal areas. This could be due to the rather non-focal characteristics of electrical as opposed to optogenetic stimulation (Gradinaru et al., 2009). Moreover, recent studies in non-human primates (Haynes and Haber, 2013) and humans (Alkemade and Forstmann, 2014) question the existence of distinct anatomical subdivisions, proposing instead that the functional zones within the STN overlap. However, the most highly evoked potential was always found in the motor area of the cortex.

Notably, a more laterally located M1 spot revealed local PAC on the one side (similar to recent reports by (Swann et al., 2015) and connectivity to STN on the other, captured via long-range PAC. However, this connection seems to be rather indirect since the effective connectivity measures projected to more medially located areas in M1. Importantly, the present study demonstrates that B-HFO in the STN is connected to both of these direct and indirect cortico-subcortical loops and may thereby serve as network hub.

Clinical relevance

There is increasing evidence to suggest that DBS of the STN is a network-modulating therapy that influences wide-spread cortical activity and synchronization in PD (Dejean et al., 2009; Weiss et al., 2015). Several lines of research have reported pathologically altered cortical physiology (Herz et al., 2014) and cortico-subcortical coupling in PD patients (Litvak et al., 2011; Williams et al., 2002), 6-ODHA-treated rats (Magill et al., 2001; Sharott et al., 2005) and MPTP-treated monkeys (Devergnas et al., 2014). In parallel to these electrophysiological findings, recent fMRI studies in PD patients also suggest that modulated functional connectivity takes place between the cortical areas involved in motor processes and the STN (Fernández-Seara et al., 2015).

In the present study, we captured local PAC and long-range PAC, both of which were reduced by therapeutic interventions in PD, i.e. the B-HFO in the STN following Levodopa administration (López-Azcárate et al., 2010) and cortical beta-coupled gamma oscillations in M1 during DBS (de Hemptinne et al., 2015). This indicates a pathophysiological origin of this neural synchronization and may suggest subthalamic PAC as a biomarker for treatment monitoring and modulation.

We detected a positive correlation between the strength of cortico-subcortical phase coupling in the upper beta band and the severity of motor symptoms (UPDRS III). This finding is consistent with two recent studies in primates (Devergnas et al., 2014) and humans (Kato et al., 2015) in which a correlation between STN-M1

coherence and severity of Parkinsonism was also found. As in our study, both the clinical evaluation and the recording of STN-M1 connectivity were obtained in resting state and in the medication OFF state. Their interaction might reflect the pathological default network in PD.

Interestingly, recent findings indicate that the cortical area with the highest STN-M1 beta band connectivity showed the most obvious power reduction during subthalamic DBS (Whitmer et al., 2012). In the same vein, recent work by de Hemptinne and colleagues revealed that exaggerated PAC in the M1 of PD patients might serve as a more robust biomarker than cortical beta power (de Hemptinne et al., 2015). Along these lines, we recently demonstrated that subthalamic stimulation facilitated movement-related desynchronization of widespread cortical activity and predicted clinical improvement from DBS (Weiss et al., 2015).

Future Perspectives

At present, the standard DBS electrode design limits the differential modulation of the reported STN markers. Since BO, HFO and B-HFO are all most prominent in the dorsal STN (de Hemptinne et al., 2013; López-Azcárate et al., 2010; Özkurt et al., 2011; Schlaier et al., 2013; Wang et al., 2014; Yang et al., 2014; Zaidel et al., 2010), i.e. within an area of about 2 mm length, they cannot be targeted specifically with the large circular electrode contacts (with a length of 1.5 mm) used nowadays in clinical practice. However, recent technological refinements have allowed for directional steering of the stimulation in pilot studies to achieve a wider therapeutic window in this patient group (Contarino et al., 2014; Pollo et al., 2014). Such increased spatial accuracy of stimulation would, for instance, enable us to specifically target the spot of B-HFO instead of the spot of peak BO in future. The clinical relevance of these markers could then be established in more powered studies while potentially reducing stimulation-induced side effects and/or addressing different PD symptoms with multi-contact DBS (Weiss et al., 2013) or phase-specific modulation (Azodi-Avval and Gharabaghi, 2015).

Conclusion

We have demonstrated for the first time that local B-HFO serve as subthalamic markers of the hyperdirect pathway between M1 and STN. By taking stepwise LFP recordings across the STN, we separated the respective peak of the B-HFO both spatially and spectrally from the peak of the local beta oscillations within the dorsal STN. More specifically, the motor cortical area with maximum cortico-subcortical phase coherence in the beta-band controlled the activity of the STN beta activity. Furthermore, the spot of maximum phase amplitude coupling within the STN, i.e. of the *local* B-HFO, was also the spot of *long-range* B-HFO between cortex and STN. These cumulative findings suggest that local B-HFO in the STN is induced by cortical activity rather than by basal-ganglia loops and might lead to refined targeting of DBS in Parkinson's disease in the future.

Materials and Methods

Patients and neurosurgical procedure

We recorded spontaneous brain activity from 12 PD patients (two females; age: 69.42±1.99 years, mean ± STD; disease duration: 13.42 ± 2.15 years) during implantation of DBS electrodes in the STN after overnight withdrawal of dopaminergic medication (Table 1). Intraoperative propofol medication was discontinued at least 30 minutes before electrophysiological recordings were initiated (Raz et al., 2008). The STN was localized via direct targeting on preoperative magnetic resonance imaging (Foltynie et al., 2011) and then intraoperatively by its firing pattern and background activity (Shamir et al., 2012; Winestone et al., 2012). The placement of the DBS electrode in the STN was confirmed by postoperative MRI; coordinates of the clinically applied active contact (DBS lead model 3389, Medtronic Inc., Minneapolis, USA) were referenced to the mid-commissural point: x = 12.91 ± 0.94 (mean ± SEM), y = 3.31 ± 2.54, z = 3.75 ± 2.54 mm for the left hemisphere, and x = 12.1 ± 1.13, y = 2.16 ± 0.66, z = 3.75 ± 0.83 mm for the right hemisphere. The study was conducted with the patients' informed consent and in accordance with the guidelines approved by the local ethics committee of the University Hospital Tuebingen.

Data collection and preprocessing

Cortical and subcortical electrophysiological signals were recorded in awake patients at rest. We evaluated LFPs with intraoperative test electrodes and up to three trajectories according to the ben-gun setup, (microTargeting FHC Inc., USA) passing through the STN region in steps of 0.5 mm, together with simultaneous scalp EEG with surface electrodes (Ag/AgCl electrodes, MedCaT GmbH, Netherlands) covering the head around the burr holes in accordance with the international 10–20 EEG system (Alpha-Omega, Nazareth, Israel). We recorded more than one trajectory in three of the twelve subjects. The clinically most effective trajectory was chosen for experimentation in these cases. The non-sterile EEG electrodes were positioned before surgery and covered intraoperatively with the conventional sterile surgical cover. We did not

apply the *micro tip* of the test electrode for our intraoperative measurements, but the non-insulated *macro tip* of the cannula, which is also known as the mactroelectrode. While its impedances are similar to those of the chronic electrode, this mactroelctrode can also record spike activity (Winestone et al., 2012). It has a surface area of approximately 12 mm^2 (diameter: ~1.0 mm; length: ~1.0 mm), whereas one contact of the chronic electrode has a surface area of 22 mm^2 (diameter, 1.27 mm; length, 1.5 mm). On the basis of these different surfaces, we expected to achieve a higher spatial resolution with the applied approach (Kent and Grill, 2014).

LFPs were recorded from -7 mm to +8 mm relative to the dorsal STN border (Fig. 1B) while EEG was recorded at 19 to 29 sensors covering central, parietal and a part of frontal regions (Fig. 1A). Although EEG electrodes were placed in a standardized clinical fashion, their exact position in relation to the underlying cortical anatomy was not clear, since no verification was performed. We refer to the C row of electrodes as the central region or M1, even though these electrodes might also capture signals from the premotor area.

This resulted in a total of 273 LFP recording sites with a mean of 28.20±4.76 seconds of recording at each level. Since the cortical sensors (EEG) remained fixed during the progression of the subcortical sensors (LFP), the EEG signals of each side could be concatenated for further analysis (e.g. cortical PAC). This resulted in a mean of 479.4118+76.8378 seconds of recording for each side. EEG and LFPs signals were continuously sampled at 1.4 KHz and amplified by a factor of 50 and 20, respectively. The reference electrodes were attached to the ears and the ground was placed on the nasion. The impedance was set at ~1 KΩ and below 0.5 KΩ, for the intracranial and the EEG electrodes, respectively. Representative raw signals are shown in Fig. 1A. Stimulation pulses (monopolar, bi-phasic, 1 Hz, 1.5 mA and 5 Hz, 2mA, 90 μsec, current-controlled) were applied in steps of 0.5 mm at the different levels of the dorsal STN region for at least 20 s at each level while the evoked potentials were captured with the cortical EEG electrodes. Some studies applied invasive recordings with subdural electrode strips to capture cortical physiology during DBS surgery (de Hemptinne et al., 2013; Qasim et al., 2016; Whitmer et al., 2012). Notably, a recent study measured simultaneously invasive (electrocorticography) and non-invasive (EEG) recordings during surgery and demonstrated no significant differences in the signal-to-noise ratio; specifically, HFO could be detected with both methods (Burnos et al.,

2016). A simulation study (Jing et al., 2007) demonstrated furthermore that EEG potentials were not affected by the bure holes if the recordings were performed at least 40 mm away; we therefore implemented a minimum distance of 50 mm between bure holes and electrodes in our set-up..

Data analysis of EEG and LFPs were performed in Matlab (version 2012b, Mathworks, Massachusetts, USA) using custom-made scripts (https://github.com; get_wplfphase.m), and in Fieldtrip, an open source analysis toolbox (Oostenveld et al., 2011). Signals were epoched in 1 s data segments and all artifacted epochs were removed by the Fieldtrip artifact rejection method. Line noise at 50 Hz and the harmonics were removed with a notch filter. Due to movement and respiration artifacts, frequencies below 3 Hz were not taken into consideration.

LFP power analysis

Power analysis of LFPs was computed using the Hanning taper (Mitra and Pesaran, 1999), providing maximum spectral estimation. We determined the individual frequency peak (95% confidence limit within a given frequency band) in the beta band (13–35 Hz) for each STN level and then averaged the power in three contiguous bins (±1 Hz) around this peak. This average maximum value was then normalized by dividing it by the total power from 3-95 Hz. This LFP power analysis is particularly well suited for identifying the predominant oscillatory areas of the STN (Trottenberg et al., 2007; Zaidel et al., 2010) and for resolving the individual variability of frequency peaks for each patient (de Solages et al., 2010).

Cross-frequency coupling

Possible cross-frequency interactions between the phase of low frequency oscillations and the amplitude of high frequency oscillations in the STN LFPs and between EEG and STN LFPs were investigated by phase amplitude coupling (PAC). To quantify PAC, we used the modulation index (MOI) (Canolty et al., 2006). The LFP signals X(t) contain both phase and amplitude components. X(t) was filtered via convolution with complex Morlet

wavelets (width 7) to extract the instantaneous phase ($X\varphi(t)$) and amplitude ($X_{Amp}(t)$). A raw MOI value was then calculated:

$$MOI = \left| \frac{1}{N} \sum_{n=1}^{N} X_{Amp}(n) e^{-iX_{\varphi}(n)} \right| \quad (1)$$

where || denotes the absolute value. Statistical significance of MOI was estimated using temporally shuffled amplitudes, creating 200 surrogate MOI values and comparing them with raw MOI to obtain a z-score measurement (Onslow et al., 2011; Penny et al., 2008). PAC was considered significant below an alpha level of 0.05 and the false discovery rate was corrected for multiple comparisons. We calculated MOI using frequencies ranging from 10–40 Hz for the phase signals and from 100-350 Hz for amplitude in 2 Hz and 4 Hz bins, respectively. This analysis was performed across all sites and for each patient. Within the STN, we determined the maximum frequency of phase (F_{φ}) and amplitude (F_{Amp}) on the site showing the maximum MOI. The total MOI for each patient was calculated by averaging the coupling between phases and amplitudes centered around the peak frequencies across each individual STN level (de Hemptinne et al., 2013). This value was normalized from 0-1 for each patient across the STN depths (Yang et al., 2014) and later used for group analysis. We next extracted the preferred coupling phase by taking the angle of phase-locking factors on the frequency range at which PAC exhibited significant values (Lega et al., 2016). The cortical PAC was quantified with the MOI as well by frequencies ranging from 10–40 Hz for the phase signals and from 50-350 Hz for the amplitude in the same frequency resolution as indicated above.

Cortico-subcortical connectivity

To investigate the cortico-subcortical functional connectivity, the Weighted Phase Lag Index (WPLI) (Vinck et al., 2011) was calculated between EEG and LFP as a measure of phase consistency between two distal regions for each level within STN (Cohen, 2014).

$$WPLI_{EEG-LFP} = \frac{n^{-1}\sum_{n=1}^{N}\left|imag\left(S_{EEG-LFP\,n}\right)\right| sgn\left(imag\left(S_{EEG-LFP\,n}\right)\right)}{n^{-1}\sum_{n=1}^{N} imag\left(S_{EEG-LFP\,n}\right)} \quad 2$$

where *S* is the cross-spectrum density matrix, *imag* the imaginary part and *sgn* the sign function. Since this measure eliminates zero phase lag signals, it is insensitive to the volume conduction of neural activity; a common challenge during EEG recordings. Due to the small number of trials, the debiased WPLI (dWPLI) was used to provide reliable phase coherence estimation (Phillips et al., 2012; Vinck et al., 2011); for stable estimations of dWPLI, the data was epoched in half-second segments. Furthermore, this measurement is more efficient in detecting true phase interaction than common phase measurements like the imaginary part of coherence (Nolte et al., 2004). In our case, dWPLI was normalized by its standard deviation, which was computed by the jackknife method; absolute values larger than 1.96 (corresponding to $p<0.05$) were considered statistically significant (Hohlefeld et al., 2013; Luft et al., 2013; Nolte et al., 2008).

Directionality between EEG and LFP, i.e. the effective connectivity, was calculated on the basis of the phase-slope index (PSI) (Nolte et al., 2008).

$$PSI_{EEG-reference} = imag\left(\sum_{f} S^{*}_{EEG-reference}\left(f\right) S_{EEG-reference\,n}\left(f+\delta f\right)\right) \quad 3$$

where * stands for the complex conjugates and δf is the frequency resolution. Here, depending on the information flow between STN (which is taken as a reference) and cortex, PSI has a positive (direction flow from cortex to STN) or negative sign (direction flow from STN to cortex). We also studied the information flow within the central region of the cortex between lateral and medial M1. Since the more lateral EEG electrode is taken as a reference, PSI has a positive (direction flow from medial to lateral M1) or negative sign (direction flow from lateral to medial M1).

Subdivisions of STN

Previous electrophysiology studies on PD regarded the STN region with prominent beta oscillations as the motor area (Deffains et al., 2014; Holdefer et al., 2010; Novak et al., 2011; Ray et al., 2008; Steigerwald et al., 2008; Zaidel et al., 2010) and considered it differed from the associative/limbic area. Moreover, these two different subregions are topographically defined as the dorsolateral and ventromedial region, respectively, with the border running halfway along the STN (Deffains et al., 2014). This approach was also taken in the present study.

Statistical analysis

Statistical analysis was conducted using the statistics toolbox for Matlab and the level for statistical significance was defined as p=0.05. Nonparametric Mann–Whitney U test was used to compare two groups and Kruskal–Wallis ANOVA with Tukey's post hoc test was conducted to evaluate statistical differences when more than two groups were compared. Correlation analysis was performed with the Spearman's rank test. Unless otherwise stated, all values were expressed as mean ± SEM. The normalization values were calculated on the basis of the following formula;

$$\mathrm{V}' = \left(V - \min\left(V\right)\right)./\left(\max\left(V\right) - \min\left(V\right)\right), \qquad 4$$

where V is the raw vector.

Acknowledgements

RA was supported by the Graduate Training Centre of Neuroscience, International Max Planck Research School for Cognitive and Systems Neuroscience, Tuebingen, Germany. AG was supported by grants from the German Research Council [DFG EC 307], and from the Federal Ministry for Education and Research [BFNT 01GQ0761, BMBF 16SV3783, BMBF 03160064B, BMBF V4UKF014]. The authors declare that they have no competing interests.

Competing interests

The authors declare that the research was conducted in the absence of any commercial or financial relationships that could be construed as a potential conflict of interest.

References

Alkemade, A., and Forstmann, B.U. (2014). Do we need to revise the tripartite subdivision hypothesis of the human subthalamic nucleus (STN)? NeuroImage 95, 326-329.

Azodi-Avval, R., and Gharabaghi, A. (2015). Phase-dependent modulation as a novel approach for therapeutic brain stimulation. Frontiers in Computational Neuroscience 9.

Brunenberg, E.J.L., Moeskops, P., Backes, W.H., Pollo, C., Cammoun, L., Vilanova, A., Janssen, M.L.F., Visser-Vandewalle, V.E.R.M., Romeny, B.M.t.H., Thiran, J.-P., and Platel, B. (2012). Structural and Resting State Functional Connectivity of the Subthalamic Nucleus: Identification of Motor STN Parts and the Hyperdirect Pathway. Plos One 7.

Burnos, S., Fedele, T., Schmid, O., Krayenbühl, N., and Sarnthein, J. (2016). Detectability of the somatosensory evoked high frequency oscillation (HFO) co-recorded by scalp EEG and ECoG under propofol. NeuroImage: Clinical 10, 318-325.

Canolty, R.T., Edwards, E., Dalal, S.S., Soltani, M., Nagarajan, S.S., Kirsch, H.E., Berger, M.S., Barbaro, N.M., and Knight, R.T. (2006). High Gamma Power Is Phase-Locked to Theta Oscillations in Human Neocortex. Science 313, 1626-1628.

Chiken, S., and Nambu, A. (2015). Mechanism of Deep Brain Stimulation: Inhibition, Excitation, or Disruption? The Neuroscientist.

Cohen, M. (2014). Analyzing neural time series data: theory and practice (MIT, Cambridge, MA).

Contarino, M.F., Bour, L.J., Verhagen, R., Lourens, M.A.J., de Bie, R.M.A., van den Munckhof, P., and Schuurman, P.R. (2014). Directional steering: A novel approach to deep brain stimulation. Neurology 83, 1163-1169.

de Hemptinne, C., Ryapolova-Webb, E.S., Air, E.L., Garcia, P.A., Miller, K.J., Ojemann, J.G., Ostrem, J.L., Galifianakis, N.B., and Starr, P.A. (2013). Exaggerated phase–amplitude coupling in the primary motor cortex in Parkinson disease. Proceedings of the National Academy of Sciences 110, 4780-4785.

de Hemptinne, C., Swann, N.C., Ostrem, J.L., Ryapolova-Webb, E.S., San Luciano, M., Galifianakis, N.B., and Starr, P.A. (2015). Therapeutic deep brain stimulation reduces cortical phase-amplitude coupling in Parkinson's disease. Nat Neurosci 18, 779-786.

de Solages, C., Hill, B.C., Koop, M.M., Henderson, J.M., and Bronte-Stewart, H. (2010). Bilateral symmetry and coherence of subthalamic nuclei beta band activity in Parkinson's disease. Experimental Neurology 221, 260-266.

Deffains, M., Holland, P., Moshel, S., de Noriega, F.R., Bergman, H., and Israel, Z. (2014). Higher neuronal discharge rate in the motor area of the subthalamic nucleus of Parkinsonian patients. Journal of Neurophysiology 112, 1409-1420.

Deffains, M., Iskhakova, L., Katabi, S., Haber, S.N., Israel, Z., and Bergman, H. (2016). Subthalamic, not striatal, activity correlates with basal ganglia downstream activity in normal and parkinsonian monkeys. eLife 5, e16443.

Dejean, C., Hyland, B., and Arbuthnott, G. (2009). Cortical Effects of Subthalamic Stimulation Correlate with Behavioral Recovery from Dopamine Antagonist Induced Akinesia. Cerebral Cortex 19, 1055-1063.

Devergnas, A., Pittard, D., Bliwise, D., and Wichmann, T. (2014). Relationship between oscillatory activity in the cortico-basal ganglia network and parkinsonism in MPTP-treated monkeys. Neurobiology of Disease 68, 156-166.

Fernández-Seara, M.A., Mengual, E., Vidorreta, M., Castellanos, G., Irigoyen, J., Erro, E., and Pastor, M.A. (2015). Resting state functional connectivity of the subthalamic nucleus in Parkinson's disease assessed using arterial spin-labeled perfusion fMRI. Human Brain Mapping 36, 1937-1950.

Fogelson, N., Williams, D., Tijssen, M., van Bruggen, G., Speelman, H., and Brown, P. (2006). Different functional loops between cerebral cortex and the subthalmic area in Parkinson's disease. Cerebral Cortex 16, 64-75.

Foltynie, T., Zrinzo, L., Martinez-Torres, I., Tripoliti, E., Petersen, E., Holl, E., Aviles-Olmos, I., Jahanshahi, M., Hariz, M., and Limousin, P. (2011). MRI-guided STN DBS in Parkinson's disease without microelectrode recording: efficacy and safety. Journal of Neurology, Neurosurgery & Psychiatry 82, 358-363.

Gradinaru, V., Mogri, M., Thompson, K.R., Henderson, J.M., and Deisseroth, K. (2009). Optical Deconstruction of Parkinsonian Neural Circuitry. Science 324, 354-359.

Haynes, W.I.A., and Haber, S.N. (2013). The Organization of Prefrontal-Subthalamic Inputs in Primates Provides an Anatomical Substrate for Both Functional Specificity and Integration: Implications for Basal Ganglia Models and Deep Brain Stimulation. Journal of Neuroscience 33, 4804-4814.

Herz, D.M., Florin, E., Christensen, M.S., Reck, C., Barbe, M.T., Tscheuschler, M.K., Tittgemeyer, M., Siebner, H.R., and Timmermann, L. (2014). Dopamine Replacement Modulates Oscillatory Coupling Between Premotor and Motor Cortical Areas in Parkinson's Disease. Cerebral Cortex 24, 2873-2883.

Hirschmann, J., Oezkurt, T.E., Butz, M., Homburger, M., Elben, S., Hartmann, C.J., Vesper, J., Wojtecki, L., and Schnitzler, A. (2011). Distinct oscillatory STN-cortical loops revealed by simultaneous MEG and local field potential recordings in patients with Parkinson's disease. Neuroimage 55, 1159-1168.

Hohlefeld, F.U., Huchzermeyer, C., Huebl, J., Schneider, G.H., Nolte, G., Brucke, C., Schonecker, T., Kuhn, A.A., Curio, G., and Nikulin, V.V. (2013). Functional and effective connectivity in subthalamic local field potential recordings of patients with Parkinson's disease. Neuroscience 250, 320-332.

Holdefer, R.N., Cohen, B.A., and Greene, K.A. (2010). Intraoperative Local Field Recording for Deep Brain Stimulation in Parkinson's Disease and Essential Tremor. Movement Disorders 25, 2067-2075.

Jahanshahi, M., Obeso, I., Rothwell, J.C., and Obeso, J.A. (2015). A fronto-striato-subthalamic-pallidal network for goal-directed and habitual inhibition. Nat Rev Neurosci 16, 719-732.

Jing, L., Kun, W., Shanan, Z., and Bin, H. (2007). Effects of holes on EEG forward solutions using a realistic geometry head model. Journal of Neural Engineering 4, 197.

Kahan, J., Urner, M., Moran, R., Flandin, G., Marreiros, A., Mancini, L., White, M., Thornton, J., Yousry, T., Zrinzo, L., *et al.* (2014). Resting state functional MRI in Parkinson's disease: the impact of deep brain stimulation on 'effective' connectivity. Brain.

Kato, K., Yokochi, F., Taniguchi, M., Okiyama, R., Kawasaki, T., Kimura, K., and Ushiba, J. (2015). Bilateral coherence between motor cortices and subthalamic nuclei in patients with Parkinson's disease. Clinical Neurophysiology 126, 1941-1950.

Kent, A.R., and Grill, W.M. (2014). Analysis of deep brain stimulation electrode characteristics for neural recording. J Neural Eng 11, 046010.

Krack, P., and Hariz, M.I. (2013). Deep brain stimulation in Parkinson's disease: reconciliation of evidence-based medicine with clinical practice. Lancet Neurology 12, 25-26.

Kühn, A.A., Kempf, F., Brücke, C., Gaynor Doyle, L., Martinez-Torres, I., Pogosyan, A., Trottenberg, T., Kupsch, A., Schneider, G.-H., Hariz, M.I., *et al.* (2008). High-Frequency Stimulation of the Subthalamic Nucleus Suppresses Oscillatory β Activity in Patients with Parkinson's Disease in Parallel with Improvement in Motor Performance. The Journal of Neuroscience 28, 6165-6173.

Kühn, A.A., Kupsch, A., Schneider, G.-H., and Brown, P. (2006). Reduction in subthalamic 8–35 Hz oscillatory activity correlates with clinical improvement in Parkinson's disease. European Journal of Neuroscience 23, 1956-1960.

Kühn, A.A., Tsui, A., Aziz, T., Ray, N., Brücke, C., Kupsch, A., Schneider, G.-H., and Brown, P. (2009). Pathological synchronisation in the subthalamic nucleus of patients with Parkinson's disease relates to both bradykinesia and rigidity. Experimental Neurology 215, 380-387.

Kuriakose, R., Saha, U., Castillo, G., Udupa, K., Ni, Z., Gunraj, C., Mazzella, F., Hamani, C., Lang, A.E., Moro, E., *et al.* (2010). The Nature and Time Course of Cortical Activation Following Subthalamic Stimulation in Parkinson's Disease. Cerebral Cortex 20, 1926-1936.

Lalo, E., Thobois, S., Sharott, A., Polo, G., Mertens, P., Pogosyan, A., and Brown, P. (2008). Patterns of bidirectional communication between cortex and basal ganglia during movement in patients with Parkinson disease. Journal of Neuroscience 28, 3008-3016.

Lega, B., Burke, J., Jacobs, J., and Kahana, M.J. (2016). Slow-Theta-to-Gamma Phase-Amplitude Coupling in Human Hippocampus Supports the Formation of New Episodic Memories. Cerebral cortex (New York, NY : 1991) 26, 268-278.

Li, Q., Ke, Y., Chan, D.C.W., Qian, Z.-M., Yung, K.K.L., Ko, H., Arbuthnott, G.W., and Yung, W.-H. (2012). Therapeutic Deep Brain Stimulation in Parkinsonian Rats Directly Influences Motor Cortex. Neuron 76, 1030-1041.

Little, S., and Brown, P. (2014). Focusing Brain Therapeutic Interventions in Space and Time for Parkinson's Disease. Current Biology 24, R898-R909.

Litvak, V., Jha, A., Eusebio, A., Oostenveld, R., Foltynie, T., Limousin, P., Zrinzo, L., Hariz, M.I., Friston, K., and Brown, P. (2011). Resting oscillatory cortico-subthalamic connectivity in patients with Parkinson's disease. Brain 134, 359-374.

López-Azcárate, J., Tainta, M., Rodríguez-Oroz, M.C., Valencia, M., González, R., Guridi, J., Iriarte, J., Obeso, J.A., Artieda, J., and Alegre, M. (2010). Coupling between Beta and High-Frequency Activity in the Human Subthalamic Nucleus May Be a Pathophysiological Mechanism in Parkinson's Disease. The Journal of Neuroscience 30, 6667-6677.

Lozano, A.M., and Lipsman, N. (2013). Probing and Regulating Dysfunctional Circuits Using Deep Brain Stimulation. Neuron 77, 406-424.

Luft, C.D.B., Nolte, G., and Bhattacharya, J. (2013). High-Learners Present Larger Mid-Frontal Theta Power and Connectivity in Response to Incorrect Performance Feedback. The Journal of Neuroscience 33, 2029-2038.

Magill, P.J., Bolam, J.P., and Bevan, M.D. (2001). Dopamine regulates the impact of the cerebral cortex on the subthalamic nucleus-globus pallidus network. Neuroscience 106, 313-330.

Mitra, P.P., and Pesaran, B. (1999). Analysis of dynamic brain imaging data. Biophysical Journal 76, 691-708.

Nambu, A., Tokuno, H., and Takada, M. (2002). Functional significance of the cortico–subthalamo–pallidal 'hyperdirect' pathway. Neuroscience Research 43, 111-117.

Nolte, G., Bai, O., Wheaton, L., Mari, Z., Vorbach, S., and Hallett, M. (2004). Identifying true brain interaction from EEG data using the imaginary part of coherency. Clinical Neurophysiology 115, 2292-2307.

Nolte, G., Ziehe, A., Nikulin, V.V., Schlögl, A., Krämer, N., Brismar, T., and Müller, K.-R. (2008). Robustly Estimating the Flow Direction of Information in Complex Physical Systems. Physical Review Letters 100, 234101.

Novak, P., Przybyszewski, A.W., Barborica, A., Ravin, P., Margolin, L., and Pilitsis, J.G. (2011). Localization of the subthalamic nucleus in Parkinson disease using multiunit activity. Journal of the Neurological Sciences 310, 44-49.

Oostenveld, R., Fries, P., Maris, E., and Schoffelen, J.-M. (2011). FieldTrip: Open Source Software for Advanced Analysis of MEG, EEG, and Invasive Electrophysiological Data. Computational Intelligence and Neuroscience 2011, 9.

Oswal, A., Beudel, M., Zrinzo, L., Limousin, P., Hariz, M., Foltynie, T., Litvak, V., and Brown, P. (2016). Deep brain stimulation modulates synchrony within spatially and spectrally distinct resting state networks in Parkinson's disease. Brain 139, 1482-1496.

Özkurt, T.E., Butz, M., Homburger, M., Elben, S., Vesper, J., Wojtecki, L., and Schnitzler, A. (2011). High frequency oscillations in the subthalamic nucleus: A neurophysiological marker of the motor state in Parkinson's disease. Experimental Neurology 229, 324-331.

Phillips, L., Litcofsky, K.A., Pelster, M., Gelfand, M., Ullman, M.T., and Charles, P.D. (2012). Subthalamic Nucleus Deep Brain Stimulation Impacts Language in Early Parkinson's Disease. Plos One 7.

Pollo, C., Kaelin-Lang, A., Oertel, M.F., Stieglitz, L., Taub, E., Fuhr, P., Lozano, A.M., Raabe, A., and Schüpbach, M. (2014). Directional deep brain stimulation: an intraoperative double-blind pilot study. Brain 137, 2015-2026.

Qasim, S.E., de Hemptinne, C., Swann, N.C., Miocinovic, S., Ostrem, J.L., and Starr, P.A. (2016). Electrocorticography reveals beta desynchronization in the basal ganglia-cortical loop during rest tremor in Parkinson's disease. Neurobiology of Disease 86, 177-186.

Ray, N.J., Jenkinson, N., Wang, S., Holland, P., Brittain, J.S., Joint, C., Stein, J.F., and Aziz, T. (2008). Local field potential beta activity in the subthalamic nucleus of patients with Parkinson's disease is associated with improvements in bradykinesia after dopamine and deep brain stimulation. Experimental Neurology 213, 108-113.

Raz, A., Bergman, H., Eimerl, D., and Israel, Z. (2008). Propofol induced changes in the neuronal activity of subthalamic nucleus neuron. Movement Disorders 23, Suppl 1:S117.

Schlaier, J.R., Habermeyer, C., Janzen, A., Fellner, C., Hochreiter, A., Proescholdt, M., Brawanski, A., and Lange, M. (2013). The influence of intraoperative microelectrode recordings and clinical testing on the location of final stimulation sites in deep brain stimulation for Parkinson's disease. Acta Neurochirurgica 155, 357-366.

Schuepbach, W.M.M., Rau, J., Knudsen, K., Volkmann, J., Krack, P., Timmermann, L., Haelbig, T.D., Hesekamp, H., Navarro, S.M., Meier, N., *et al.* (2013). Neurostimulation for Parkinson's Disease with Early Motor Complications. New England Journal of Medicine 368, 610-622.

Shamir, R.R., Zaidel, A., Joskowicz, L., Bergman, H., and Israel, Z. (2012). Microelectrode Recording Duration and Spatial Density Constraints for Automatic Targeting of the Subthalamic Nucleus. Stereotactic and Functional Neurosurgery 90, 325-334.

Sharott, A., Magill, P.J., Bolam, J.P., and Brown, P. (2005). Directional analysis of coherent oscillatory field potentials in the cerebral cortex and basal ganglia of the rat. Journal of Physiology-London 562, 951-963.

Shimamoto, S.A., Ryapolova-Webb, E.S., Ostrem, J.L., Galifianakis, N.B., Miller, K.J., and Starr, P.A. (2013). Subthalamic Nucleus Neurons Are Synchronized to Primary Motor Cortex Local Field Potentials in Parkinson's Disease. The Journal of Neuroscience 33, 7220-7233.

Steigerwald, F., Pötter, M., Herzog, J., Pinsker, M., Kopper, F., Mehdorn, H., Deuschl, G., and Volkmann, J. (2008). Neuronal Activity of the Human Subthalamic Nucleus in the Parkinsonian and Nonparkinsonian State. Journal of Neurophysiology 100, 2515-2524.

Swann, N.C., de Hemptinne, C., Aron, A.R., Ostrem, J.L., Knight, R.T., and Starr, P.A. (2015). Elevated synchrony in Parkinson disease detected with electroencephalography. Annals of Neurology 78, 742-750.

Trottenberg, T., Kupsch, A., Schneider, G.-H., Brown, P., and Kuehn, A.A. (2007). Frequency-dependent distribution of local field potential activity within the subthalamic nucleus in Parkinson's disease. Experimental Neurology 205, 287-291.

van Wijk, B.C.M., Beudel, M., Jha, A., Oswal, A., Foltynie, T., Hariz, M.I., Limousin, P., Zrinzo, L., Aziz, T.Z., Green, A.L., *et al.* (2016). Subthalamic nucleus phase–amplitude coupling correlates with motor impairment in Parkinson's disease. Clinical Neurophysiology 127, 2010-2019.

Vinck, M., Oostenveld, R., van Wingerden, M., Battaglia, F., and Pennartz, C.M.A. (2011). An improved index of phase-synchronization for electrophysiological data in the presence of volume-conduction, noise and sample-size bias. NeuroImage 55, 1548-1565.

Walker, H.C., Huang, H., Gonzalez, C.L., Bryant, J.E., Killen, J., Cutter, G.R., Knowlton, R.C., Montgomery, E.B., Guthrie, B.L., and Watts, R.L. (2012). Short latency activation of cortex during clinically effective subthalamic deep brain stimulation for Parkinson's disease. Movement Disorders 27, 864-873.

Wang, J., Hirschmann, J., Elben, S., Hartmann, C.J., Vesper, J., Wojtecki, L., and Schnitzler, A. (2014). High-frequency oscillations in Parkinson's disease: Spatial distribution and clinical relevance. Movement Disorders 29, 1265-1272.

Weiss, D., Klotz, R., Govindan, R.B., Scholten, M., Naros, G., Ramos-Murguialday, A., Bunjes, F., Meisner, C., Plewnia, C., Krüger, R., and Gharabaghi, A. (2015). Subthalamic stimulation modulates cortical motor network activity and synchronization in Parkinson's disease. Brain 138, 679-693.

Weiss, D., Walach, M., Meisner, C., Fritz, M., Scholten, M., Breit, S., Plewnia, C., Bender, B., Gharabaghi, A., Waechter, T., and Krueger, R. (2013). Nigral stimulation for resistant axial motor impairment in Parkinson's disease? A randomized controlled trial. Brain 136, 2098-2108.

Whitmer, D., de Solages, C., Hill, B., Yu, H., Henderson, J.M., and Bronte-Stewart, H. (2012). High frequency deep brain stimulation attenuates subthalamic and cortical rhythms in Parkinson's disease. Frontiers in Human Neuroscience 6.

Williams, D., Tijssen, M., van Bruggen, G., Bosch, A., Insola, A., Di Lazzaro, V., Mazzone, P., Oliviero, A., Quartarone, A., Speelman, H., and Brown, P. (2002). Dopamine-dependent changes in the functional connectivity between basal ganglia and cerebral cortex in humans. Brain 125, 1558-1569.

Winestone, J.S., Zaidel, A., Bergman, H., and Israel, Z. (2012). The use of macroelectrodes in recording cellular spiking activity. Journal of Neuroscience Methods 206, 34-39.

Yang, A.I., Vanegas, N., Lungu, C., and Zaghloul, K.A. (2014). Beta-Coupled High-Frequency Activity and Beta-Locked Neuronal Spiking in the Subthalamic Nucleus of Parkinson's Disease. The Journal of Neuroscience 34, 12816-12827.

Zaidel, A., Spivak, A., Grieb, B., Bergman, H., and Israel, Z. (2010). Subthalamic span of β oscillations predicts deep brain stimulation efficacy for patients with Parkinson’s disease. Brain 133, 2007-2021.

Figures:

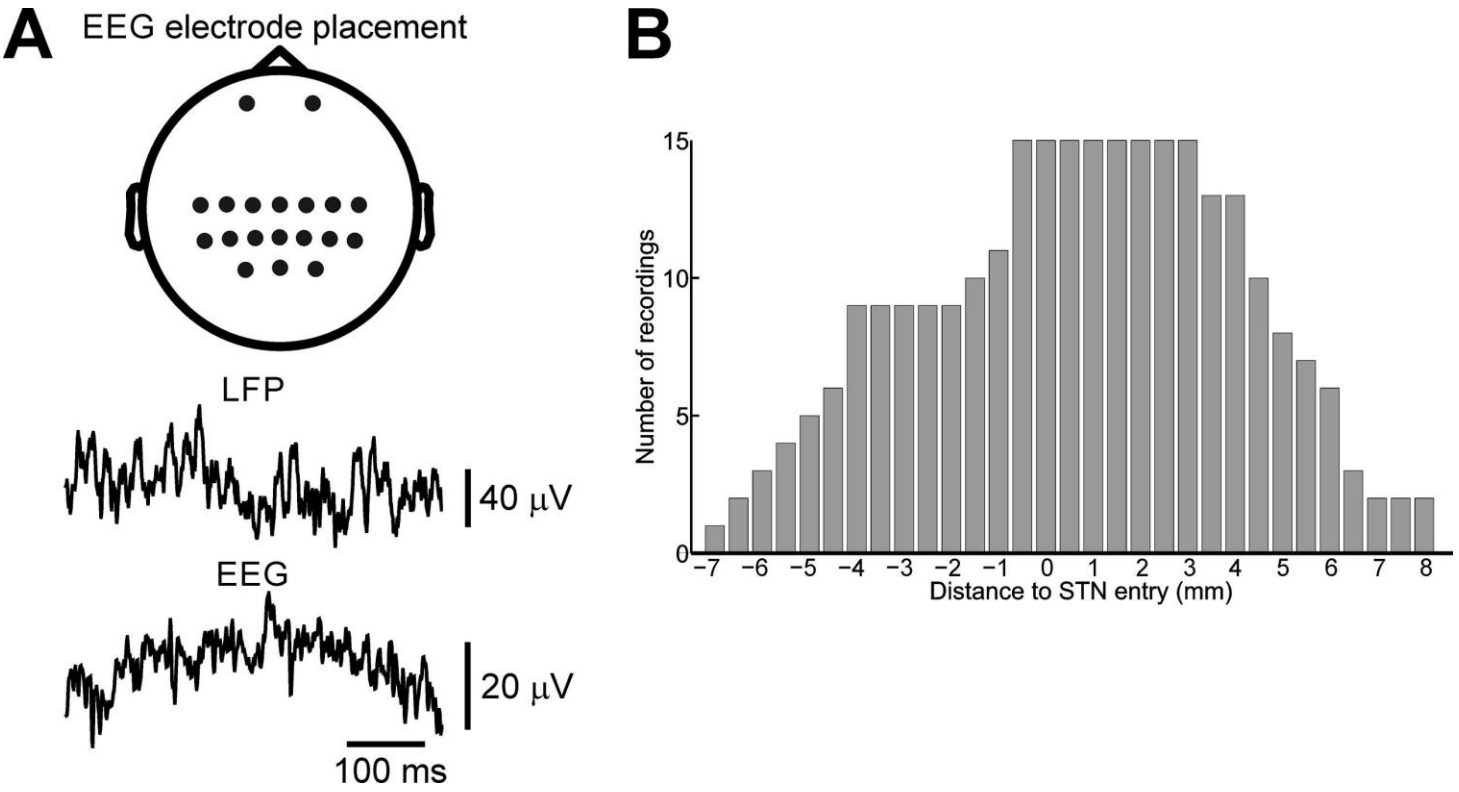

Figure 1: Experimental setup**. (**A) Topography of EEG electrode placement during DBS surgery and raw signals of simultaneous STN-LFP and EEG recordings of one representative PD patient. (B) Cumulative number of analyzed LFP recordings at each recording depth.

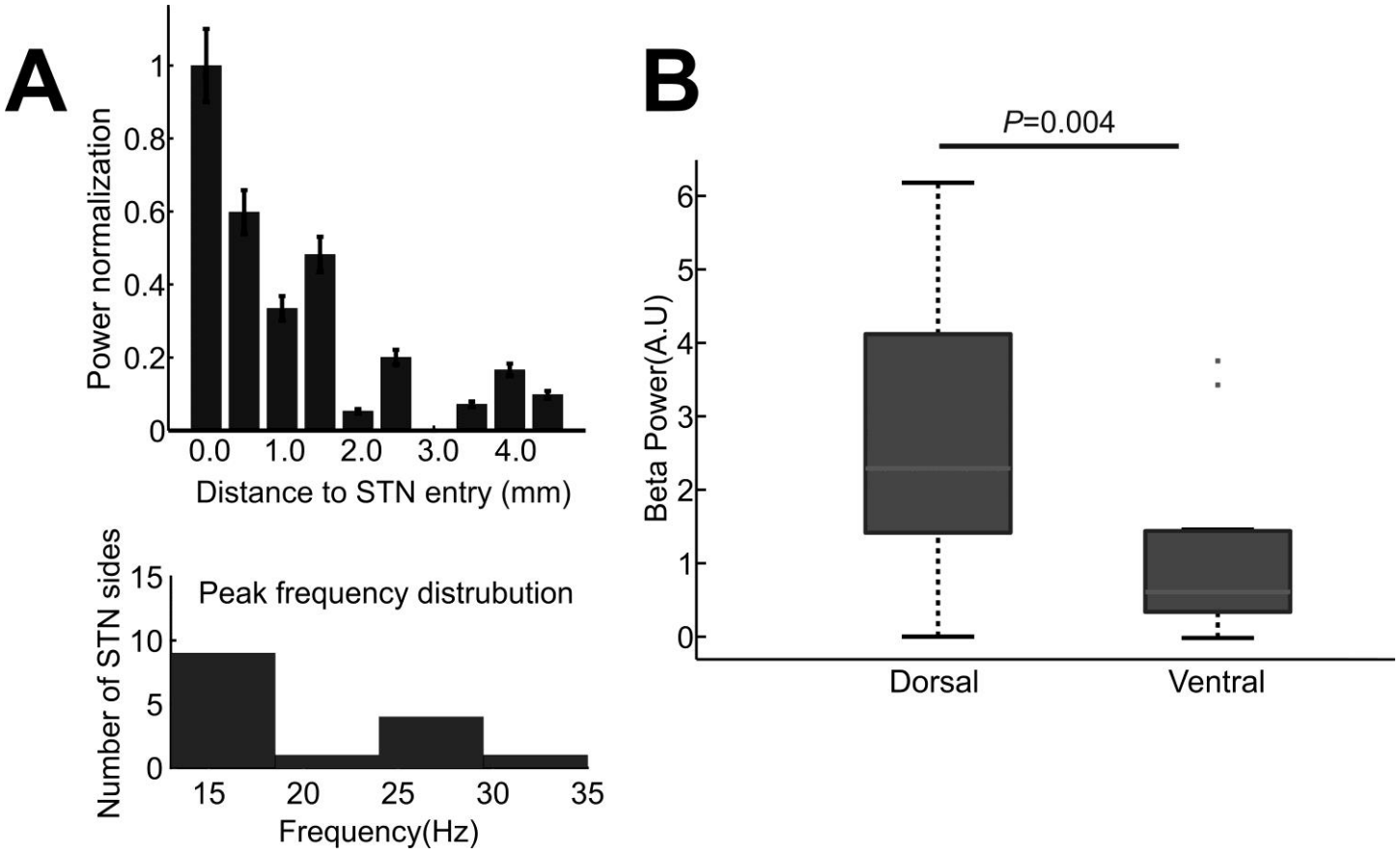

Figure 2: Group data of neural oscillations in the STN. (A) Histogram (upper plot) of beta (13-35 Hz) activity in relation to the STN entry. Distribution (lower plot) of peak frequencies (in 5 Hz bins) of the highest beta band power of each patient. (B) Significant beta oscillation in dorsal-STN; box plots show the median, the $25^{th}/75^{th}$ percentiles and the maximum/minimum values of the beta oscillations in the dorsal and ventral STN, respectively. Outliers are depicted by crosses.

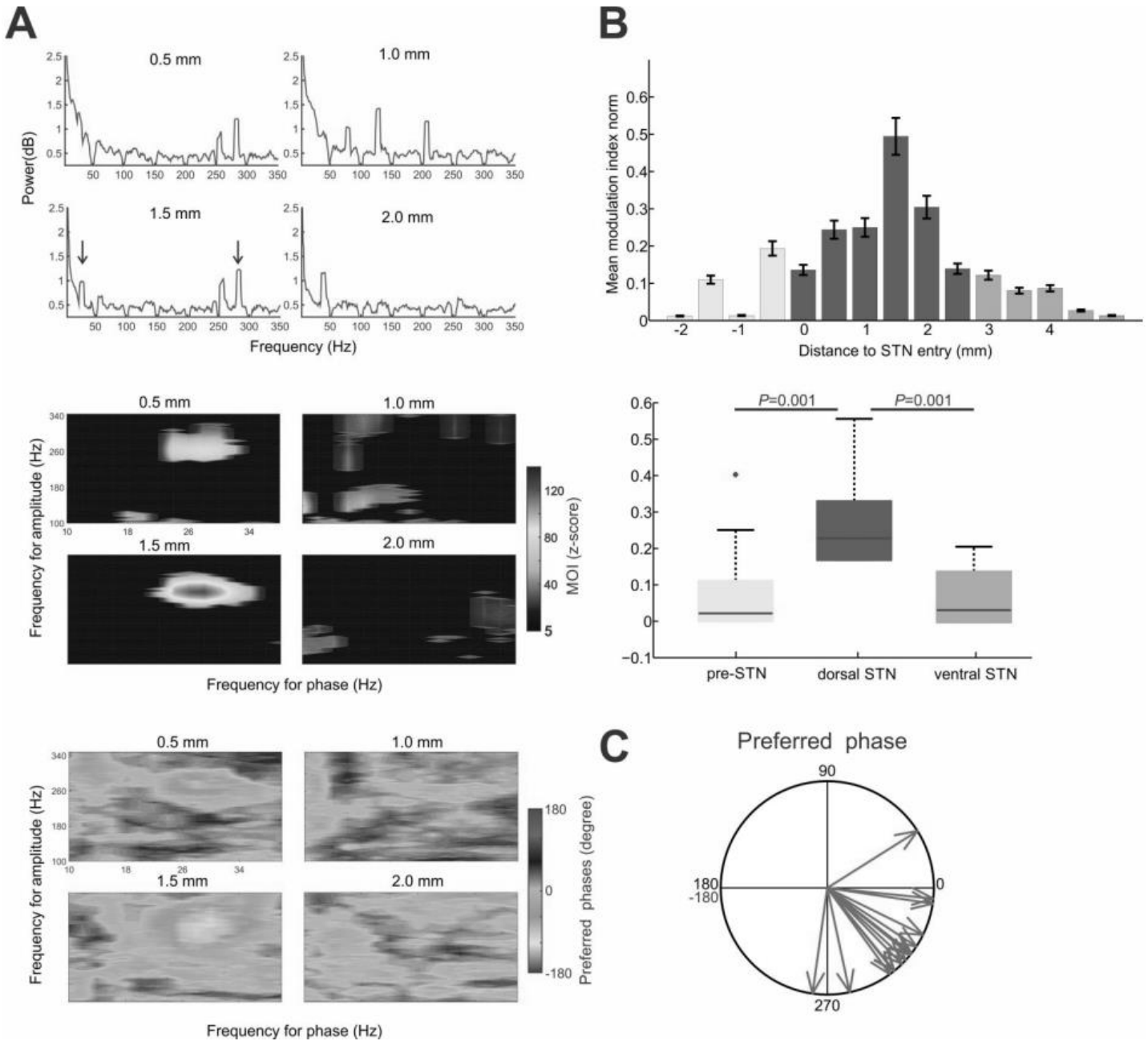

Figure 3: Phase-amplitude coupling in the STN. (A) Power spectrum, B-HFO and preferred coupling phase (lower plot) for one representative patient at different depths of the dorsal STN shows a peak at a depth of 1.5 mm below STN entry. (B) Group results of averaged B-HFO at different STN depths reveal spatial specificity in the dorsal part of STN (left). Box plots show the median, the 25^{th}/75^{th} percentiles and the maximum/minimum values of the B-HFO in pre-STN, dorsal and ventral STN, respectively. Outliers are depicted by crosses (right). (C) Multiple individual results of preferred phase coupling of B-HFO in STN.

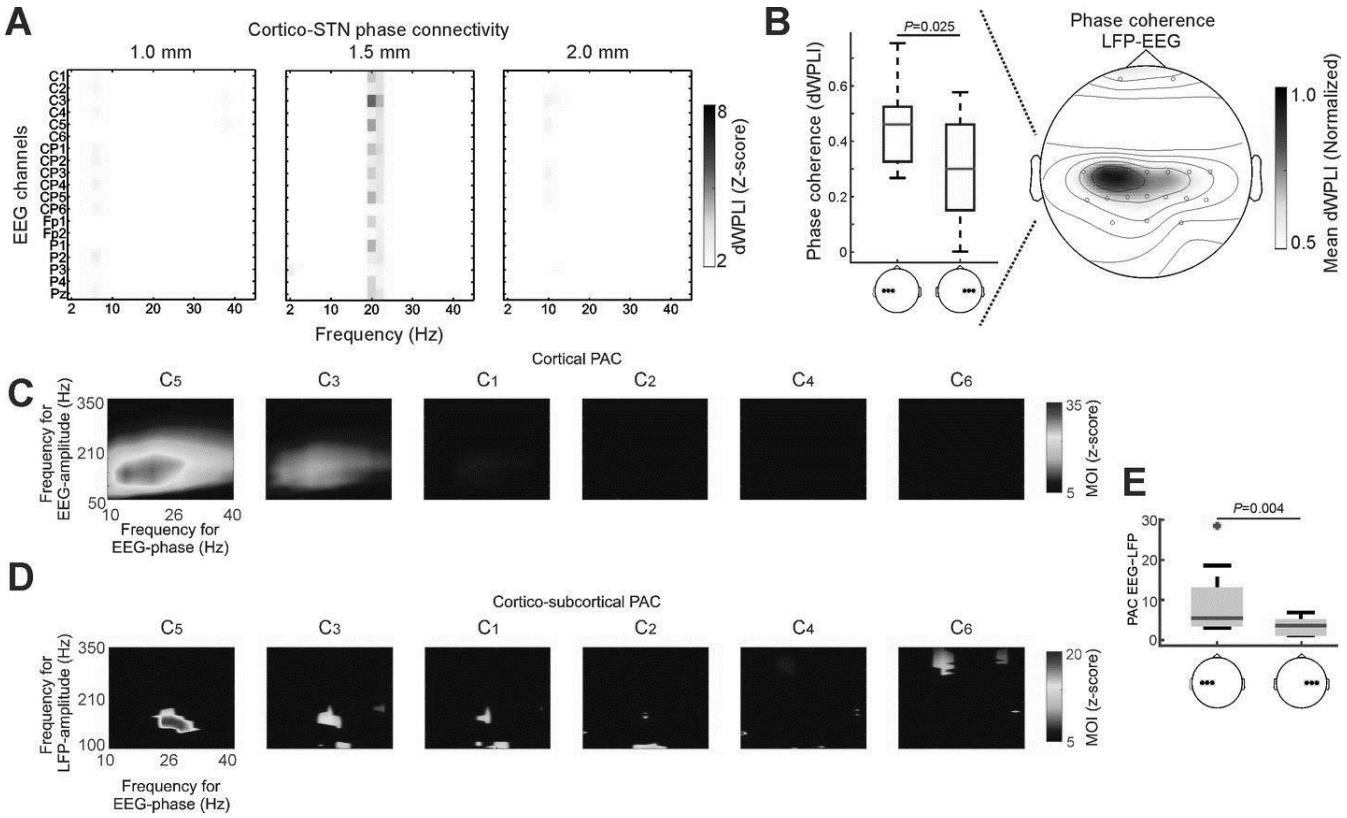

Figure 4: Cortico-subcortical connectivity and cross-frequency coupling. (A) Phase coherence between left STN-LFP and all EEG electrodes in one representative patient across different STN depths. (B) Topographic group data showing the spatial specificity of LFP-EEG phase coherence, i.e. C1/3; results for the right LFP-EEG coherence were flipped to the left side. Box plot compares ipsi- and contralateral phase coherence of the central region. (C) Cortical beta phase-broadband gamma coupling and (D) B-HFO between cortical BO and high-frequency activity in the STN of the central region in one representative patient. (E) Group data showing box plots with the median, the 25^{th}/75^{th} percentiles and the maximum/minimum values of the cortico-STN B-HFO for the central EEG electrodes ipsi- and contralateral, respectively.

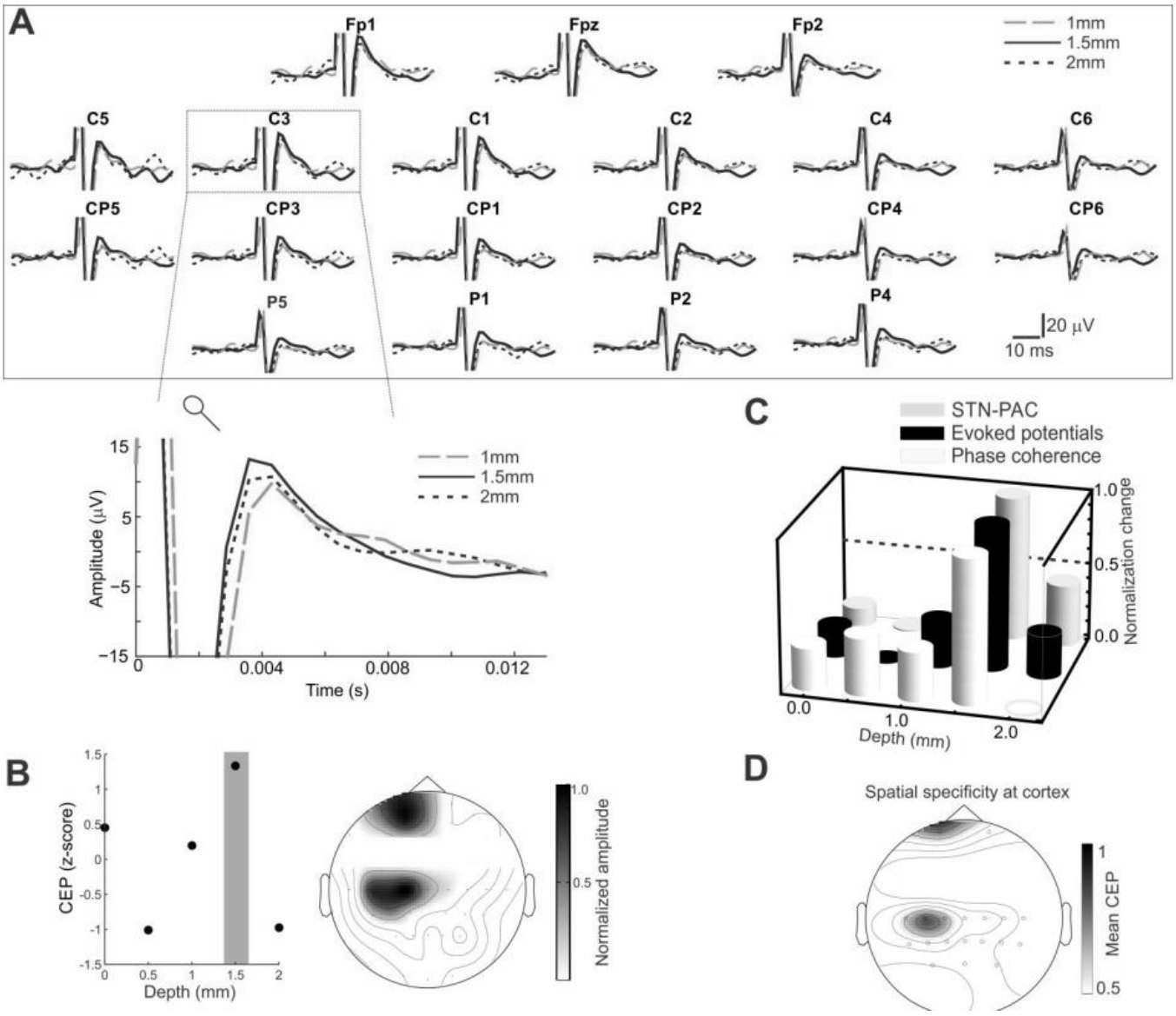

Figure 5: Evoked potentials and relationship between different physiological STN markers (A) Cortical-evoked potential recorded at various cortical sites following 1 Hz electrical stimulation in the STN at different depths for one representative patient. (B) The amplitude (left side) of the cortical-evoked potentials (CEP) recorded at C3 for one representative patient following 1 Hz electrical stimulation at different STN depths with the corresponding cortical topography at maximum CEP (right side). (C) Cortical topography of maximum CEP over nine hemispheres. (D) Group results of cortical evoked potential, PAC and dWPLI across different STN depths.

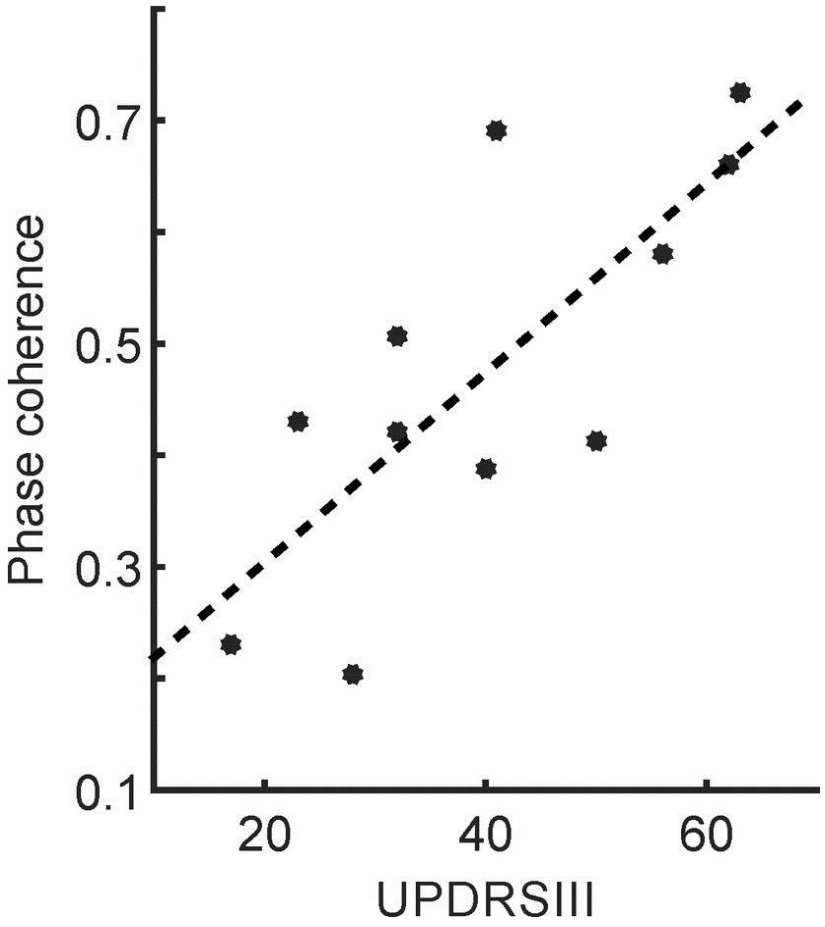

Figure 6: Correlation between cortico-subcortical connectivity and motor symptoms. The phase coherence between STN and motor cortex correlated significantly with the severity of motor symptoms (UPDRS III in OFF state).

Table 1: Demographic and clinical data of the twelve patients analyzed in this study.

F = female; M = male. L=left; R=right; + = cathode; − = anode; G = IPG case

Case	Age (years)/ gender	Recording side(s)	UPDRS III OFF/ON	DBS contacts right/left	DBS frequency/ amplitude/duration
PD1	66/ M	L+R	17/11	10-/G+	125/2.0/60
				2-/G+	125/2.3/60
PD2	69/ M	L+R	41/28	10-/G+	130/1.7/60
				2-/G+	130/1.7/60
PD3	63/ M	L	23/21	10-/G+	130/0.9/60
				2-/G+	130/1.6/60
PD4	72/ M	L+R	62/41	10-/G+	130/1.5/60
				2-/G+	130/1.8/90
PD5	73/ M	L	40/20	10-/G+	130/2.2/90
				2-/G+	130/2.0/90
PD6	73/ F	L	32/18	11-/G+	130/3.0/60
				3-/G+	130/3.0/60
PD7	71/ M	L	32/19	10-/+G	130/1.0/60
				2-/+G	130/1.0/60
PD8	66/ M	R	63/45	10-/G+	120/1.5/60
				3-/G+	120/1.5/60
PD9	67/ F	L	28/14	10-/G+	130/1.8/60
				2-/G+	130/1.8/60
PD10	73/ M	L	36/31	8-/G+	125/1.5/60
				3-/G+	125/1.5/60
PD11	67/ M	R	50/37	10-/G+	130/2.4/90
				2-/G+	130/2.2/90
PD12	73/ M	R	56/21	10-/G+	130/1.2/60
				2-/G+	130/1.8/60

Table 2: Relationship between different physiological markers (A) and correlation with motor symptoms (B).

A

Spatial relationship between different physiological markers	**R^2**	**P-value**
BO and local B-HFO (STN)	0.366	0.218
BO and phase coherence (dWPLI)	0.369	0.214
Local B-HFO and phase coherence (dWPLI)	0.76	**0.003**

B

Correlation between UPDRS III and physiological markers	**R^2**	**P-value**
Beta power in STN (BO)	0.519	0.102
Cortical PAC	0.134	0.713
Local B-HFO (STN)	0.359	0.309
Cortico-subcortical coherence	0.724	**0.0142**
Long range B-HFO (cortico-subcortical)	0.116	0.845

Spatial specificity of beta oscillation and cortico-subthalamic connectivity in Parkinson's disease

Ramin Azodi-Avval, Alireza Gharabaghi*

Division of Functional and Restorative Neurosurgery, and Centre for Integrative Neuroscience, Eberhard Karls University Tuebingen, Germany

* Correspondence: Prof. Dr. Alireza Gharabaghi, Division of Functional and Restorative Neurosurgery, Eberhard Karls University, Otfried-Mueller-Str.45, 72076 Tuebingen, Germany, Tel: +49 7071 29 83550, Fax: +49 7071 29 25104, E-Mail address: alireza.gharabaghi@uni-tuebingen.de

Abbreviations: DBS=deep brain stimulation; dWPLI=debiased weighted phase lag index; BO=beta oscillations; LFP=local field potential; M1=motor cortex; MEG=magnetoencephalography; MOI=modulation index; PSI=phase-slope index; STN=subthalamic nucleus; UPDRS III=Unified Parkinson's Disease Rating Scale.

Abstract

Deep brain stimulation (DBS) of the subthalamic nucleus (STN) is a common intervention for the treatment of Parkinson's disease. However, the underlying neurophysiology in the STN and related cortico-subcortical networks mediating the therapeutic effects is still unclear. To address this, we simultaneously recorded electroencephalography and local field potentials (LFP) with chronic DBS electrodes at various depths along the trajectory to STN in 21 patients with Parkinson's disease (PD). We show empirically the power spectrum of monopolar LFP recordings to be a robust and reliable tool for detecting specific oscillatory regions in the STN. Using this novel technique, we identified the oscillatory beta area in the STN which was robustly detectable across different DBS electrode contacts during mapping. Intracranial LFP measurements together with intraoperative EEG recordings revealed strong cortico-subthalamic phase coupling to the ipsilateral motor area. At this site, the information flowed was mediated from the cortical motor cortex to the STN in the oscillatory high beta band suggesting a pathologically synchronized network with a direct connection, i.e.via the hyperdiect pathway. The STN site connected to the cortical motor area was spatially specific and located differently than the oscillatory beta region in the STN. While the spectral peak of the cortico-subthalamic connectivity was in the high beta-band, the oscillatory region showed its peak in the low beta-range. Moreover, the cortico-subthalamic synchronization correlated with the severity of the motor symptoms in the medication OFF state. These findings provide evidence for the existence of two distinct networks in the dorsal STN which could be detected during surgery.

Introduction

Parkinson's disease is a neurodegenerative disorder which is characterized by pathological electrophysiological changes caused by dopamine depletion (Brittain and Brown, 2014; Little and Brown, 2014). The lack of dopamine in the basal ganglia loop seems particularly relevant for the appearance of pathological bursts during single-cell recording (Filion and Tremblay, 1991; Sharott et al., 2005) and of beta oscillations during in local field potentials recordings (Weinberger et al., 2006). In this regard, both the reduction of pathological activity during therapeutic deep brain stimulation (DBS) and the neural activity of subthalamic nucleus (STN) at rest have repeatedly been shown to correlate with the pathophysiology of PD (de Hemptinne et al., 2015; Hirschmann et al., 2016; Sharott et al., 2014; Zaidel et al., 2010). Intraoperative electrophysiological measurements of single-unit neuronal activity is the most common techniques to detect the borders of the STN (Hutchison et al., 1998; Novak et al., 2011). However, this method suffers from a number of limitations during DBS surgery. Increased surgery-related risk factors, such as hemorrhages, or misplacement of the chronic DSB lead while replacing the test electrode are concerns related to the microelectrode recording procedure (McClelland, 2011; Paffi et al., 2015; Zrinzo et al., 2012). Macroelectrode recording with the chronic DBS electrode could instead offer a novel approach to target subcortical structure. Local field potentials (LFP) recorded by the chronic DBS lead are a summation signal of excitatory and inhibitory potentials (Buzsáki et al., 2012). These signals have recently been used for feedback control of adaptive DBS in PD (Little et al., 2013). Features in LFP oscillations have been shown to highly correlate with single-cell activity, particularly with regard to the beta oscillations of LFPs and the beta oscillatory cells within the STN (Weinberger et al., 2006). Hence, LFPs could be a reliable candidate for STN localization. Accordingly, some studies have shown LFP spectral features to be informative with regard to the clinically most effective DBS location in the STN (Chen et al., 2006; Yoshida et al., 2010).

However, bioplorization of the electrode contacts and relatively large step sizes during recording have reduced the spatial accuracy during STN mapping in pervious studies.

A direct link between the STN and the motor cortex, i.e. the hyperdirect pathway, has been suggested to play a prominent role during therapeutic stimulation for disrupting pathological oscillatory activity and reducing motor symptoms of PD (Gradinaru et al., 2009; Li et al., 2012). The STN-motor cortex interaction has been shown to be clinically relevant for the state of the disease during the administration of L-dopa medication or STN-DBS (de Hemptinne et al., 2015; Litvak et al., 2011; Oswal et al., 2016). However, previous studies performed cortico-subcortical coherence analysis while the position of the DBS electrode contacts was fixed, thereby, providing only poor spatial resolution in the targeted area. Despite this importance of local STN activity and pathological brain networks in PD (Hirschmann et al., 2011; Litvak et al., 2011; Oswal et al., 2016), to date research on both local and network biomarkers during STN mapping is scarce. Furthermore, optimal positioning of the implanted DBS leads plays a vital role in the treatment effectiveness and long-term life quality in PD patients with DBS therapy (Deuschl et al., 2006; Guo et al., 2013; Maks et al., 2009). Hence, we hypothesized that combined intraoperative EEG and stepwise LFP recordings with the chronic electrode along the trajectory to STN will reveal STN-cortex connectivity patterns and their relationship to local STN biomarkers. To the best of our knowledge, this is the first study on the spatial and spectral specificity of the hyperdirect pathway and its relationship to local electrophysiological markers during STN mapping.

Materials and methods

Patients and neurosurgical procedure

We recorded brain activity from 21 patients who were diagnosed with idiopathic Parkinson's disease (seven females; age: 67.05±3.53 years, mean ± STD; disease duration: 13.40 ± 2.33

years) during bilateral implantation of deep brain stimulation electrodes in the STN. Intraoperative propofol medication was stopped at least 30 minutes before electrophysiological recordings were initiated (Azodi-Avval and Gharabaghi, 2015). During the neurophysiological recordings, patients were not under sedation and awake. The study was conducted with the patients' informed consent and according to the guidelines approved by the local ethics committee of the University Hospital Tuebingen.

Data collection and preprocessing

Cortical and subcortical electrophysiological signals were recorded in awake patients at rest. We evaluated LFPs with chronic DBS electrodes (quadripolar DBS lead model 3389; 1.27 mm in diameter, 1.5 mm contact length and 0.5 mm contact-to-contact separation, Medtronic Inc., Minneapolis, USA) along the trajectory throughout the STN region in steps of 1 mm. Simultaneously we recorded scalp EEG with surface electrodes (Ag/AgCl electrodes, MedCaT GmbH, Netherlands) covering the head around the burr holes in accordance with the international 10–20 EEG system (Alpha-Omega, Nazareth, Israel). The non-sterile EEG electrodes were placed before surgery and covered intraoperatively with the conventional sterile surgical covering procedure. LFPs were recorded from -8 mm to +9 mm relative to the upper STN border, while EEG was measured at 32 to 38 sensors covering frontal, central, temporal, midline and parietal regions (Fig. 1A). Although EEG electrodes were placed in a standardized clinical fashion, their exact position in relation to the underlying cortical anatomy remains clear. We will refer to the C row of electrodes as the central region or M1, even though these electrodes might capture signals from the premotor area as well.

For online recordings and evaluation, the LFP and EEG signals were streaming to a dedicated system running Matlab; the communication link was established through an Ethernet network. We gathered the data in blocks of 10 ms; at the end of the recording period, signal blocks were concatenated without any missing sample for further analysis. The data were also

stored offline by the data acquisition system (Alpha-Map, Alpha-Omega, Israel). We considered 30 seconds of recordings of simultaneous EEG and LFP at each depth for further analysis. Cortical and intracranial signals were continuously sampled at 1.4 KHz and amplified by a factor of 50 and 20, respectively. The reference electrodes were attached to the ears and the ground was placed on the nasion. The impedance was set at ~1 KΩ and below 0.5 KΩ for the intracranial and the EEG electrodes, respectively. Representative raw signals are shown in Fig. 1A.

Data analysis of EEG and LFPs was performed in Matlab (version 2014b, Mathworks, Massachusetts, USA) using custom-made scripts, and in Fieldtrip, an open source analysis toolbox (Oostenveld et al., 2011, http://fieldtrip.fcdonders.nl/). Signals were epoched in half second data segments, and all artifacted epochs were removed by the Fieldtrip artifact rejection method. Line noise at 50 Hz and the harmonics were removed with a notch filter. Due to movement and respiration artifacts, frequencies below 3 Hz were not taken into consideration.

Online and offline power spectrum and coherence analysis

The power spectrum of monopolar LFP channels was computed using the Hanning taper (Mitra and Pesaran, 1999) for both online and offline analysis. For group analysis of LFP power, the beta frequency power was normalized by dividing it by the total power from 3-95 Hz; this was based on the individual beta frequency peak for each patient. During the intraoperative online recording, we calculated the power spectrum of all four DBS electrode contacts separately between 5-45 Hz, as well as the phase coherence coupling between DBS contact pairs (01-12-23) and all EEG cortical activity in the same frequency range. This procedure was done at each depth along the trajectory towards the target in the steps of 1 mm. Phase coherence coupling was measured with the Weighted Phase Lag Index (WPLI) (Vinck et al., 2011) between EEG and LFP. This method is more efficient in detecting genuine phase interaction than common phase measurements like the imaginary part of coherence (Nolte et

al., 2004). Directionality between cortical EEG and subcortical LFP was calculated on the basis of the phase-slope index (PSI) (Nolte et al., 2008). Here, depending on the information flow between the subcortical site (which is taken as a reference) and the cortex, PSI has a positive (flow direction from cortex to subcortical site) or negative sign (flow direction from subcortical site to cortex). In this study, dWPLI and PSI were normalized by their standard deviation, which was computed by the jackknife method; absolute values larger than 1.96 (corresponding to $p<0.05$) were considered statistically significant (Hohlefeld et al., 2013; Luft et al., 2013; Nolte et al., 2008).

Considering the physical characteristics of DBS contacts and the step size resolution, the spatial position of the lowest DBS contact (contact 0) will be covered by the second lowest contact (contact 1) after descending the lead by 2 mm. This technique allowed us to determine the reliability of detected oscillatory region by moving the electrode across the STN, thereby, recording each position several times by different electrode contacts (Fig. 1B).

Results

Spectral changes along the trajectory of a DBS electrode

The power spectrum calculation of the DBS contacts (0-3) at each depth is shown in Fig. 2A along the trajectory to the STN. The power spectrum shows the spectral and spatial specificity, in the beta band and at the position of 0 mm. In fact, the persistence of the beta peak pattern in the same spatial location captured with different DBS contacts at different time points underlined the reliability of the detected beta oscillatory region. This beta oscillatory region was confirmed in the whole patient group and revealed a mean peak frequency of 16.94±0.87 Hz (Fig. 2B). The same pattern was demonstrated with both monopolar and bipolar recordings (Fig. 2C). Moreover, the linear correlation between the normalized beta power at the upper STN border recorded with different contacts revealed the high reliability of the technique (Fig.

2C, lower plot; for monopolar R=0.84, P=0.00001 and bipolar R=0.87, P=0.00001). Notably, the reliability of bipolar LFP recordings was less in comparison to monopolar measurements. Comparative analysis of all recordings of pre-STN, dorsal and ventral STN revealed a significantly higher average beta oscillatory power in the dorsal STN than in the pre-STN and ventral STN for both the monopolar and bipolar analysis (Fig. 2D).

Spatial and spectral specificity of STN-motor cortex connectivity

We furthermore investigated whether the cortex, particularly the motor area had a functional or effective connection to a specific part of the STN. This cortico-subcortical connectivity analysis with dWPLI was performed between all DBS contact pairs (01, 12, 23) and cortical EEG electrodes. We explored whether the STN-cortical coupling had spatial and spectral specificity across PD. Fig. 3 shows significant STN-ipsilateral motor network phase coupling at 2 mm in the high beta-frequency (22.43±1.75 Hz) range for the contact pair 01. This result was confirmed in the same spectral range with the contact pair 12 when it passed the same spatial location. Interestingly, the effective connectivity analysis with PSI confirmed the ipsilateral medial motor area as the region with the highest cortico-subcortical information flow from the cortex to the same site in the STN and in the same frequency range (21.29±1.72 Hz).

The group average cortical topography revealed a specific spatial pattern at the cortical level, (electrodes projecting to the medial motor cortex of the ipsilateral hemisphere, i.e. the C1/3 electrodes, Fig. 4A) as well as within the STN (peaking in the dorsal part of the STN 1.59±0.56 mm below the STN entry). There was no difference between the cortical topography and the subcortical location of effective and functional connectivity, and also no difference in the frequency range. Phase coherence and PSI of the ipsilateral motor cortical region was significantly higher than of the other cortical areas ($p = 0.01$; Mann–Whitney U test, Fig. 4B).

Electrophysiological biomarkers and clinical correlation

The prominent beta oscillatory (BO) region within the STN (16.94±0.87 Hz) peaked at the STN entry and decreased gradually from the dorsal to the ventral border, whereas the STN-motor coupling (22.43±1.75 Hz) peaked at 1.59±0.56 mm below the STN entry. Statistical analysis revealed that the peak beta frequencies of both STN (16.94±0.87 Hz) and coherence (22.43±1.75 Hz) differed significantly from each other (P= 0.0004; Mann–Whitney U test and P= 0.01). In each patient, the sites of maximum BO (r=0.18; P=0.36) did not show any correlation to the site of maximum cortico-subcortical phase coherence to the ipsilateral M1. Notably, the cortico-subthalamic synchronization was the only physiological marker that significantly correlated (r=0.61, P=0.006) with the severity of motor symptoms in the medication OFF state (Fig. 5).

Discussion

Deep brain stimulation of the STN provides an intervention to directly perturb pathological brain oscillations in PD (Little and Brown, 2014). But the spatial specificity of STN DBS with respect to the neurophysiological activity within STN and its coupling to the cortex is still less clear. In this study, we applied a novel intraoperative mapping approach and could identify the maximum neural oscillatory region in STN and the site which had the most relevant phase coherence to the ipsilateral motor area, i.e. indicative for the hyperdirect pathway.

Beta oscillatory region in the STN

Applying microelectrodes for single-cell or LFP recording is the most established way to delineate the STN boundary (Benazzouz et al., 2002; Contarino et al., 2012; Hutchison et al., 1998; Novak et al., 2011). However, there are some concerns employing this method for DBS lead implantation. Misplacement of the final electrode (Paffi et al., 2015), when replacing the test electrodes for microrecording, and surgical risks such as hemorrhages might be related to this procedure (Zrinzo et al., 2012). Here, we proposed and evaluated a novel recording method

which could potentially resolve the issues related to the use of test electrodes. Our findings showed that monopolar recordings of LFP channels from the final electrode are a robust and reproducible way to monitor the oscillatory regions in the STN, particularly the beta-band oscillations. A local increase of beta LFP oscillation in the STN has been shown to correlate with the pathophysiology of the disease and with single-cell recordings (Kühn et al., 2009; Sharott et al., 2014). This pathological beta oscillation in the low beta-range was reduced during therapeutic stimulation and has recently been used as a feedback signal for closed-loop DBS in PD patients (Little et al., 2013). Therefore, the close relationship between beta LFP oscillations and pathophysiology of PD could provide a reliable biomarker to targeting the respective area in the STN. Previous studies that searched for the STN boundary through LFP measurements with the chronic electrode, bipolarized the electrode contacts and used a stepwise mapping of 2mm (Chen et al., 2006; Telkes et al., 2016). Based on our findings with monopolar recordings in steps of 1 mm, we conclude that these previous approaches were limited in detecting the beta band oscillatory region with high spatial accuracy.

Strong subthalamic cortical motor coupling

Our findings demonstrated significant functional and effective connectivity between the STN and ipsilateral motor area. Notably, the results were reproducible in the same spatial location of STN at different time points and with different electrode contacts. This finding underlined the existence of an STN region with strong connectivity to the motor cortical area. Both postoperative EEG and MEG recordings with simultaneous STN LFP recordings have previously provided evidence for the functional STN-M1 connectivity in the high beta-band (Litvak et al., 2011; Oswal et al., 2016; van Wijk et al., 2016). These results were confirmed by electrocorticography (ECoG) measurements as well which offered a better localization and higher signal-to-noise ratio (Whitmer and White, 2012). In this line of research, the clinical effectiveness of activated DBS contacts located in the dorsal STN was shown to positively

correlate with connectivity to the superior frontal gyrus and the thalamus when using probabilistic tractography with diffusion tensor imaging (DTI) (Vanegas-Arroyave et al., 2016). Another DTI study, correlated the STN anatomy and predominant beta oscillatory activity in STN with the connect pattern to the cortex (Accolla et al., 2016). However, these studies were limited by the relatively poor spatial resolution of DTI; moreover, the position of the DBS lead was fixed due to the postoperative recordings, thereby, limiting the specificity of the findings within the STN. These issues could be solved in this study by step-wise (in 1 mm steps) recordings during surgery capturing cortico-subcortical connectivity across the STN, enabling us to have a better spatial resolution in compare the neuroimaging localization.

Direct glutamatergic projections of the motor cortex to STN, i.e. the hyperdirect pathway, plays a prominent role in mediating the DBS effects by regulating abnormal activity in M1 (Chiken and Nambu, 2015; Gradinaru et al., 2009; Li et al., 2012). Hence, the identification of a hyperdirect M1-subthalamic nucleus pathway could be the key element for the clinical effects and optimal electrode placement. Although some studies have attempted to localize the STN-cortex connection based on preoperative tractography (Petersen et al., 2016; Whitmer et al., 2012b), it is not clear to what extent this method can use for the individual DBS treatment planning. The main concern with this technique is the brain shift (Khan et al., 2008) that may occur during stereotactic surgery and the poor spatial resolution of DTI which may lead to targeting errors during electrode implantation (Accolla et al., 2016). However, the intraoperative online measurement of cortico-subcortical connectivity by combined recording of EEG and LFP signals with the final electrode will likely reduce these potential targeting errors. Furthermore, the presented technique may allow targeting the pathological network in PD by disturbing abnormal activity between the STN and motor area.

Implications for clinic therapy

There is increasing electrophysiological evidence to suggest that STN-DBS is modulating abnormal cortical and subcortical activity, as well as their functional coupling during therapeutic high-frequency stimulation (Dejean et al., 2009; Weiss et al., 2015). Reduction of the excessive beta synchronization in the cortical motor area and of subthalamic-motor cortex coherence in the high beta-band during DBS indicated that clinical importance of the STN-motor network functional connection for the pathophysiology PD (de Hemptinne et al., 2015; Oswal et al., 2016). Furthermore, experimental data with a non-human primate model of PD showed the disease severity to correlate positively with STN-M1 coherence in beta band (Devergnas et al., 2014). In the present study, we demonstrated that the severity of PD motor symptoms can be predict by STN phase coupling to the ipsilateral motor cortex. The spatial specificity of this connectivity in the STN could be considered as a marker for targeting this pathological network during DBS in PD.

Author contributions

R.A. and A.G. collected data, designed and performed research, analyzed data and wrote the paper.

Acknowledgements

RA was supported by the Graduate Training Centre of Neuroscience, International Max Planck Research School for Cognitive and Systems Neuroscience, Tuebingen, Germany. AG was supported by grants from the German Research Council [DFG EC 307], and from the Federal Ministry for Education and Research [BFNT 01GQ0761, BMBF 16SV3783, BMBF 03160064B, BMBF V4UKF014]. The authors declare that they have no competing interests.

Reference

Accolla, E.A., Herrojo Ruiz, M., Horn, A., Schneider, G.-H., Schmitz-Hübsch, T., Draganski, B., and Kühn, A.A. (2016). Brain networks modulated by subthalamic nucleus deep brain stimulation. Brain.

Azodi-Avval, R., and Gharabaghi, A. (2015). Phase-dependent modulation as a novel approach for therapeutic brain stimulation. Frontiers in Computational Neuroscience 9.

Benazzouz, A., Breit, S., Koudsie, A., Pollak, P., Krack, P., and Benabid, A.L. (2002). Intraoperative microrecordings of the subthalamic nucleus in Parkinson's disease. Movement disorders : official journal of the Movement Disorder Society 17 Suppl 3, S145-149.

Brittain, J.-S., and Brown, P. (2014). Oscillations and the basal ganglia: Motor control and beyond. NeuroImage 85, Part 2, 637-647.

Buzsáki, G., Anastassiou, C.A., and Koch, C. (2012). The origin of extracellular fields and currents — EEG, ECoG, LFP and spikes. Nat Rev Neurosci 13, 407-420.

Chen, C.C., Pogosyan, A., Zrinzo, L.U., Tisch, S., Limousin, P., Ashkan, K., Yousry, T., Hariz, M.I., and Brown, P. (2006). Intra-operative recordings of local field potentials can help localize the subthalamic nucleus in Parkinson's disease surgery. Experimental Neurology 198, 214-221.

Chiken, S., and Nambu, A. (2015). Mechanism of Deep Brain Stimulation: Inhibition, Excitation, or Disruption? The Neuroscientist.

Contarino, M.F., Bour, L.J., Bot, M., van den Munckhof, P., Speelman, J.D., Schuurman, P.R., and de Bie, R.M. (2012). Tremor-specific neuronal oscillation pattern in dorsal subthalamic nucleus of parkinsonian patients. Brain Stimulation 5, 305-314.

de Hemptinne, C., Swann, N.C., Ostrem, J.L., Ryapolova-Webb, E.S., San Luciano, M., Galifianakis, N.B., and Starr, P.A. (2015). Therapeutic deep brain stimulation reduces cortical phase-amplitude coupling in Parkinson's disease. Nat Neurosci 18, 779-786.

Deuschl, G., Schade-Brittinger, C., Krack, P., Volkmann, J., Schäfer, H., Bötzel, K., Daniels, C., Deutschländer, A., Dillmann, U., Eisner, W., *et al.* (2006). A Randomized Trial of Deep-Brain Stimulation for Parkinson's Disease. New England Journal of Medicine 355, 896-908.

Devergnas, A., Pittard, D., Bliwise, D., and Wichmann, T. (2014). Relationship between oscillatory activity in the cortico-basal ganglia network and parkinsonism in MPTP-treated monkeys. Neurobiology of Disease 68, 156-166.

Filion, M., and Tremblay, L.o. (1991). Abnormal spontaneous activity of globus pallidus neurons in monkeys with MPTP-induced parkinsonism. Brain Research 547, 140-144.

Gradinaru, V., Mogri, M., Thompson, K.R., Henderson, J.M., and Deisseroth, K. (2009). Optical Deconstruction of Parkinsonian Neural Circuitry. Science 324, 354-359.

Guo, S., Zhuang, P., Hallett, M., Zheng, Z., Zhang, Y., Li, J., and Li, Y. (2013). Subthalamic deep brain stimulation for Parkinson's disease: Correlation between locations of oscillatory activity and optimal site of stimulation. Parkinsonism & Related Disorders 19, 109-114.

Hirschmann, J., Butz, M., Hartmann, C.J., Hoogenboom, N., Özkurt, T.E., Vesper, J., Wojtecki, L., and Schnitzler, A. (2016). Parkinsonian Rest Tremor Is Associated With Modulations of Subthalamic High-Frequency Oscillations. Movement Disorders, n/a-n/a.

Hohlefeld, F.U., Huchzermeyer, C., Huebl, J., Schneider, G.H., Nolte, G., Brucke, C., Schonecker, T., Kuhn, A.A., Curio, G., and Nikulin, V.V. (2013). Functional and effective connectivity in subthalamic local field potential recordings of patients with Parkinson's disease. Neuroscience 250, 320-332.

Hutchison, W.D., Allan, R.J., Opitz, H., Levy, R., Dostrovsky, J.O., Lang, A.E., and Lozano, A.M. (1998). Neurophysiological identification of the subthalamic nucleus in surgery for Parkinson's disease. Annals of Neurology 44, 622-628.

Khan, M.F., Mewes, K., Gross, R.E., and Škrinjar, O. (2008). Assessment of Brain Shift Related to Deep Brain Stimulation Surgery. Stereotactic and Functional Neurosurgery 86, 44-53.

Kühn, A.A., Tsui, A., Aziz, T., Ray, N., Brücke, C., Kupsch, A., Schneider, G.-H., and Brown, P. (2009). Pathological synchronisation in the subthalamic nucleus of patients with Parkinson's disease relates to both bradykinesia and rigidity. Experimental Neurology 215, 380-387.

Li, Q., Ke, Y., Chan, D.C.W., Qian, Z.-M., Yung, K.K.L., Ko, H., Arbuthnott, G.W., and Yung, W.-H. (2012). Therapeutic Deep Brain Stimulation in Parkinsonian Rats Directly Influences Motor Cortex. Neuron 76, 1030-1041.

Little, S., and Brown, P. (2014). Focusing Brain Therapeutic Interventions in Space and Time for Parkinson’s Disease. Current Biology 24, R898-R909.

Little, S., Pogosyan, A., Neal, S., Zavala, B., Zrinzo, L., Hariz, M., Foltynie, T., Limousin, P., Ashkan, K., FitzGerald, J., *et al.* (2013). Adaptive Deep Brain Stimulation In Advanced Parkinson Disease. Annals of Neurology 74, 449-457.

Litvak, V., Jha, A., Eusebio, A., Oostenveld, R., Foltynie, T., Limousin, P., Zrinzo, L., Hariz, M.I., Friston, K., and Brown, P. (2011). Resting oscillatory cortico-subthalamic connectivity in patients with Parkinson's disease. Brain 134, 359-374.

Luft, C.D.B., Nolte, G., and Bhattacharya, J. (2013). High-Learners Present Larger Mid-Frontal Theta Power and Connectivity in Response to Incorrect Performance Feedback. The Journal of Neuroscience 33, 2029-2038.

Maks, C.B., Butson, C.R., Walter, B.L., Vitek, J.L., and McIntyre, C.C. (2009). Deep brain stimulation activation volumes and their association with neurophysiological mapping and therapeutic outcomes. Journal of Neurology, Neurosurgery & Psychiatry 80, 659-666.

McClelland, S. (2011). A cost analysis of intraoperative microelectrode recording during subthalamic stimulation for Parkinson's disease. Movement Disorders 26, 1422-1427.

Nolte, G., Bai, O., Wheaton, L., Mari, Z., Vorbach, S., and Hallett, M. (2004). Identifying true brain interaction from EEG data using the imaginary part of coherency. Clinical Neurophysiology 115, 2292-2307.

Nolte, G., Ziehe, A., Nikulin, V.V., Schlögl, A., Krämer, N., Brismar, T., and Müller, K.-R. (2008). Robustly Estimating the Flow Direction of Information in Complex Physical Systems. Physical Review Letters 100, 234101.

Novak, P., Przybyszewski, A.W., Barborica, A., Ravin, P., Margolin, L., and Pilitsis, J.G. (2011). Localization of the subthalamic nucleus in Parkinson disease using multiunit activity. Journal of the Neurological Sciences 310, 44-49.

Oswal, A., Beudel, M., Zrinzo, L., Limousin, P., Hariz, M., Foltynie, T., Litvak, V., and Brown, P. (2016). Deep brain stimulation modulates synchrony within spatially and spectrally distinct resting state networks in Parkinson's disease. Brain 139, 1482-1496.

Paffi, A., Camera, F., Apollonio, F., d'Inzeo, G., and Liberti, M. (2015). Numerical characterization of intraoperative and chronic electrodes in deep brain stimulation. Frontiers in Computational Neuroscience 9, 2.

Petersen, M.V., Lund, T.E., Sunde, N., Frandsen, J., Rosendal, F., Juul, N., and Østergaard, K. (2016). Probabilistic versus deterministic tractography for delineation of the cortico-subthalamic hyperdirect pathway in patients with Parkinson disease selected for deep brain stimulation. Journal of Neurosurgery, 1-12.

Sharott, A., Gulberti, A., Zittel, S., Tudor Jones, A.A., Fickel, U., Münchau, A., Köppen, J.A., Gerloff, C., Westphal, M., Buhmann, C., *et al.* (2014). Activity Parameters of Subthalamic Nucleus Neurons Selectively Predict Motor Symptom Severity in Parkinson's Disease. The Journal of Neuroscience 34, 6273-6285.

Sharott, A., Magill, P.J., Bolam, J.P., and Brown, P. (2005). Directional analysis of coherent oscillatory field potentials in the cerebral cortex and basal ganglia of the rat. Journal of Physiology-London 562, 951-963.

Telkes, I., Jimenez-Shahed, J., Viswanathan, A., Abosch, A., and Ince, N.F. (2016). Prediction of STN-DBS Electrode Implantation Track in Parkinson's Disease by Using Local Field Potentials. Frontiers in Neuroscience 10, 198.

van Wijk, B.C.M., Beudel, M., Jha, A., Oswal, A., Foltynie, T., Hariz, M.I., Limousin, P., Zrinzo, L., Aziz, T.Z., Green, A.L., *et al.* (2016). Subthalamic nucleus phase–amplitude coupling correlates with motor impairment in Parkinson's disease. Clinical Neurophysiology 127, 2010-2019.

Vanegas-Arroyave, N., Lauro, P.M., Huang, L., Hallett, M., Horovitz, S.G., Zaghloul, K.A., and Lungu, C. (2016). Tractography patterns of subthalamic nucleus deep brain stimulation. Brain.

Vinck, M., Oostenveld, R., van Wingerden, M., Battaglia, F., and Pennartz, C.M.A. (2011). An improved index of phase-synchronization for electrophysiological data in the presence of volume-conduction, noise and sample-size bias. NeuroImage 55, 1548-1565.

Weinberger, M., Mahant, N., Hutchison, W.D., Lozano, A.M., Moro, E., Hodaie, M., Lang, A.E., and Dostrovsky, J.O. (2006). Beta oscillatory activity in the subthalamic nucleus and its relation to dopaminergic response in Parkinson's disease. Journal of Neurophysiology 96, 3248-3256.

Whitmer, D., de Solages, C., Hill, B.C., Yu, H., Henderson, J.M., and Bronte-Stewart, H. (2012). High frequency deep brain stimulation attenuates subthalamic and cortical rhythms in Parkinson's disease. Frontiers in Human Neuroscience 6.

Whitmer, D., and White, C.N. (2012). Evidence of Human Subthalamic Nucleus Involvement in Decision Making. Journal of Neuroscience 32, 8753-8755.

Yoshida, F., Martinez-Torres, I., Pogosyan, A., Holl, E., Petersen, E., Chen, C.C., Foltynie, T., Limousin, P., Zrinzo, L.U., Hariz, M.I., and Brown, P. (2010). Value of subthalamic nucleus local field potentials recordings in predicting stimulation parameters for deep brain stimulation in Parkinson's disease. Journal of neurology, neurosurgery, and psychiatry 81, 885-889.

Zaidel, A., Spivak, A., Grieb, B., Bergman, H., and Israel, Z. (2010). Subthalamic span of β oscillations predicts deep brain stimulation efficacy for patients with Parkinson's disease. Brain 133, 2007-2021.

Zrinzo, L., Foltynie, T., Limousin, P., and Hariz, M. (2012). Image-verified deep brain stimulation reduces risk and cost with no apparent impact on efficacy. Movement Disorders 27, 1585-1586.

Figures:

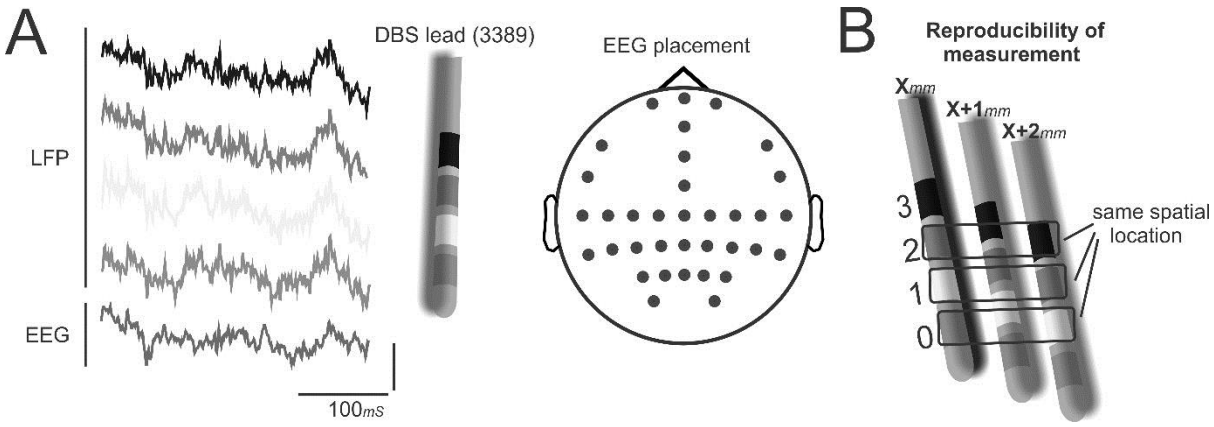

Figure 1: Experimental setup and LFP recorded in STN-cortex loop**. (**A) An example of recorded EEG and LFP signals with the quadripolar DBS electrode along the trajectory to the STN (left plot). The topography of EEG electrode placement during DBS surgery (right plot). (B) Pictogram shows the subcortical mapping procedure while descending the DBS lead. The DBS electrode contains four macroelectrode contacts (length 1.5 mm each), which are separated by 0.5 mm. Contact 0 was the most caudal and contact 3 the most rostral electrode contact.

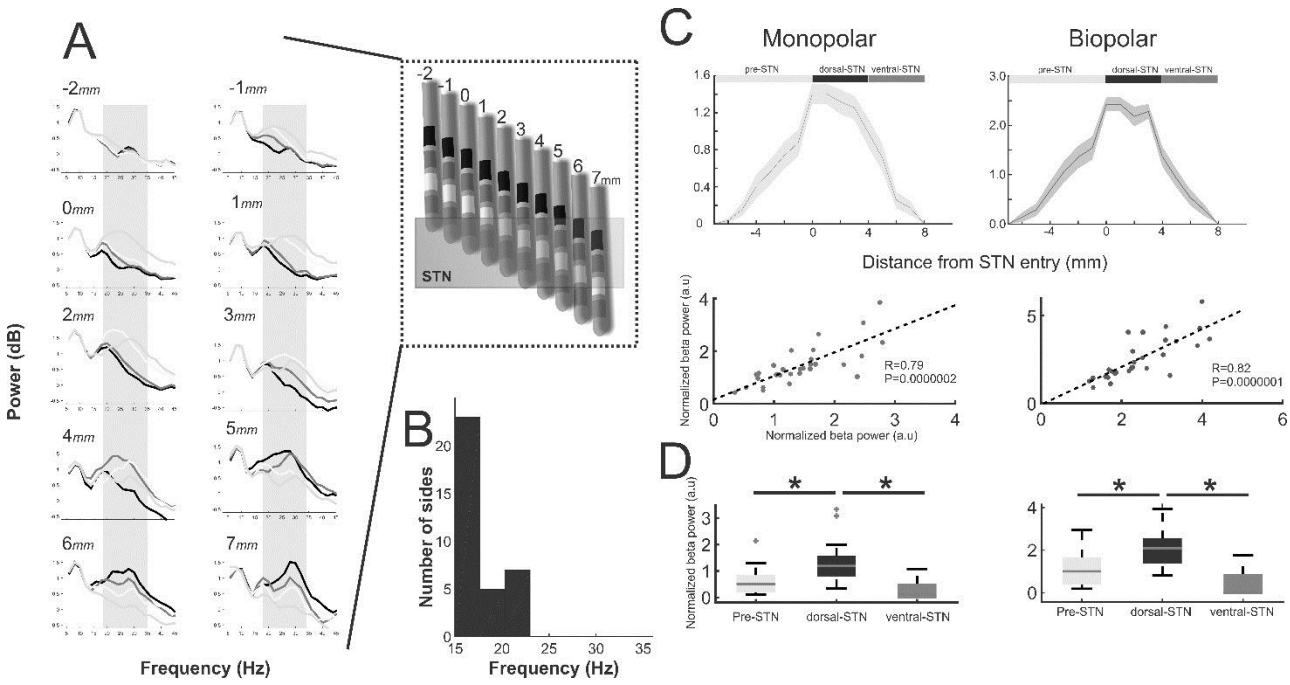

Figure 2: Oscillatory power spectrum in the STN. (A) An example of LFP signals recorded with the chronic DBS electrode (spectral plot from 5-45 Hz) while descending it in steps of 1 mm. The shaded area indicates the spatial extend of the STN (B) Distribution of beta peak in the STN. (C) Group normalized beta oscillation for the monopolar DBS contact 0 and the biplorized pair 01 along the trajectory throughout the STN (upper plot). Correlation between contact 0 / contact 1 (left plot) and contact pair 01 / contact pair 12 (right plot), respectively, at the upper STN border. (D) Significant beta oscillation in the dorsal STN with both monopolar (contact-0) and bioplorized (pair contact 01) analysis; box plots show the median, the 25^{th}/75^{th} percentiles and the maximum/minimum values of the beta oscillations in the dorsal and ventral STN, respectively. Outliers are depicted by crosses.

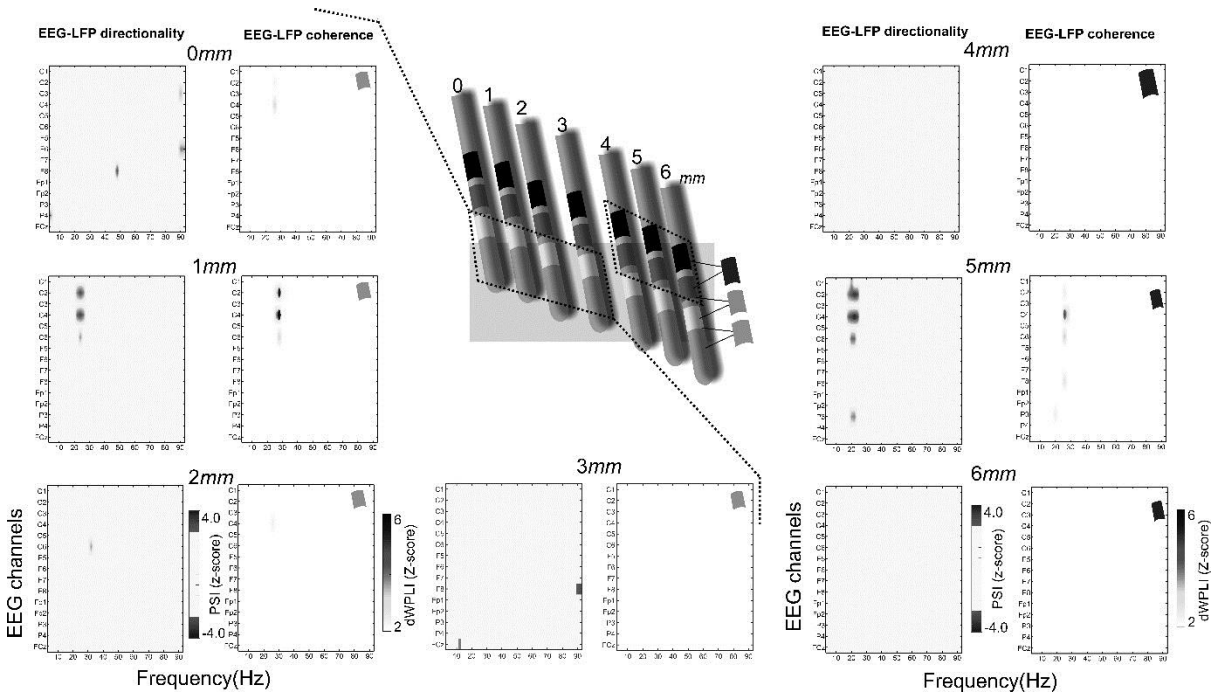

Figure 3: Cortico-subcortical connectivity measurement. Reproducibility of phase coherence and directionality between left STN-LFP and EEG electrodes in one representative PD patient across different STN depths.

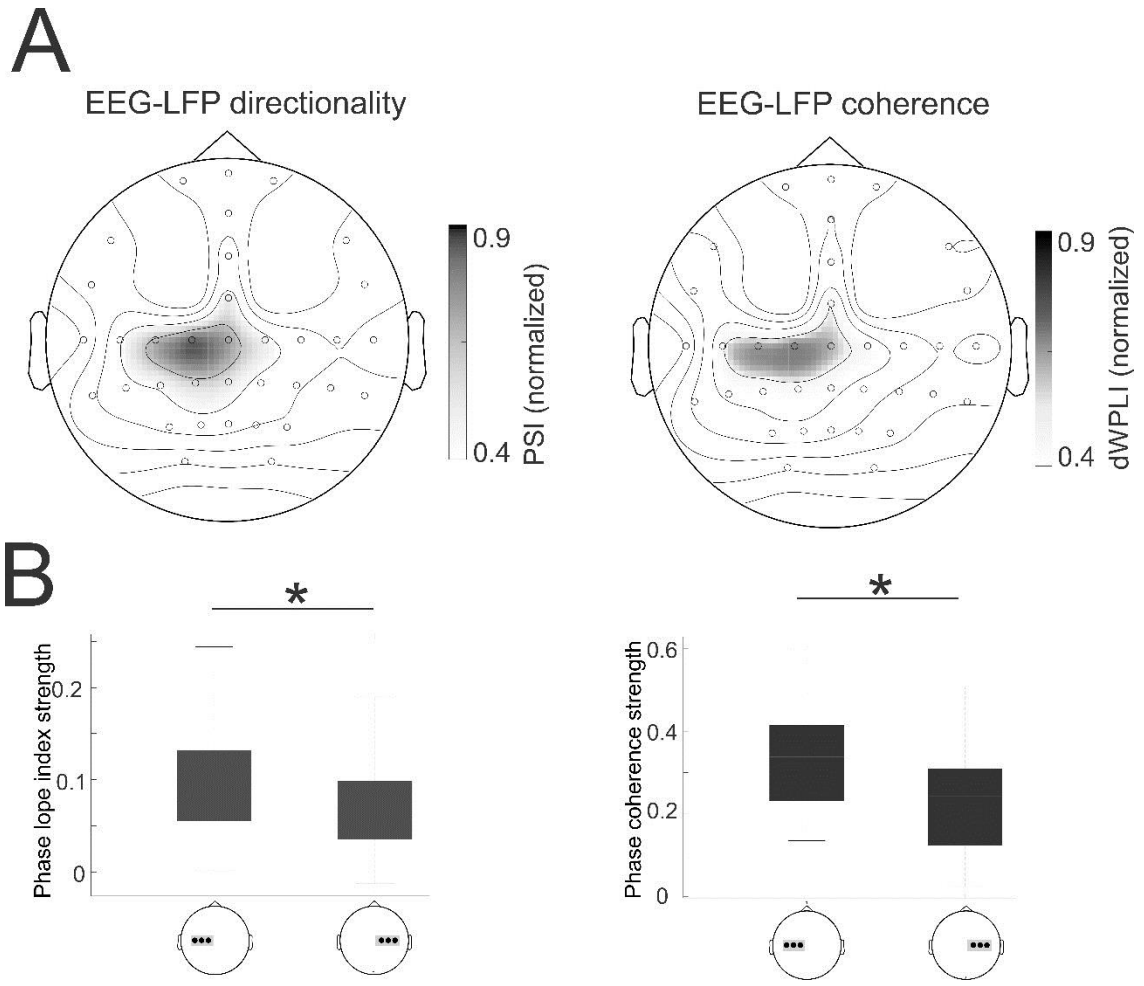

Figure 4: (A) Topographic group data are showing the spatial specificity of LFP-EEG phase coherence and effective connectivity (left plot). (B) The STN-motor cortex connectivity shows significant laterality to the ipsilateral side.

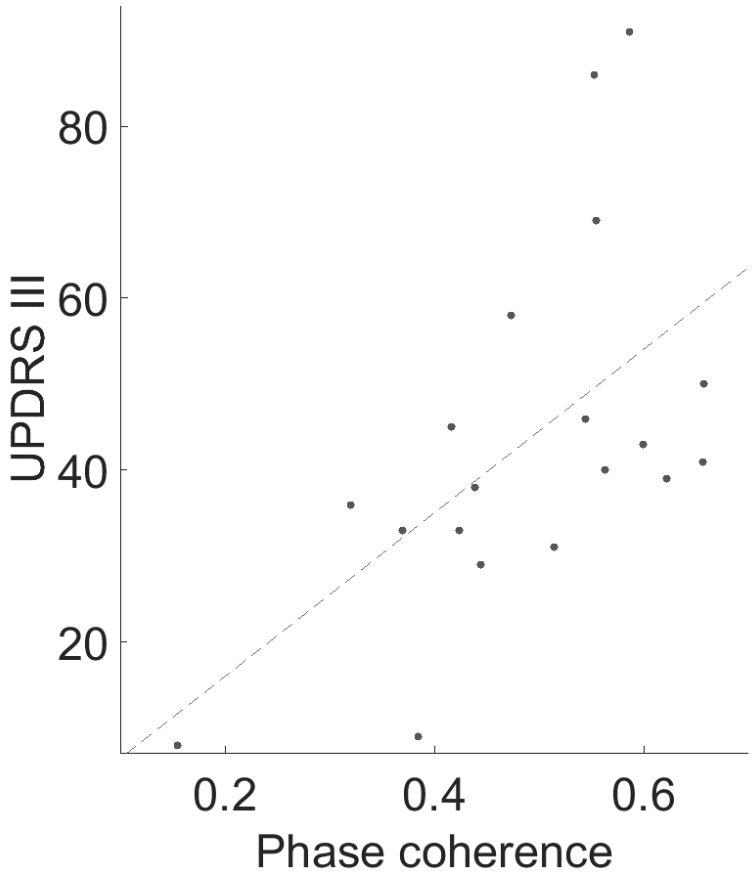

Figure 5: Correlation between cortico-subcortical connectivity and motor symptoms. The phase coherence between STN and motor cortex correlated significantly with the severity of motor symptoms (UPDRS III in the medication OFF state).

Subthalamic resonance properties predict cortico-subcortical motor network connectivity and deep brain stimulation effects in Parkinson's disease

Ramin Azodi-Avval, Alireza Gharabaghi*

Division of Functional and Restorative Neurosurgery, and Centre for Integrative Neuroscience, Eberhard Karls University Tuebingen, Germany

* Correspondence: Prof. Dr. Alireza Gharabaghi, Division of Functional and Restorative Neurosurgery, Eberhard Karls University, Otfried-Mueller-Str.45, 72076 Tuebingen, Germany, Tel: +49 7071 29 83550, Fax: +49 7071 29 25104, E-Mail address: alireza.gharabaghi@uni-tuebingen.de

Abbreviations: DBS=deep brain stimulation; dWPLI=debiased weighted phase lag index; BO=beta oscillations; HFO= high frequency oscillation; LFP=local field potential; STN=subthalamic nucleus; sEPs= subcortical evoked potentials.

Abstract

Deep brain stimulation (DBS) of the subthalamic nucleus (STN) is an established therapy for the symptomatic treatment of Parkinson's disease (PD). The subcortical dynamics in response to DBS in relation to local STN biomarkers and electrophysiological motor network patterns are still unclear. To address this, we simultaneously recorded electroencephalography and stepwise local field potentials (LFPs) with quadripolar chronic DBS electrode along the surgical trajectory to the STN in 13 PD patients. In the resting state, two oscillatory regions were found in STN, in the beta-band and high frequency oscillation (HFO)-band. Furthermore, the LFP activity in responses to DBS at different stimulation frequencies and in different subcortical depths across the STN was investigated. We observed that the subcortical evoked potentials (sEPs) had distinct spatial and temporal properties in STN. The sEPs were prominent in the dorsal part of the STN; their location in the STN correlated highly with the region in the STN where the resting motor-subthalamic coherence and the HFO reached their highest values as well. There was, however, no correlation with the beta oscillatory region. Moreover, an oscillation model was applied to the sEPs to extract the dynamic properties at different subcortical depths. The findings indicated that the area with the most prominent sEPs in the dorsal STN was also the one with the least resistant to DBS (i.e. low damping values) and the maximum energy absorption (i.e. resonance properties). During therapeutic stimulation, the damping of the system increased, reflecting a resonance inhibiting effect. The spatial location of the clinically most effective contact matched with the location of the strongest sEPs. These findings suggest that this spot in the STN may facilitate the electrical stimulation effects by decoupling the pathological STN-motor cortex coupling during therapeutic DBS.

Introduction

Deep brain stimulation (DBS) of the subthalamic nucleus (STN) is the most common neurosurgical procedure for the symptomatic treatment of Parkinson's disease (PD) (Krack and Hariz, 2013; Lozano and Lipsman, 2013; Odekerken et al., 2013b). However, the optimal site of stimulation within the STN for effective treatment is still not completely understood. Higher discharge rates (Deffains et al., 2014), synchronization in the beta oscillation frequencies range (BO, 14-35 Hz) (Priori et al., 2004; Ray et al., 2008; Yoshida et al., 2010), high frequency oscillations (Hirschmann et al., 2016; Wang et al., 2014), and beta-coupled high frequency oscillations have all been located in the dorsolateral motor part of the STN (Yang et al., 2014); this area has, therefore, been suggested as the best site for DBS. This region in the STN is anatomically linked to the motor cortical circuit (Chiken and Nambu, 2015; Haynes and Haber, 2013) and has significant functional connectivity in the oscillatory beta band to motor/premotor cortical areas (Fogelson et al., 2006; Hirschmann et al., 2011; Li et al., 2012; Litvak et al., 2011; Oswal et al., 2016; van Wijk et al., 2016). Moreover, relevant correlations between each these different electrophysiological biomarkers and the severity of different PD motor symptoms has been demonstrated (Hirschmann et al., 2016; Kato et al., 2015; Kühn et al., 2009; López-Azcárate et al., 2010; Wang et al., 2014; Weiss et al., 2015). Given the spatial and spectral diversity of oscillatory activity in basal ganglia loop (Brittain and Brown, 2014; Little and Brown, 2014), choosing the best site for effective treatment seems to remain an ongoing challenge.

Nonetheless, both pharmacological treatment with L-dopa (Barbeau, 1969; Chaudhuri and Schapira, 2009; Nagatsu and Sawada, 2009) and neurostimulation by DBS (Lozano and Lipsman, 2013; Odekerken et al., 2013a; Schuepbach et al., 2013) have shown promising results in the alleviation of PD symptoms. There are several lines of research reporting changes of pathological beta synchronization both at the local level (STN or cortical region) and in the long-distance cortico-subcortical communication by the administration of dopaminergic medication (Litvak et al., 2011; Oswal et al., 2016). Similarly, neural modulation by delivering subthalamic high-frequency DBS led

to the suppression of beta oscillations within the STN in the low beta-band (Kühn et al., 2008; Whitmer et al., 2012); and to the reduction of coupling between the phase of the beta rhythm and the amplitude of broadband gamma activity in the primary motor cortex of PD patients (de Hemptinne et al., 2013; de Hemptinne et al., 2015). Furthermore, long range STN–cortical interactions could be functionally decoupled during DBS (Oswal et al., 2016). However, the impact of DBS modulation on neural oscillations in relation to the site of stimulation within the STN is still not well investigated.

Direct perturbation of neural activity by electrical stimulation can be used to probe dynamical system properties. In fact, if the applied frequency of the electrical stimulation is close enough to the natural frequency of the system, the amplitude of the evoked response reaches maximum values; accordingly, maximum power absorption of the stimulation occurs in the system (=minimum energy dissipation). This kind of response is also referred to as resonance. In a study by Eusebio and colleagues (Eusebio et al., 2009), different STN DBS stimulation frequencies revealed the natural frequency (resonance frequency) of the system in PD to the at 20 Hz; the maximum cortical evoked potential occurred at 20 Hz STN DBS. In parallel to this approach, the intrinsic dynamical properties of different cortical areas were revealed by transcranial magnetic stimulation (Rosanova et al., 2009). However, no study has investigated the subcortical dynamical properties of DBS and their relationship to local and distant physiological biomarkers.

We hypothesized that the effectiveness of DBS would be predicted by the dynamical properties of local oscillatory activity and its cortico-subcortical functional coupling. In order to test this, we recorded scalp EEG signals covering the central, frontal, partial, and midline regions during intraoperative mapping of the STN via LFPs acquired from the quadripolar chronic DBS electrode during DBS implantation surgery. We expected that the local oscillatory responses to stimulation in the STN region would reveal their involvement in different cortico-subcortical loops.

Materials and Methods

Patients and neurosurgical procedure

Thirteen patients (two females; age: 66.07±4.46 years, mean ± STD; disease duration: 11.38 ± 2.32 years), who underwent implantation of DBS electrodes in the STN, were recruited for this study. Patients did not receive dopamine for at least 12h before surgery according to the standard operational procedures. Intraoperative propofol medication was discontinued at least 30 minutes before electrophysiological recordings were initiated (Azodi-Avval and Gharabaghi, 2015). The study was conducted with the patients' informed consent and in accordance with the guidelines approved by the local ethics committee of the University Hospital Tuebingen.

Data collection and pre-processing

Spontaneous cortical activity was recorded with EEG surface electrodes (Ag/AgCl electrodes, MedCaT GmbH, Netherlands) during DBS operation from 30 up to 39 sensors covering frontal, central and parietal regions (Fig. 1A). EEG signals were sampled at 1.4 kHz and stored in the NeuroOmega system for further offline analyses. LFP activity from the quadripolar DBS electrode lead (four ring contacts, Medtronic, Model 3387) was collected at two sampling rates, 1.4 kHz and 4.8 kHz simultaneously, while the electrode was descended in steps of 1 mm for mapping of the STN region. Recording LFP with a high sampling rate provides a better temporal resolution for detecting fast evoked responses to electrical stimulation.

LFP signals were first recorded for at least 30 seconds with the chronic DBS electrode at each depth; thereafter, stimulation pulses (bi-phasic, 1 Hz, 1.5 mA; 5 Hz, 1 / 2 / 3 mA, 100 μsec, current-controlled) were applied at the same depth for 30 seconds as well. The reference electrodes were attached to the ears and the ground was placed on the nasion. The impedance was set at ~1 KΩ and below 0.5 KΩ, for the intracranial and the EEG electrodes, respectively.

Data analysis of EEG and LFPs were performed in Matlab (version 2014b, Mathworks, Massachusetts, USA) using custom-made scripts, and in Fieldtrip, an open source analysis toolbox

(Oostenveld et al., 2011, http://fieldtrip.fcdonders.nl/). Signals were epoched in half seconds segments for resting-state data recording, and all artifacts epochs were removed by the Fieldtrip artifact rejection method. Line noise at 50 Hz and the harmonics were removed with a notch filter.

LFP power analysis

Power analysis of LFPs was computed using the Hanning taper for the lower frequency band (5-45 Hz) and discrete prolate spheroidal sequences tapers (DPSS, smoothing bandwidth ± 5 Hz) for the higher frequency band (60-350) (Fries et al., 2008; Mitra and Pesaran, 1999; Schoffelen et al., 2011). This LFP power analysis is particularly well suited for identifying the predominant oscillatory areas of the STN (Trottenberg et al., 2007; Zaidel et al., 2010) and for resolving the individual variability of frequency peaks for each patient (de Solages et al., 2010).

To calculate high oscillatory activity at each depth, we determined the individual frequency peak (within a given frequency band) for each STN level and then averaged the power in three contiguous bins (± 5 Hz) around this peak. This maximum average value was then normalized by dividing it by the total power from 50-350 Hz.

Cortico-subcortical connectivity

To investigate the cortico-subcortical functional coupling, the Weighted Phase Lag Index (WPLI) (Vinck et al., 2011) was calculated between EEG and LFP as a measure of phase consistency between two distal regions for each level within the STN (Azodi-Avval and Gharabaghi, 2015).

$$WPLI_{EEG-LFP} = \frac{n^{-1}\sum_{n=1}^{N}\left|imag\left(S_{EEG-LFP\,n}\right)\right| sgn\left(imag\left(S_{EEG-LFP\,n}\right)\right)}{n^{-1}\sum_{n=1}^{N} imag\left(S_{EEG-LFP\,n}\right)} \quad 1$$

where S is the cross-spectrum density matrix, imag the imaginary part and sgn the sign function. Since this measure eliminates zero phase lag signals, it is insensitive to the volume conduction of neural activity; a common challenge during EEG recordings. Due to the small number of trials, the debiased WPLI (dWPLI) was used to provide reliable phase coherence estimation (Vinck et al., 2011; Phillip et al., 2014). In our case, dWPLI was normalized by its standard deviation, which was computed by the

jackknife method; absolute values larger than 1.96 (corresponding to $p<0.05$) were considered statistically significant (Hohlefeld et al., 2013; Luft et al., 2013; Nolte et al., 2008).

Resonance properties in subcortical region

In order to establish damping measurements of different subcortical sites in response to electrical stimulations, an oscillation model was used. Here, damping refers to the energy dissipation properties of a brain region under electrical stimulation. If the amplitude of the evoked potentials response (sEPs) to a single DBS pulse (such as a 1 Hz stimulation) undergoes many oscillations (EPs) before dumping (i.e. the inherent resistance) brings it to baseline again, this response is known as the underdamped oscillation (Fig. 2A). A high damping factor of a brain site prevents the system from being resonant (with high sEPs after stimulation), while a low damping value of the stimulated area results in response with many oscillations. The damping factor becomes important when the system (e.g. the brain site) is under continuous electrical stimulation; the closer the stimulation frequency is to the natural frequency of the system, the higher the number of cycles (longer decay time) (Fig. 2B). Here, to capture the damping properties of the underdamped oscillation, a mathematical model was applied. The oscillation can be written as a second-order autonomous differential equations,

$$\ddot{x} + 2\varsigma\omega_0\dot{x} + \omega_0^2 x = 0 \qquad 2$$

where ω_0 is the angular frequency and dimensionless and ξ is a constant called the damping ratio. Assuming $2\varsigma < \omega_0$, we can model the resulting evoked response after stimulation with the following equation, which is the solution of the equation (2),

$$x(t) = Ae^{-\varsigma\omega_n t}\sin\left(\omega_d t + \phi\right) \qquad 3$$

where,

$$\omega_d = \omega_n\sqrt{1-\varsigma^2} = 2\pi/\left(t_2 - t_1\right)$$

where ω_d is the damped frequency reflecting how the sinusoidal oscillation decays exponentially over time, and ω_n is the underdamped frequency. To estimate the damping experimentally from real data,

the logarithmic decrement method was used. This method is based on the ratios of two peak oscillations written as following,

$$\frac{x_1}{x_2} = \frac{x_1(t)}{x_1(t+nT)} = \frac{e^{-\varsigma\omega_n t}}{e^{-\varsigma\omega_n (t+nT)}} = e^{-\varsigma\omega_n n(t_2-t_1)} \quad 4$$

Taking the natural logarithm from this expression, we have a logarithmic decrement as following,

$$\delta = In\left(\frac{x_1(t)}{x_1(t+nT)}\right) = \varsigma\omega_n(t_2-t_1) = \frac{2\pi\varsigma}{\sqrt{1-\varsigma^2}} \quad 5$$

Moreover, when solving this equation with regard to the damping, we have

$$\varsigma = \sqrt{\frac{1}{(2\pi/\delta)^2}} \quad 6$$

In this study, by delivering DBS at fixed frequencies in different subcortical depths along the surgical trajectory, the resonance area within the STN could be revealed.

Statistical analysis

The statistical analysis was conducted by using the statistics toolbox for Matlab, and the level of statistical significance was defined as p=0.05. Nonparametric Mann–Whitney U-test was used to compare two groups. Correlation analysis was performed with the Spearman's rank test. Unless otherwise stated, all values were expressed as mean ± SEM. The normalization values were calculated on the basis of the following formula:

$$\mathrm{V}' = (V - \min(V))./(\max(V) - \min(V)), \quad 7$$

where V is the raw vector.

Results

The patients enrolled in this study were examined before surgery using the motor part of the Unified Parkinson's Disease Rating Scale (UPDRS III) while applying the L-Dopa test (medication "ON" and "OFF"). The mean UPDRS III score was 24.15±7.80 and 49.77±12.58 in the ON state and OFF states,

respectively. The clinical information is summarized in Table 1. Intraoperative recordings during DBS surgery were performed in 13 PD patients.

STN mapping: power evaluation

We evaluated the power spectrum of the four DBS contacts (0 to 3) during mapping the STN. The calculation of the spectrum revealed spectral and spatial specificity for all patients. There was a prominent peak in the beta band, which was validated with other DBS contacts when the electrode was moved towards the target. The physical properties of the DBS lead provided the opportunity to record in same spatial STN location for several times (Fig. 1B). The resulting exemplary power spectrograms of one PD patient during STN mapping procedure is showed in Fig. 1B: The first peak in beta range appeared in the lowest contact (DBS 0) at 0 mm, i.e. when it entered the STN. Which descending the electrode further (after 2 mm), the same oscillatory region was detectable with the second lowest contact (DBS 1). The same pattern could be observed at DBS contact 2 (when descending another 2 mm), i.e when the lowest DBS contact 0 was at a depth of 4 mm below the STN entry (Fig. 1B). With this approach, the beta oscillatory region in the STN could be identified in all patients in an effective and robust way; the peak beta frequency was concentrated in the low beta-band 16.17±0.89 Hz.

Resting state cortico-subcortical connectivity

We next investigated the dynamic communication between simultaneously recorded subcortical neural activity in the STN and with ongoing cortical oscillations with the robust measure of phase coherence. To examine the spatial or spectral specificity of this phase coupling the respective coherence values were calculated at each depth during mapping the STN. The phase coupling between the STN and cortical sensors showed significant functional connectivity in the high beta-band. Exemplary data is shown for two PD (Fig. 3A). Group analysis revealed the spectral specificity of LFP-EEG coherence for the high beta-band (22.17±4.46 Hz; Fig. 3B), a spatial specificity at 2.41± 0.56 mm blow STN border. The peak of group cortical topography of this cortico-subthalamic coherence was located in the ipsilateral motor area (Fig. 3B).

Spatial and temporal properties of diminishing evoked potentials

To examine the responses of the STN region to low frequency stimulation at different subcortical depths, we DBS with 5 Hz and with 1 Hz. In the case of 5Hz stimulation, the intensity was randomly changed between 1 to 3 mA in steps of 1 mA. Fig. 4A shows the average response of subcortical evoked responses at different sites to 1 and 5 Hz DBS in two exemplary patients. The sEPs during mapping of STN show temporal and spatial specificity as well. Notably, various current intensities lead to the same spatial and temporal properties of sEPs, indicating that the intensity did not alter the latency and spatial location of sEPs. The variability of sEP amplitudes and temporal properties across the patient group (Fig. 4B), thus, reflects the related anatomical and oscillatory properties of the respective regions. Prominent sEPs occurred at 2.83±0.71 mm below STN border with a latency of 5.11±0.25 msec, 8.08±0.34 msec and 11.18±0.42 msec for P_1, P_3 and P_5, respectively (Fig. 5C). The amplitudes of these peaks were 513.82±139.55 µV, 270.76±109.31 µV and 162.3±116.62 µV. To check whether these peaks declined linearly, we next ran the Spearman's rank test (Fig. 4C, right).

High-frequency oscillations in the STN

Spectral analysis was performed in both resting state and during low frequency stimulation and detected HFO activity 2.50 ± 0.88 mm below the upper STN boundary, respectively. Fig. 5A, B display the power activity in the high-frequency range from 50 Hz to 400 Hz. Interestingly, the resting state HFO peak (322.54±3.72 Hz) and frequency of oscillating sEPs (338.12±12.56 Hz) were significantly correlated with each other (r=0.60, P=0.02).

Damping of subcortical regions

The subcortical responses to DBS revealed different morphologies of evoked responses which reflect the oscillatory properties of the respective area. Here, we measured the damping by using equation 6. Fig. 6A shows the damping factors for two exemplary patients; the results revealed a bell-shaped pattern of these factors within the STN for all patients. Consistent with the equations 2 and 3, both factors depended on the nature of the post-stimulation diminishing sEPs and had an inverse

relationship to each other (Fig. 6A). The lower damping factor of each patient correlated significantly with the highest HFO value in the STN (Fig. 6B).

Local HFO activity in STN and STN-motor network predict damping properties

The maximum local HFO activity (2.50±0.88 mm) in the STN co-located with the ipsilateral STN-motor cortex phase coupling in the beta-band (22.17±4.46) which was 2.41±0.56 mm below the STN entry; this finding is compatible with a motor cortex-STN interaction via a direct connection (hyperdirect pathway). Moreover, the spatial location of the most prominent sEPs (lowest subthalamic damping) was 2.83±0.71 mm below STN border. In each patient, the sites of maximum sEPs ($r=0.91$; $P=0.0003$; Spearman test) in the STN and highest local HFO, but not the site of maximum beta oscillations, correlated highly with the ipsilateral STN-motor cortex phase coherence. Notably, the location of maximum HFO power was different from the location of maximum beta oscillations, but correlated significantly with the location of maximum sEPs ($r=0.84$; $P=0.0005$; Spearman test).

Discussion

STN-DBS can serve as a powerful therapeutic tool for symptomatic PD treatment, reducing the pathological activity at both local and network levels (Oswal et al., 2016). Despite considerable research on the neurophysiology in PD patients and during STN-DBS, it is still not completely understood which physiologically defined spot within the STN may provide the best clinical response to electrical stimulation. We demonstrated for the first time that the dynamical properties of the STN region may be informative with regard to other pathological biomarkers in the basal ganglia loop and may even predict the best spot for therapeutic effects.

Different roles of beta-band and HFO oscillatory regions

Prominent beta oscillations play a crucial role in the state of Parkinson's disease (Brittain and Brown, 2014; Eusebio and Brown, 2007); there is considerable evidence supporting the claim that the degree of changes in beta synchronization in the STN and the cortical motor circuit, induced by L-

dopa medication, correlates with bradykinesia and rigidity (Kühn et al., 2009; Litvak et al., 2011(Fogelson et al., 2006). More recently, resting tremor in PD has been linked to the appearance of HFO in the STN (Hirschmann et al., 2016), which in turn has been inversely correlated with contralateral akinesia/rigidity scores (Wang et al., 2014). It has. Therefore, been suggested that local and long-range neural activities, particularly beta oscillation and their coupling with broadband gamma oscillations, may play a crucial role in the state of the Parkinson's disease (de Hemptinne et al., 2013; Swann et al., 2015). In fact, pathological low beta oscillations in STN decreased during high-frequency DBS, while the high beta-range seemed to play a critical role in STN-motor cortex coupling (Oswal et al., 2016; van Wijk et al., 2016). However, to the best of our knowledge, the evoked responses to DBS have not been studied in the different subcortical regions yet; nor have these local sEPs be compared to cortico-subcortical coupling or different local oscillatory patterns in the STN.

Delivering electrical stimulation at different subcortical depths across the STN will result in evoked responses on the basis of the neurophysiological properties of a stimulated region. Perturbing corticothalamic circuits by transcranial magnetic stimulation showed intrinsic electrophysiological properties of cortical sites (Rosanova et al., 2009). To date, no study has used a similar approach for different subcortical regions or in the PD state. Therefore, this study represented the first attempt to identify distinct oscillatory regions in the STN while simultaneously tracing cortico-subcortical interactions during DBS surgery. We observed different sEPs after the onset of DBS, reflecting the dynamical properties of the stimulated region. High spatial and spectral correlation between HFO and prominent sEPs suggested that the appearance of short-latency evoked activity most likely reflects the perturbation of the HFO oscillatory region. This argument is confirmed by the observation that short- and long-latency sEPs co-located with HFO and BO, respectively. (Supplementary figure)

Damping might facilitate cortico-subcortical DBS modulation

In the pathophysiology of PD patients, DBS is known to disrupt afferent and efferent coupling and information flow of cortico-subcortical communication in the cortico-STN loop (Chiken and Nambu,

2015; Li et al., 2012). In our study, we demonstrated the co-location of HFO-STN, low damping site and strong STN-motor cortex coupling. Consistent with our results, HFO-STN has previously been shown to correlate with motor symptoms and to be involved in motor circuit pathophysiology (Hirschmann et al., 2016; Wang et al., 2014). Notably, the temporal properties of sEPs in our study were consistent for different stimulation frequencies (1 Hz, 5Hz and 130 Hz) and intensities. It is, thus, likely that the frequency of sEPs conveys information about the neuronal characteristics of the stimulated region.

Eusebio and colleagues recorded cortical evoked potentials while stimulating at various DBS frequencies (between 5 and 30 Hz, in steps of 5 Hz) in the STN of PD patients and showed that the amplitude of cEP (recorded from the skull) increased significantly in the ipsilateral sensorimotor cortex at 20 Hz compared to other DBS frequencies. This indicated that, in PD patients, 20 Hz may be the frequency at which the basal ganglia-cortical network involving the STN tends to resonate. They also pointed out that under L-dopa administration the damping was raised in the basal ganglia-cortical network, thereby potentially limiting this loop to resonance at 20 Hz oscillation. Our results complement this study; instead of limiting the resonance effect with dopamine medication, we rather applied therapeutic stimulation to achieve a similar phenomenon. In fact, the reduction in sEPs during high- frequency stimulation suggests that the damping of the cortico-subcortical system (Fig. 7) increased, thereby, changing the system from the pathological resonance state to a rather normal condition. These results could offer practical and reliable markers for closed-loop stimulation, as sEPs have been to dynamically change with respect to the underlying neural activity.

Reference

Azodi-Avval, R., and Gharabaghi, A. (2015). Phase-dependent modulation as a novel approach for therapeutic brain stimulation. Frontiers in Computational Neuroscience 9.

Barbeau, A. (1969). L-Dopa Therapy in Parkinson's Disease: A Critical Review of Nine Years' Experience. Canadian Medical Association Journal 101, 59-68.

Brittain, J.-S., and Brown, P. (2014). Oscillations and the basal ganglia: Motor control and beyond. NeuroImage 85, Part 2, 637-647.

Chaudhuri, K.R., and Schapira, A.H.V. (2009). Non-motor symptoms of Parkinson's disease: dopaminergic pathophysiology and treatment. The Lancet Neurology 8, 464-474.

Chiken, S., and Nambu, A. (2015). Mechanism of Deep Brain Stimulation: Inhibition, Excitation, or Disruption? The Neuroscientist.

de Hemptinne, C., Ryapolova-Webb, E.S., Air, E.L., Garcia, P.A., Miller, K.J., Ojemann, J.G., Ostrem, J.L., Galifianakis, N.B., and Starr, P.A. (2013). Exaggerated phase-amplitude coupling in the primary motor cortex in Parkinson disease. Proceedings of the National Academy of Sciences of the United States of America 110, 4780-4785.

de Hemptinne, C., Swann, N.C., Ostrem, J.L., Ryapolova-Webb, E.S., San Luciano, M., Galifianakis, N.B., and Starr, P.A. (2015). Therapeutic deep brain stimulation reduces cortical phase-amplitude coupling in Parkinson's disease. Nat Neurosci 18, 779-786.

de Solages, C., Hill, B.C., Koop, M.M., Henderson, J.M., and Bronte-Stewart, H. (2010). Bilateral symmetry and coherence of subthalamic nuclei beta band activity in Parkinson's disease. Experimental Neurology 221, 260-266.

Deffains, M., Holland, P., Moshel, S., de Noriega, F.R., Bergman, H., and Israel, Z. (2014). Higher neuronal discharge rate in the motor area of the subthalamic nucleus of Parkinsonian patients. Journal of Neurophysiology 112, 1409-1420.

Eusebio, A., and Brown, P. (2007). Oscillatory activity in the basal ganglia. Parkinsonism & Related Disorders 13, S434-S436.

Eusebio, A., Pogosyan, A., Wang, S., Averbeck, B., Gaynor, L.D., Cantiniaux, S., Witjas, T., Limousin, P., Azulay, J.-P., and Brown, P. (2009). Resonance in subthalamo-cortical circuits in Parkinsons disease. Brain 132, 2139-2150.

Fogelson, N., Williams, D., Tijssen, M., van Bruggen, G., Speelman, H., and Brown, P. (2006). Different functional loops between cerebral cortex and the subthalmic area in Parkinson's disease. Cerebral Cortex 16, 64-75.

Fries, P., Womelsdorf, T., Oostenveld, R., and Desimone, R. (2008). The Effects of Visual Stimulation and Selective Visual Attention on Rhythmic Neuronal Synchronization in Macaque Area V4. The Journal of Neuroscience 28, 4823-4835.

Haynes, W.I.A., and Haber, S.N. (2013). The Organization of Prefrontal-Subthalamic Inputs in Primates Provides an Anatomical Substrate for Both Functional Specificity and Integration: Implications for Basal Ganglia Models and Deep Brain Stimulation. Journal of Neuroscience 33, 4804-4814.

Hirschmann, J., Butz, M., Hartmann, C.J., Hoogenboom, N., Özkurt, T.E., Vesper, J., Wojtecki, L., and Schnitzler, A. (2016). Parkinsonian Rest Tremor Is Associated With Modulations of Subthalamic High-Frequency Oscillations. Movement Disorders, n/a-n/a.

Hohlefeld, F.U., Huchzermeyer, C., Huebl, J., Schneider, G.H., Nolte, G., Brucke, C., Schonecker, T., Kuhn, A.A., Curio, G., and Nikulin, V.V. (2013). Functional and effective connectivity in subthalamic local field potential recordings of patients with Parkinson's disease. Neuroscience 250, 320-332.

Kato, K., Yokochi, F., Taniguchi, M., Okiyama, R., Kawasaki, T., Kimura, K., and Ushiba, J. (2015). Bilateral coherence between motor cortices and subthalamic nuclei in patients with Parkinson’s disease. Clinical Neurophysiology 126, 1941-1950.

Krack, P., and Hariz, M.I. (2013). Deep brain stimulation in Parkinson's disease: reconciliation of evidence-based medicine with clinical practice. Lancet Neurology 12, 25-26.

Kühn, A.A., Kempf, F., Brücke, C., Gaynor Doyle, L., Martinez-Torres, I., Pogosyan, A., Trottenberg, T., Kupsch, A., Schneider, G.-H., Hariz, M.I., *et al.* (2008). High-Frequency Stimulation of the Subthalamic Nucleus Suppresses Oscillatory β Activity in Patients with Parkinson's Disease in Parallel with Improvement in Motor Performance. The Journal of Neuroscience 28, 6165-6173.

Kühn, A.A., Tsui, A., Aziz, T., Ray, N., Brücke, C., Kupsch, A., Schneider, G.-H., and Brown, P. (2009). Pathological synchronisation in the subthalamic nucleus of patients with Parkinson's disease relates to both bradykinesia and rigidity. Experimental Neurology 215, 380-387.

Li, Q., Ke, Y., Chan, D.C.W., Qian, Z.-M., Yung, K.K.L., Ko, H., Arbuthnott, G.W., and Yung, W.-H. (2012). Therapeutic Deep Brain Stimulation in Parkinsonian Rats Directly Influences Motor Cortex. Neuron 76, 1030-1041.

Little, S., and Brown, P. (2014). Focusing Brain Therapeutic Interventions in Space and Time for Parkinson’s Disease. Current Biology 24, R898-R909.

López-Azcárate, J., Tainta, M., Rodríguez-Oroz, M.C., Valencia, M., González, R., Guridi, J., Iriarte, J., Obeso, J.A., Artieda, J., and Alegre, M. (2010). Coupling between Beta and High-Frequency Activity in the Human Subthalamic Nucleus May Be a Pathophysiological Mechanism in Parkinson's Disease. The Journal of Neuroscience 30, 6667-6677.

Lozano, Andres M., and Lipsman, N. (2013). Probing and Regulating Dysfunctional Circuits Using Deep Brain Stimulation. Neuron 77, 406-424.

Luft, C.D.B., Nolte, G., and Bhattacharya, J. (2013). High-Learners Present Larger Mid-Frontal Theta Power and Connectivity in Response to Incorrect Performance Feedback. The Journal of Neuroscience 33, 2029-2038.

Mitra, P.P., and Pesaran, B. (1999). Analysis of dynamic brain imaging data. Biophysical Journal 76, 691-708.

Nagatsu, T., and Sawada, M. (2009). L-dopa therapy for Parkinson's disease: Past, present, and future. Parkinsonism & Related Disorders 15, Supplement 1, S3-S8.

Nolte, G., Ziehe, A., Nikulin, V.V., Schlögl, A., Krämer, N., Brismar, T., and Müller, K.-R. (2008). Robustly Estimating the Flow Direction of Information in Complex Physical Systems. Physical Review Letters 100, 234101.

Odekerken, V.J.J., de Haan, R.J., Schurrman, P.R., and de Bie, R.M.A. (2013a). Subthalamic versus globus pallidus deep brain stimulation Reply. Lancet Neurology 12, 329-329.

Odekerken, V.J.J., van Laar, T., Staal, M.J., Mosch, A., Hoffmann, C.F.E., Nijssen, P.C.G., Beute, G.N., van Vugt, J.P.P., Lenders, M.W.P.M., Contarino, M.F., *et al.* (2013b). Subthalamic nucleus versus globus pallidus bilateral deep brain stimulation for advanced Parkinson's disease (NSTAPS study): a randomised controlled trial. Lancet Neurology 12, 37-44.

Oswal, A., Beudel, M., Zrinzo, L., Limousin, P., Hariz, M., Foltynie, T., Litvak, V., and Brown, P. (2016). Deep brain stimulation modulates synchrony within spatially and spectrally distinct resting state networks in Parkinson’s disease. Brain 139, 1482-1496.

Priori, A., Foffani, G., Pesenti, A., Tamma, F., Bianchi, A.M., Pellegrini, M., Locatelli, M., Moxon, K.A., and Villani, R.M. (2004). Rhythm-specific pharmacological modulation of subthalamic activity in Parkinson's disease. Experimental Neurology 189, 369-379.

Ray, N.J., Jenkinson, N., Wang, S., Holland, P., Brittain, J.S., Joint, C., Stein, J.F., and Aziz, T. (2008). Local field potential beta activity in the subthalamic nucleus of patients with Parkinson's disease is associated with improvements in bradykinesia after dopamine and deep brain stimulation. Experimental Neurology 213, 108-113.

Rosanova, M., Casali, A., Bellina, V., Resta, F., Mariotti, M., and Massimini, M. (2009). Natural Frequencies of Human Corticothalamic Circuits. The Journal of Neuroscience 29, 7679-7685.

Schoffelen, J.-M., Poort, J., Oostenveld, R., and Fries, P. (2011). Selective Movement Preparation Is Subserved by Selective Increases in Corticomuscular Gamma-Band Coherence. The Journal of Neuroscience 31, 6750-6758.

Schuepbach, W.M.M., Rau, J., Knudsen, K., Volkmann, J., Krack, P., Timmermann, L., Haelbig, T.D., Hesekamp, H., Navarro, S.M., Meier, N., *et al.* (2013). Neurostimulation for Parkinson's Disease with Early Motor Complications. New England Journal of Medicine 368, 610-622.

Swann, N.C., de Hemptinne, C., Aron, A.R., Ostrem, J.L., Knight, R.T., and Starr, P.A. (2015). Elevated synchrony in Parkinson disease detected with electroencephalography. Annals of Neurology 78, 742-750.

Trottenberg, T., Kupsch, A., Schneider, G.-H., Brown, P., and Kuehn, A.A. (2007). Frequency-dependent distribution of local field potential activity within the subthalamic nucleus in Parkinson's disease. Experimental Neurology 205, 287-291.

van Wijk, B.C.M., Beudel, M., Jha, A., Oswal, A., Foltynie, T., Hariz, M.I., Limousin, P., Zrinzo, L., Aziz, T.Z., Green, A.L., *et al.* (2016). Subthalamic nucleus phase–amplitude coupling correlates with motor impairment in Parkinson's disease. Clinical Neurophysiology 127, 2010-2019.

Vinck, M., Oostenveld, R., van Wingerden, M., Battaglia, F., and Pennartz, C.M.A. (2011). An improved index of phase-synchronization for electrophysiological data in the presence of volume-conduction, noise and sample-size bias. NeuroImage 55, 1548-1565.

Wang, J., Hirschmann, J., Elben, S., Hartmann, C.J., Vesper, J., Wojtecki, L., and Schnitzler, A. (2014). High-frequency oscillations in Parkinson's disease: Spatial distribution and clinical relevance. Movement Disorders 29, 1265-1272.

Weiss, D., Klotz, R., Govindan, R.B., Scholten, M., Naros, G., Ramos-Murguialday, A., Bunjes, F., Meisner, C., Plewnia, C., Krüger, R., and Gharabaghi, A. (2015). Subthalamic stimulation modulates cortical motor network activity and synchronization in Parkinson's disease. Brain 138, 679-693.

Whitmer, D., de Solages, C., Hill, B., Yu, H., Henderson, J.M., and Bronte-Stewart, H. (2012). High frequency deep brain stimulation attenuates subthalamic and cortical rhythms in Parkinson's disease. Frontiers in Human Neuroscience 6.

Yang, A.I., Vanegas, N., Lungu, C., and Zaghloul, K.A. (2014). Beta-Coupled High-Frequency Activity and Beta-Locked Neuronal Spiking in the Subthalamic Nucleus of Parkinson's Disease. The Journal of Neuroscience 34, 12816-12827.

Yoshida, F., Martinez-Torres, I., Pogosyan, A., Holl, E., Petersen, E., Chen, C.C., Foltynie, T., Limousin, P., Zrinzo, L.U., Hariz, M.I., and Brown, P. (2010). Value of subthalamic nucleus local field potentials recordings in predicting stimulation parameters for deep brain stimulation in Parkinson's disease. Journal of neurology, neurosurgery, and psychiatry 81, 885-889.

Zaidel, A., Spivak, A., Grieb, B., Bergman, H., and Israel, Z. (2010). Subthalamic span of β oscillations predicts deep brain stimulation efficacy for patients with Parkinson’s disease. Brain 133, 2007-2021.

Figures:

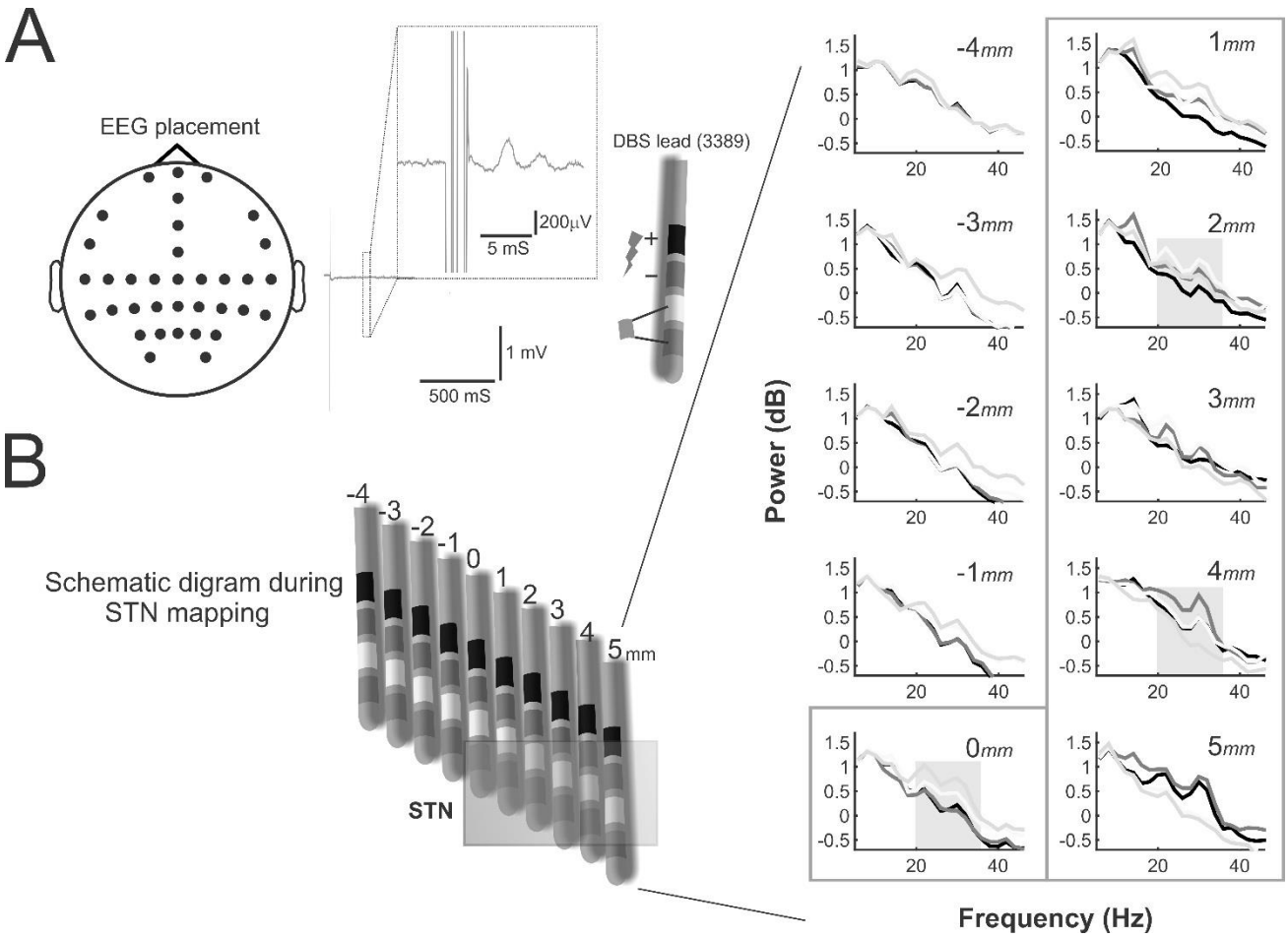

Figure 1: Experimental setup and recordings in the cortico-subcortical loop. (A) An example of recoded LFP signals with the quadripolar chronic DBS electrode during low-frequency stimulation; LFPs were recorded bipolarly from contacts 01 and stimulation was performed with contact 2 as an active and contact 3 as a return contact (right plot). Topography of EEG electrode placement during DBS surgery (left plot). (B) Identification of the STN boundary by calculating the power spectrum during mapping of the STN with four DBS contacts (0 to 3), showing the distinct spatial and spectral specificity of the beta oscillatory region starting at a depth of 0 mm (STN entry).

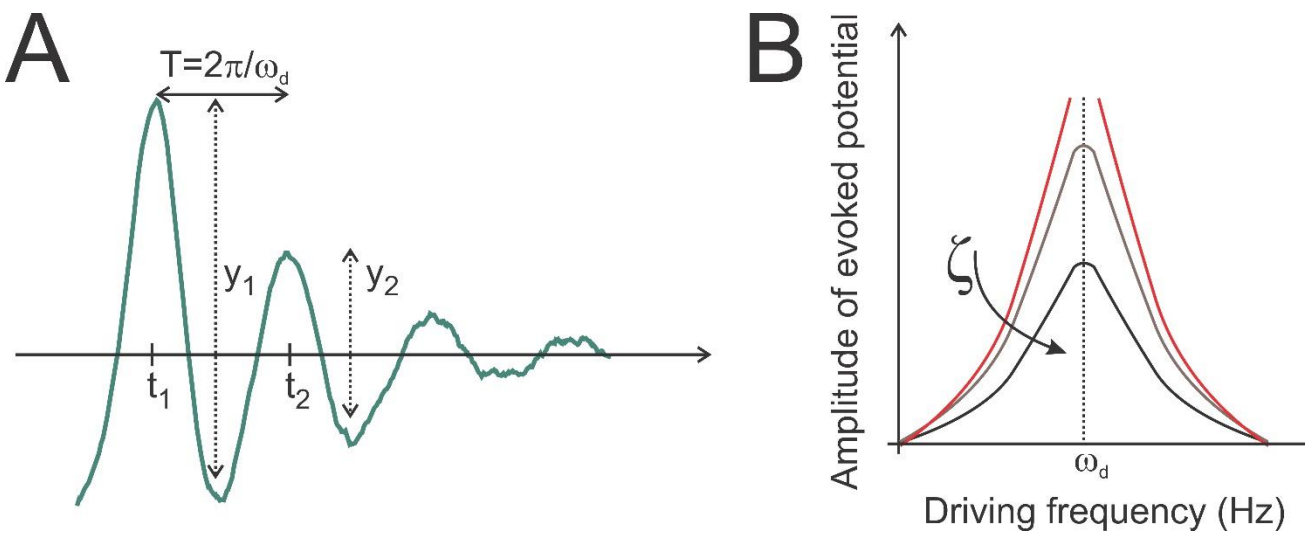

Figure 2: Underdamped oscillations and damping. (A) An example of an underdamped oscillation where the amplitude gradually decreased over time. y_1/ y_2 and t_1/ t_2 are representing the maximum first and second peak to peak amplitude and the period of oscillations, respectively. T refers to the period of oscillations and ω_d is the damped frequency. (B) The plot indicates the relationship between the amplitude of evoked response and the stimulation frequency in terms of decreasing damping. The lower the damping, the more resonance in the system.

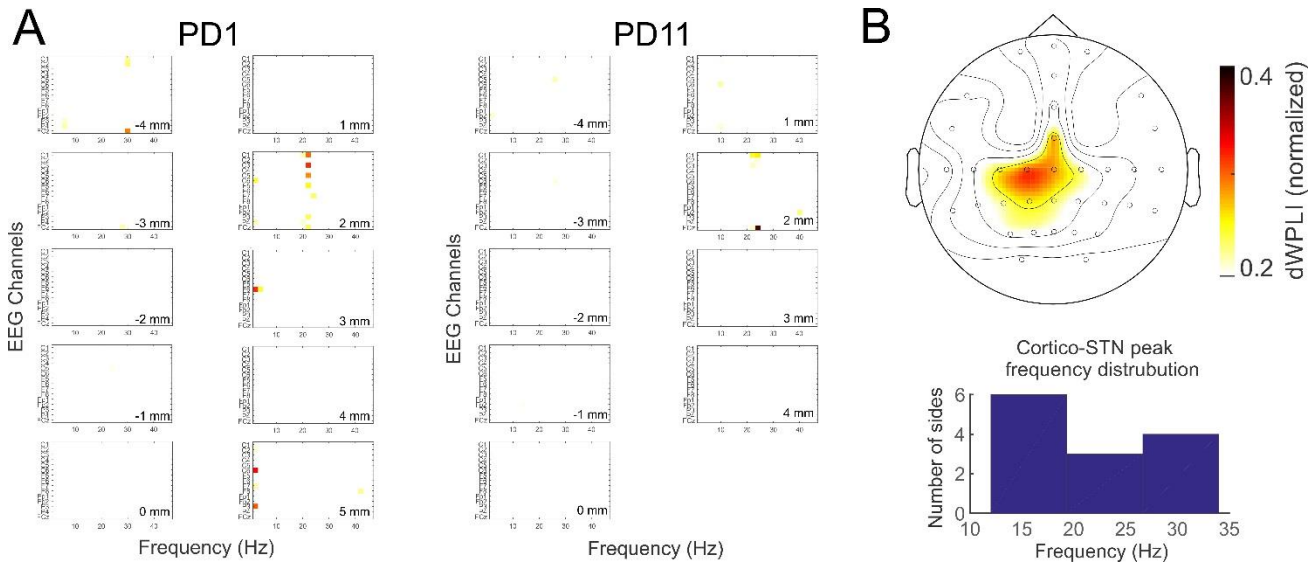

Figure 3: Cortico-subcortical functional connectivity. (A) Phase coherence between left STN-LFP and all EEG electrodes in two representative patients across different STN depths. (B) Topographic group data showing the spatial specificity of LFP-EEG phase coherence, i.e. C1/3; results for the right LFP-EEG coherence were flipped to the left side (upper plot). Distribution of peak frequencies (in 5 Hz bins) of the significant STN-cortex of each patient (lower plot).

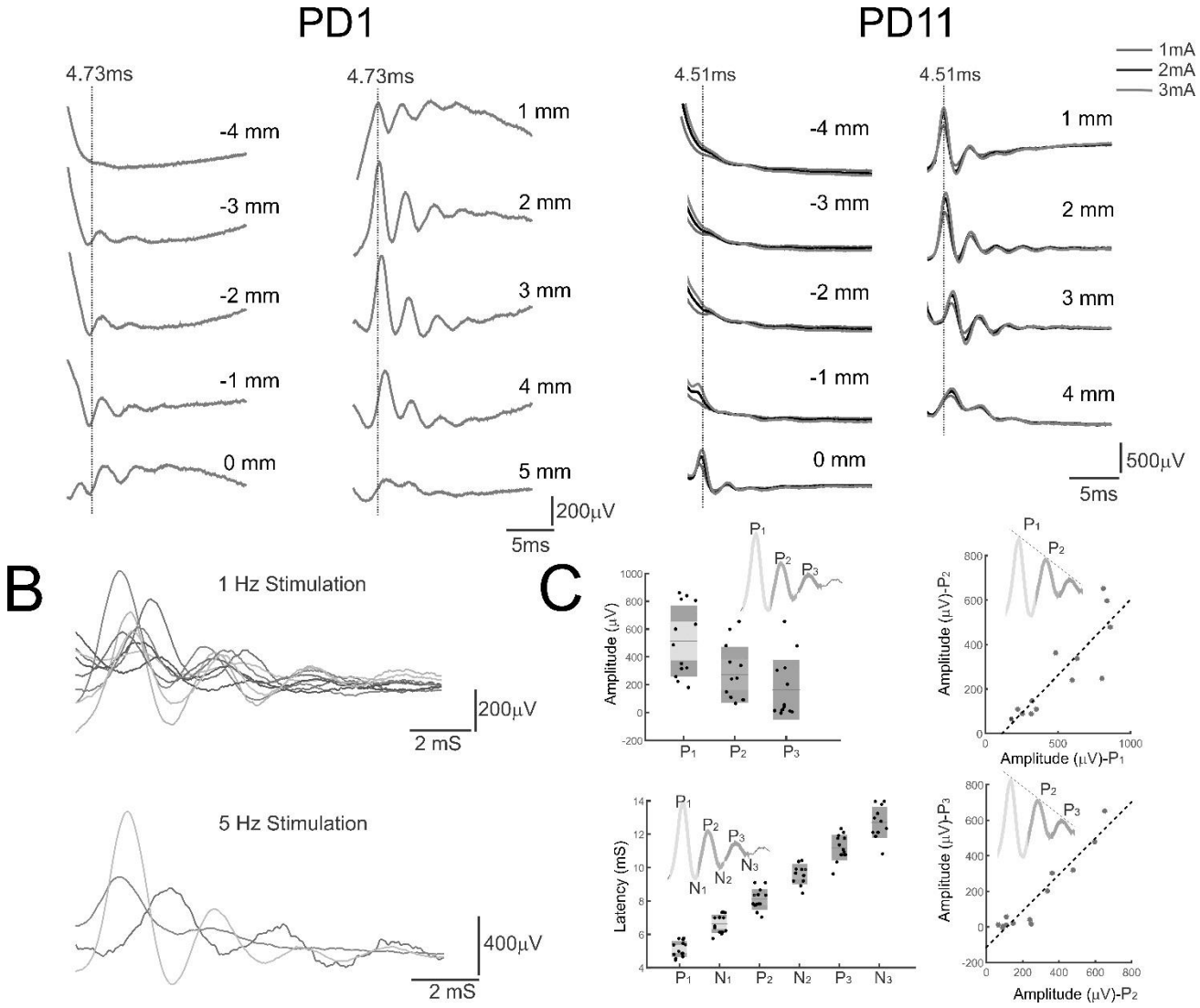

Figure 4: Temporal and spatial characteristics of short-latency evoked response. (A) Two representative patients: LFPs were recorded bipolarly from contacts 01 while contacts 2- 3+ were stimulated with 1 Hz (left plot) and 5 Hz (right plot) across different sites. (B) Variability of evoked responses to 1 Hz and 5 Hz DBS across patients. (C) Box plots are showing amplitudes and latencies for all patients; each dot represents a PD patient (Left). Significant correlation between the amplitude of P_1-P_2 and P_2-$P_{3\,is}$ indicating a linear decreas of the diminishing oscillations.

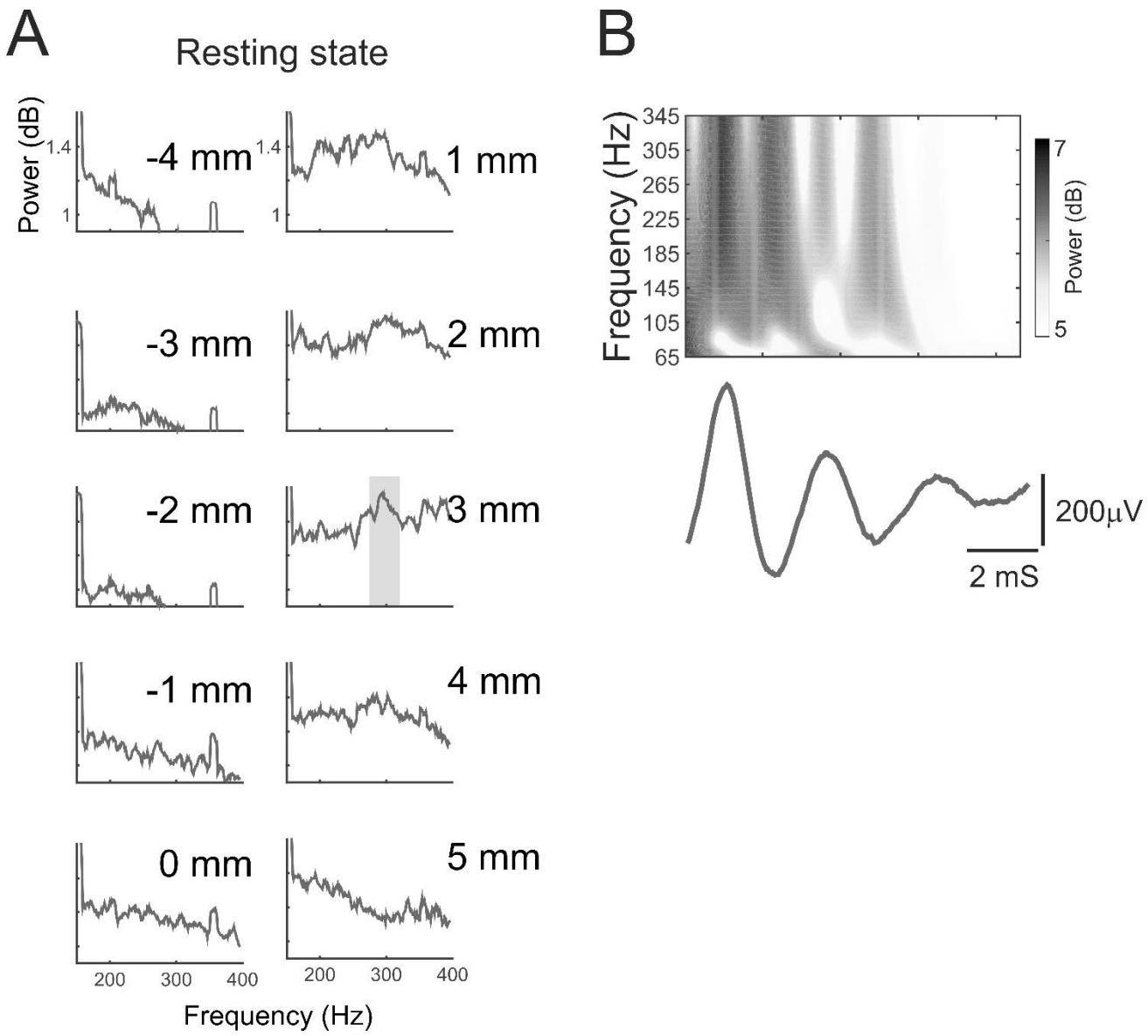

Figure 5: High-frequency oscillation in the STN. (A) Power spectrum in one representative patient. (B) Time-frequency analysis after low-frequency stimulation.

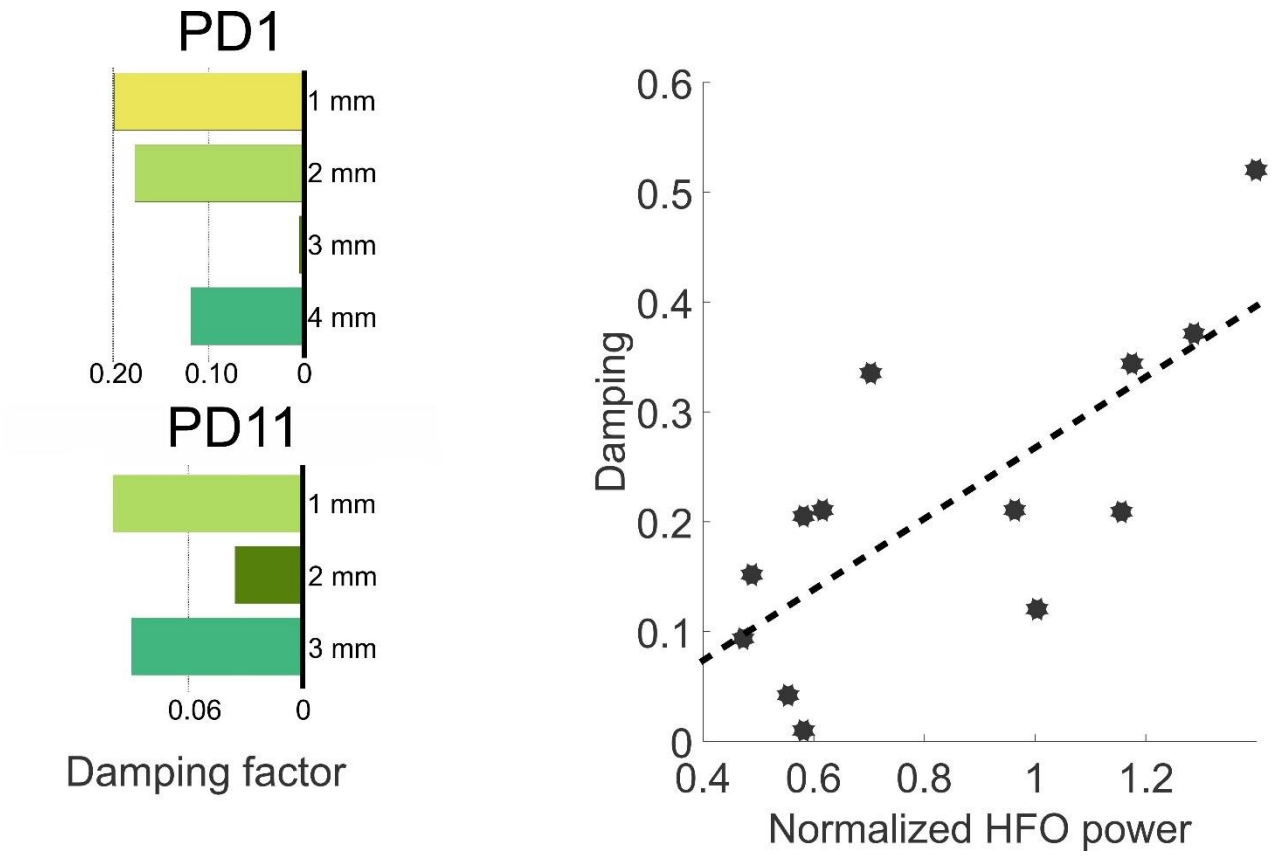

Figure 6: (A) Damping values of two patients PD1 and PD11. (B) Significant correlation between damping factor ξ and normalized HFO power (r=0.79, P=0.001).

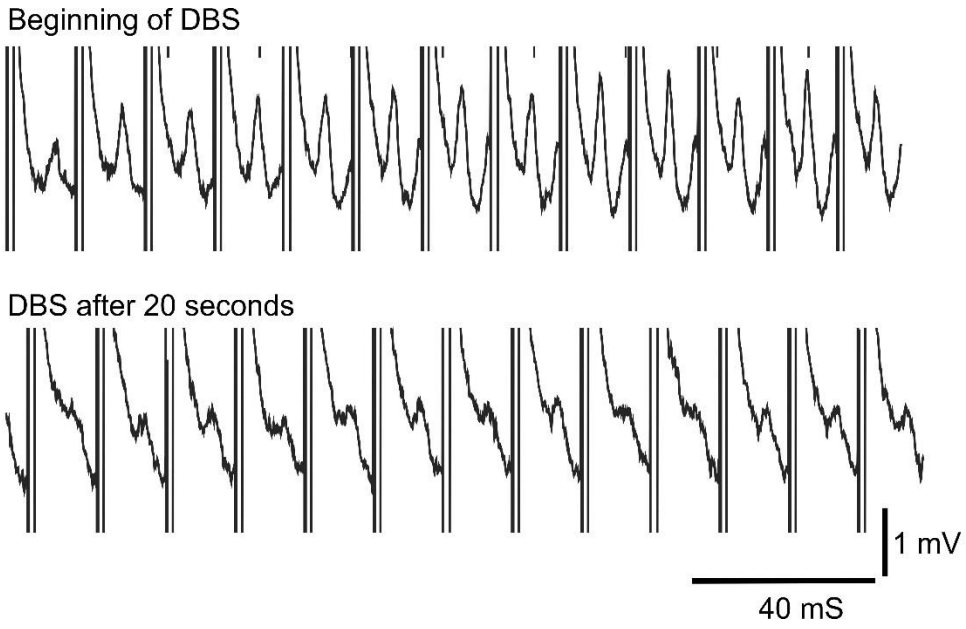

Figure 7: Recorded sEPs during 130 HZ stimulation and reduction of its amplitue after 20 sec of stimulation.

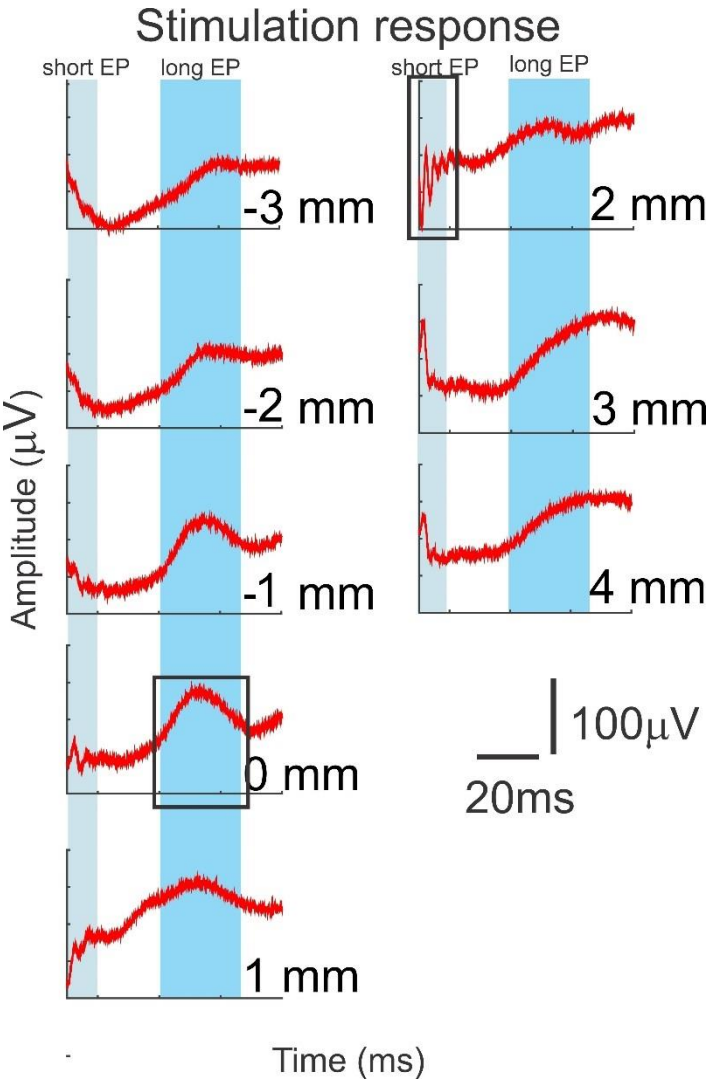

Supplementary figure: Recorded LFP and sEPs during resting state and low-frequency stimulation. It is evident that the maximum HFO (2 mm) and beta oscillatory region (0 mm) co-locate with the regions of maximum short and long sEPs after DBS.

frontiers in
COMPUTATIONAL NEUROSCIENCE

ORIGINAL RESEARCH ARTICLE
published: 26 February 2015
doi: 10.3389/fncom.2015.00026

Phase-dependent modulation as a novel approach for therapeutic brain stimulation

Ramin Azodi-Avval*[1,2] *and Alireza Gharabaghi*[1,2]*

[1] *Division of Functional and Restorative Neurosurgery and Division of Translational Neurosurgery, Department of Neurosurgery, Eberhard Karls University, Tuebingen, Germany*
[2] *Neuroprosthetics Research Group, Werner Reichardt Centre for Integrative Neuroscience, Eberhard Karls University, Tuebingen, Germany*

Edited by:
Julien Modolo, Western University, Canada

Reviewed by:
Jesus M. Cortes, Ikerbasque. Biocruces Health Research Institute, Spain
Chiun-Fan Chen, Spaulding Neuromodulation Center and Harvard Medical School, USA

****Correspondence:***
Alireza Gharabaghi, Division of Functional and Restorative Neurosurgery and Division of Translational Neurosurgery, Department of Neurosurgery, Eberhard Karls University, Otfried-Mueller-Str.45, 72076 Tuebingen, Germany
e-mail: alireza.gharabaghi@uni-tuebingen.de

Closed-loop paradigms provide us with the opportunity to optimize stimulation protocols for perturbation of pathological oscillatory activity in brain-related disorders. In this vein, spiking activity of motor cortex neurons and beta activity of local field potentials in the subthalamic nucleus have both been used independently of each other as neuronal signals to trigger deep brain stimulation for alleviating Parkinsonism. These approaches were superior to the standard continuous high-frequency stimulation protocols used in daily practice. However, they achieved their effects by bursts of stimulation that were applied at high-frequency as well, i.e., independent of the phase information in the stimulated region. In this context, we propose that, by timing stimulation pulses relative to the ongoing oscillation, an alternative approach, namely the targeted perturbation of pathological rhythms, could be obtained. In this modeling study, we first captured the underlying dynamics of neuronal oscillations in the human subthalamic nucleus by phased coupled neuronal oscillators. We then quantified the nature of the interaction between these coupled oscillators by obtaining a physiologically informed phase response curve from local field potentials. Reconstruction of the phase response curve predicted the sensitivity of the phase oscillator to external stimuli, revealing phase intervals that optimally maximized the degree of perturbation. We conclude that our specifically timed intervention based on the coupled oscillator concept will enable us to identify personalized ways of delivering stimulation pulses in closed-loop paradigms triggered by the phase of pathological oscillations. This will pave the way for novel physiological insights and substantial clinical benefits. In addition, this precisely phased modulation may be capable of modifying the effective interactions between oscillators in an entirely new manner.

Keywords: brain state-dependent stimulation, closed-loop stimulation, biophysical model, coupled neuronal oscillators, phase response curve, Parkinson's disease, deep brain stimulation

INTRODUCTION

Brain neuromodulation by deep brain stimulation (DBS) is meanwhile a recognized form of treatment for several neurological and neuropsychiatric disorders such as severe Parkinson's disease (PD) (Schuepbach et al., 2013), dystonia (Vidailhet et al., 2005), and essential tremor (Deuschl et al., 2011). However, general application of this therapeutic modality remains limited. This might be due to stimulation-induced side effects and/or partial efficacy of the intervention which is probably related to a misalignment between stimulation parameters and the current disease state (Moro et al., 2006; Mure et al., 2011). While patients often display variable clinical symptoms, the stimulation parameters, such as continuous high-frequency stimulation, are predefined and remain unchanged until manual modifications are performed by the physician in charge.

Closed-loop paradigms modulating the stimulation parameters on the basis of online recorded physiological markers provide us with the opportunity to adjust stimulation protocols and improve therapeutic efficacy. In this regard, the first studies in both non-human primates (Rosin et al., 2011) and Parkinsonian patients (Little et al., 2013) addressed the current limitations by applying stimulation in an adaptive manner only when specific physiological markers were detected. More specifically, adaptive DBS of the globus pallidus internus controlled by spiking activity of motor cortex neurons was more effective than continuous high-frequency stimulation in a non-human primate model of PD (Rosin et al., 2011). In a recent clinical study, adaptive DBS of the subthalamic nucleus (STN)—triggered by beta-band activity (a physiological marker of motor impairment in PD) and recorded in the immediate vicinity of the stimulating electrode in the STN—was shown to be more energy-efficient than, and clinically superior to continuous high-frequency DBS (Little et al., 2013). Despite being superior to the standard stimulation protocols, these closed-loop approaches nonetheless achieved their effects by bursts of stimulation applied at high frequency independent of the phase information in the stimulated region (Rosin et al., 2011; Little et al., 2013).

In this context, we propose that, by timing stimulation pulses relative to the ongoing oscillation in the respective area, an alternative approach—namely the targeted perturbation of pathological rhythms—can be introduced. We therefore performed a modeling study to determine the essential dynamics of neuronal oscillations in the human subthalamic nucleus by phased coupled neuronal oscillators in an aim to identify those phase intervals in which stimulation would maximize the degree of perturbation of pathological rhythms.

MATERIALS AND METHODS

The present modeling study is based on intraoperative electrophysiological recordings of two PD patients who underwent standard DBS surgery with bilateral electrode implantation in the STN and was performed in accordance with the guidelines of the local ethics committee of the Medical Faculty of the University of Tuebingen. This data represents spontaneous brain activity recorded for about 3 min through the final quadripolar DBS electrode (model 3389, Medtronic, Inc., Minneapolis, MN) which was implanted in one brain hemisphere while electrode insertion was prepared for the second side. The STN was localized via direct targeting on preoperative magnetic resonance imaging (Foltynie et al., 2011) and then during surgery with online electrophysiology (Chen et al., 2006; Holdefer et al., 2010). In accordance with standard operating procedures, dopamine medication was not administered for the last time 12 or more hours prior to surgery to avoid interference with intraoperative recordings and clinical testing (Hammond et al., 2007). In addition, intraoperative propofol medication was discontinued about 30 min before electrophysiological recordings were initiated (Raz et al., 2010). Local field potential (LFP) signals were continuously sampled at 1.4 KHz and amplified by factor 50. The reference electrodes were attached to the ears and the ground was placed on the nasion. The impedance for the intracranial electrode was ∼1 KΩ. Stereotactic planning (Machado et al., 2006) was based on multimodal preoperative images (1 mm slice thickness) from contrast-enhanced magnetic resonance imaging (MRI) and computer tomography (CT) imaging (Siemens, Erlangen, Germany). Standard electrophysiological recordings (AlphaOmega, Nazareth, Israel) and clinical test stimulation were performed intraoperatively to adjust electrode localization. This was later confirmed by postoperative MR and CT imaging.

PHASE SYNCHRONIZATION

The implanted quadripolar electrode (**Figure 1A**) enabled us to independently record four oscillatory sources, i.e., local field potentials (LFP), in the target region and to quantify their neural interaction. For this purpose, we used the phase approach proposed by Rosenblum and Pikovsky (2001) to reconstruct the phase response curve (PRC) of the LFP signals recorded in the STN. The concept of phase synchronization between coupled oscillators has not been used to derive a phase-response curve of brain signals yet, but has already been applied in several electrophysiological studies in different functional systems (Kralemann et al., 2013; Zhu et al., 2013). However, brain signals are particularly suited for such an approach as filtered LFP signals at a given frequency band have a sinusoidal waveform similar to an oscillator. Therefore, phase modeling might capture the neural network dynamics of coupled oscillators (Wang, 2010).

Data analysis of LFPs were performed in Matlab (The Mathworks, Natick, Massachusetts, USA) using custom-made scripts, DAMOCO toolbox (Kralemann et al., 2007, 2008) and Fieldtrip, an open source analysis toolbox (Oostenveld et al., 2011). To reconstruct the PRC, the power of LFP was first computed by the multitaper method. Maximum spectral estimation was provided by a single Hanning taper (Mitra and Pesaran, 1999). This approach enabled us to identify the specific electrode contact that displayed pronounced oscillatory activity in the beta-band—a known pathophysiological marker of motor impairment in PD (Little and Brown, 2012)—and which we used as a reference for the further computing. We next applied the Weighted Phase Lag Index (WPLI) (Vinck et al., 2011) to detect the electrode contact displaying the most prominent phase synchronization with this reference electrode. WPLI is defined as follows:

$$WPLI_{LFP-LFP} = \frac{n^{-1}\sum_{n=1}^{N} \left| imag\left(S_{LFP-LFP\,n}\right)\right| sgn\left(imag\left(S_{LFP-LFP\,n}\right)\right)}{n^{-1}\sum_{n=1}^{N} imag\left(S_{LFP-LFPn}\right)} \quad (1)$$

where S is the cross-spectrum density matrix, *imag* the imaginary part and *sgn* the sign function. Moreover, WPLI is insensitive to volume conduction effects since it eliminates zero phase lag signals. Thereby, it is more sensitive to detect true phase interaction as compared to common phase measurements such as the imaginary part of coherence (Nolte et al., 2004). The value of WPLI was standardized by an estimate of its standard deviation and values beyond threshold of 3 (corresponding $p < 0.003$) were considered statistically significant (Nolte et al., 2004; Hohlefeld et al., 2013, 2014). This statistically significant frequency range (see **Figure 2B**) was used for further analysis, i.e., phase extraction.

PHYSIOLOGICALLY INFORMED PHASE RESPONSE CURVE

Having determined the significant frequency interval of neural interaction for each patient, we went on to filter the LFP in that particular, i.e., patient-specific, frequency range using a Kaiser FIR filter with the MATLAB filtfilt function to avoid phase distortions. The unwrapped phase of each sample of the filtered LFP was then computed using the Hilbert transform (**Figure 1B**). The method proposed by Rosenblum and collaborators (Kralemann et al., 2007, 2008) was then used to empirically reconstruct the phase coupling function between the two electrode contacts in the STN that had already been determined. This method adapts the empirical phases to a generic model of two coupled oscillators as follows:

$$\begin{aligned} \dot{\varphi}_1 &= \omega_1 + F_{2\longrightarrow 1}(\varphi_1, \varphi_2) \\ \dot{\varphi}_2 &= \omega_2 + F_{1\longrightarrow 2}(\varphi_2, \varphi_1) \end{aligned} \quad (2)$$

where the dot represents the derivative, while φ and ω are the phase and autonomous frequency, respectively. Since the extracted phase is non-universe $\theta_{1,2}$, a transformation is needed to provide an invariant description of the coupled dynamics. The

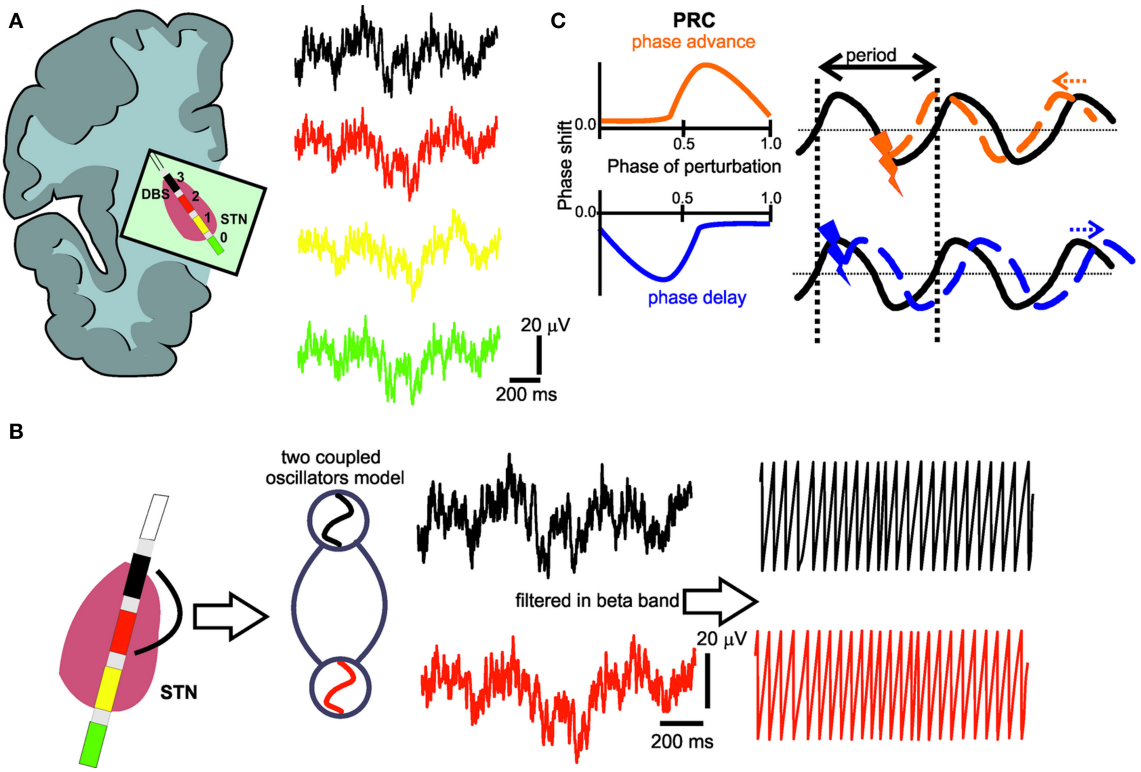

FIGURE 1 | (A) Deep brain stimulation lead positioned in the subthalamic nucleus region with four electrode contacts (0–3) and respective local field potential (LFP) recordings. **(B)** The LFPs from the electrode contact (black) with the most pronounced oscillatory activity in the beta-band and the electrode contact (red) with the most prominent phase synchronization to the first contact are captured as coupled neural oscillators. In a second step, the phase of these oscillators is extracted by Hilbert transform. **(C)** Illustration of the typical characteristics of a phase response curve (PRC) with positive (orange) or negative (blue) values indicating an earlier or later start of the perturbated cycle, respectively, i.e., the perturbation could cause a positive (orange) phase shift (phase advance), or a negative (blue) phase shift (phase delay), depending on the timing of the perturbating stimulus. The black curve represents the ongoing oscillation in the absence of any perturbation.

transformation from the unwrapped phase to the genuine phase of N observations is defined as following,

$$\varphi = \theta + 2\pi \sum_{n \neq 1} \frac{S_n}{in} \left(e^{in\theta} - 1 \right) \tag{3}$$

where

$$S_n = \frac{1}{N} \sum_{j=1}^{N} e^{in\theta(j)}.$$

After this phase correction is performed, the coupling function F of two coupled systems can be approximated by the Fourier series:

$$F = \sum_{n,m} A_{n,m} e^{-i(n\varphi_2 + m\varphi_1)} \tag{4}$$

with coefficients

$$A_{n,m} = \int_0^{2\pi} \int \varphi_1 e^{-in\varphi_1 - im\varphi_2}$$

where n and m are indices synonymous to the n:m phase locking the indices of two oscillators and A refers to the coefficients of the respective Fourier series (Kralemann et al., 2007, 2008). The resulting PRC reflects the interaction of the oscillators. When the PRC results in positive or negative values (Smeal et al., 2010), it indicates the cycle to start sooner or later, respectively, i.e., a perturbation could cause a positive phase shift (phase advance), or a negative phase shift (phase delay) (**Figure 1C**).

RESULTS

The recording of local field potentials (LFP) revealed that the most upper electrode contact of the quadripolar lead has the highest spectral power in the beta-frequency band (15–30 Hz, **Figure 2A**), indicating that it is located in the sensorimotor part of the STN (**Figure 2A**) (Holdefer et al., 2010; Yoshida et al., 2010; Zaidel et al., 2010; Novak et al., 2011; Deffains et al., 2014). Using this electrode contact as a reference, the neighboring contact revealed the most prominent phase synchronization when applying the Weighted Phase Lag Index (WPLI). This phase coherence showed a significant synchronization in the frequency range between 23–27 and 17–22 Hz for P1 and P2, respectively (**Figure 2B**), indicating that there is a pathological increase of functional connectivity in the sensorimotor part of the STN

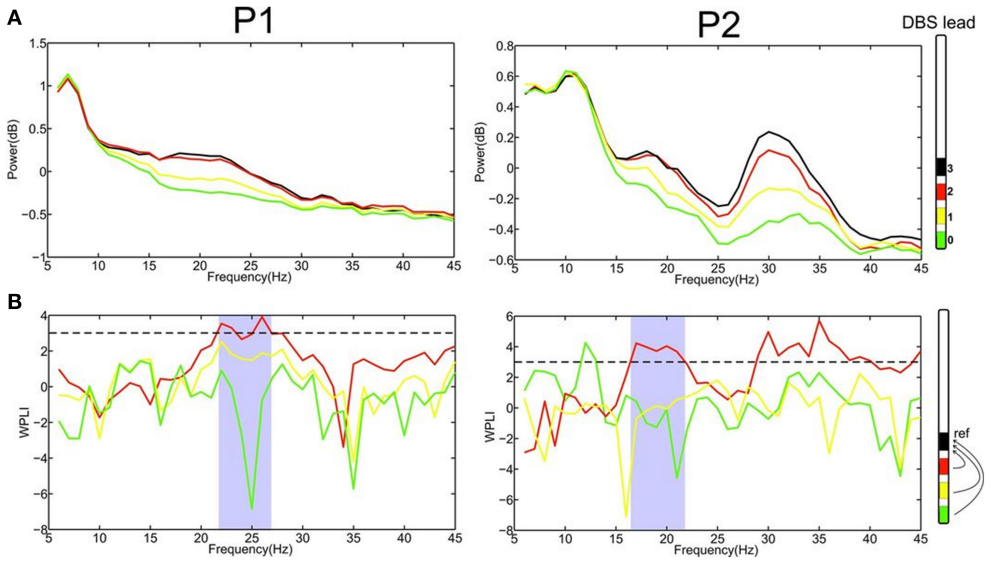

FIGURE 2 | (A) Power spectrum of LFPs recordings at the four different contacts (0–3) for patient 1 and 2, respectively, revealed that the most upper electrode contact (3, black) of the quadripolar lead has the highest spectral power in the beta-frequency band. **(B)** Computing phase synchronization between electrode contact 3 (black) and the others applying the Weighted Phase Lag Index (WPLI) showed that the most prominent coupling is with contact 2 (red). The statistically significant frequency range for WPLI is indicated in gray. The dashed line represents the significance threshold (3, corresponding $p < 0.003$).

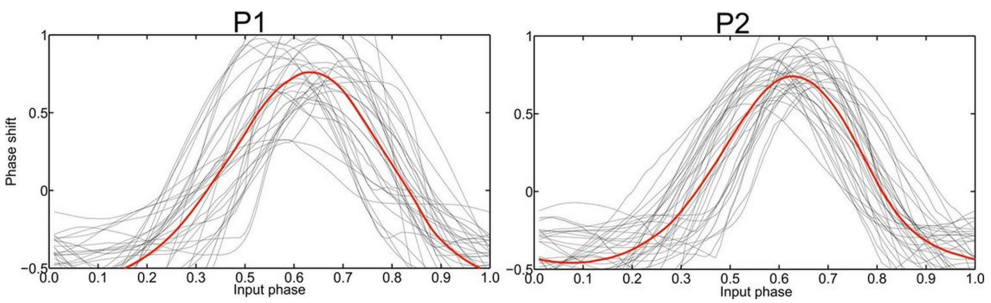

FIGURE 3 | Empirically determined PRC phase response curves (PRC) of patient 1 and 2, respectively, with the averaged curve indicated in red. The strongest phase-coupling effect in both P1 and P2 was observed around $\varphi = 0.6$ with the highest positive value, i.e., the maximum phase advance.

(Pogosyan et al., 2010). By applying a modeling approach of two neural oscillators characterized by phase dependency, we succeeded in quantifying this interaction by a phase response curve. The inherent variability of the PCRs resulting from the empirical data was resolved using the similarity method (Kralemann et al., 2013). PRC extracted from both P1 and P2 showed a similar pattern with two different domains (**Figure 3**): a phase delay in the $0 < \varphi <\sim 0.3$ and $\sim 0.7 < \varphi < 1.0$ intervals and a strong phase advance in the $\sim 0.3 < \varphi < 0.7$ interval. The strongest phase-coupling effect was observed around $\varphi = 0.6$.

DISCUSSION

The beta-band functional connectivity observed within the STN tallies well-with earlier work, indicating that this synchronization reflects a pathological marker for different motor features of PD (Pogosyan et al., 2010; Hohlefeld et al., 2013). We also located the most prominent phase synchronization in the dorsal, sensorimotor part of the STN (Pogosyan et al., 2010), i.e., the area known to be clinically most effective in suppressing PD symptoms during DBS (Herzog et al., 2004; Yokoyama et al., 2006; Schlaier et al., 2014). It remains to be experimentally disentangled, whether additional physiological markers may capture a broader spectrum of PD symptoms and may therefore be better suited for closed-loop applications. However, more sophisticated approaches of simultaneous sensing and stimulation with online signal processing may decrease the battery life span and should therefore be balanced with potential clinical benefits (Little and Brown, 2014).

On the basis of these findings, phase-specific interventions appear to be the most straightforward approach for specifically perturbating pathological synchronization. The PRC disentangles the timing of the regional interaction in the dorsal STN to

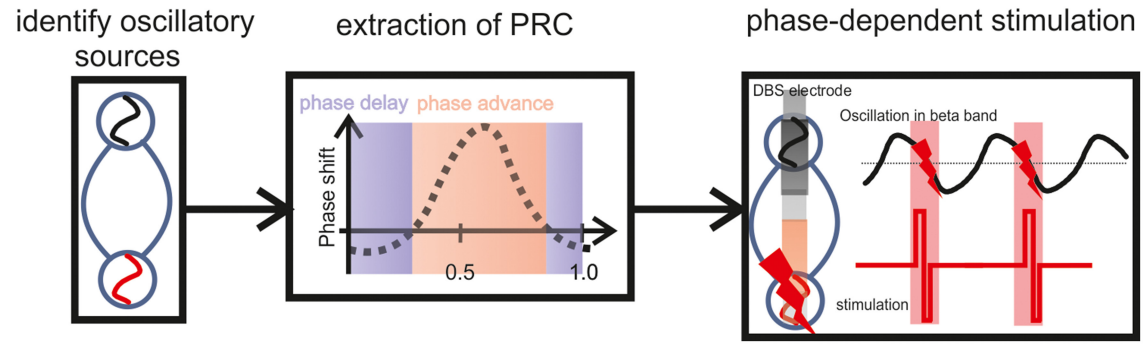

FIGURE 4 | Illustration of a closed-loop modulation protocol, recording and stimulating with two adjacent DBS electrode contacts in the STN, triggered by the ongoing oscillatory phase estimated on the basis of the PRC curve. To determine this precise timing, a closed-loop system will require a physiological calibration for each patient including the estimation of WPLI and PRC based on the individual *vivo* recordings. After this calibration, i.e., based on the subject-specific frequency range and the precise phase of maximum perturbation, the respective phase information will be the feedback signal to control the stimulation.

reveal the highest synchronization between the two oscillators at phase 0.6 (**Figure 4**). In fact, the PRC also reveals phase sensitivity of an oscillator to external perturbation (Smeal et al., 2010). We therefore propose that the application of DBS stimuli at this phase, i.e., replacing one of the two oscillators by an external stimulus, maximizes perturbation of the pathological state. Along these lines, the effect of a perturbation on an oscillating system is known to depend on the phase at which the perturbation is applied (Pikovsky et al., 2001; Kralemann et al., 2013). This assumption is further supported by physiologically calibrated modeling results which suggest that precisely timed stimulation pulses could indeed be used to shift the phase of oscillations (Witt et al., 2013).

Moreover, when stimuli are properly phased with respect to ongoing oscillations, they might even induce long-term potentiation/depotentiation (LTP/LTD) effects (Martin et al., 2000; Kauer and Malenka, 2007): both *in vitro* (Huerta and Lisman, 1993) and *in vivo* (Pavlides et al., 1988) experimental studies reported LTD induction when stimuli were applied during the positive phase of the theta rhythm. Similarly, depotentiation of existing LTP was achieved when stimuli were phase-locked to the negative phase of theta (Huerta and Lisman, 1995). Phase-specific pulses may therefore induce bidirectional modifications of synaptic strength (Martin et al., 2000) with the potential to turn a whole network into a synchronized or a desynchronized state (Pfister and Tass, 2010).

Future closed-loop modulation protocols will require simultaneous recording and stimulation. The presented findings suggest that two adjacent DBS electrode contacts in the STN may be used for this purpose, i.e., to record and to stimulate, respectively. In such a scenario the stimulating contact would be triggered by the ongoing oscillatory phase recorded at the adjacent electrode and estimated on the basis of the PRC curve. To determine the precise timing, a physiological calibration of the closed-loop system will be required for each patient beforehand, including the estimation of WPLI and PRC based on the individual *vivo* recordings. After this calibration, i.e., based on the subject-specific frequency range and the precise phase of maximum perturbation, the respective phase information will be the feedback signal to control the stimulation. This approach can be implemented with online algorithms, i.e., real-time calculation of the instantaneous phase based on the Hilbert transform (**Figure 4**).

Phase-dependent stimulation protocols may therefore be capable of modifying the effective interactions between oscillators in an entirely new fashion, potentially inducing lasting effects mediated by LTP/LTD. Furthermore, with regard to different neurological and neuropsychiatric disorders, such an approach would transform brain stimulation from a symptomatic intervention and temporary modulation—displaying its effects only for the duration of stimulation—to a treatment option that induces long-term plastic changes and durable effects lasting beyond stimulation.

ACKNOWLEDGMENTS

RA was supported by the Graduate Training Centre of Neuroscience, International Max Planck Research School, Tuebingen, Germany. AG was supported by grants from the German Research Council (DFG EC 307), and from the Federal Ministry for Education and Research (BFNT 01GQ0761, BMBF 16SV3783, BMBF 03160064B, BMBF V4UKF014). We acknowledge support by Deutsche Forschungsgemeinschaft and Open Access Publishing Fund of University of Tübingen.

REFERENCES

Chen, C. C., Pogosyan, A., Zrinzo, L. U., Tisch, S., Limousin, P., Ashkan, K., et al. (2006). Intra-operative recordings of local field potentials can help localize the subthalamic nucleus in Parkinson's disease surgery. *Exp. Neurol.* 198, 214–221. doi: 10.1016/j.expneurol.2005.11.019

Deffains, M., Holland, P., Moshel, S., de Noriega, F. R., Bergman, H., and Israel, Z. (2014). Higher neuronal discharge rate in the motor area of the subthalamic nucleus of Parkinsonian patients. *J. Neurophysiol.* 112, 1409–1420. doi: 10.1152/jn.00170.2014

Deuschl, G., Raethjen, J., Hellriegel, H., and Elble, R. (2011). Treatment of patients with essential tremor. *Lancet Neurol.* 10, 148–161. doi: 10.1016/S1474-4422(10)70322-7

Foltynie, T., Zrinzo, L., Martinez-Torres, I., Tripoliti, E., Petersen, E., Holl, E., et al. (2011). MRI-guided STN DBS in Parkinson's disease without microelectrode

recording: efficacy and safety. *J. Neurol. Neurosurg. Psychiatry* 82, 358–363. doi: 10.1136/jnnp.2010.205542

Hammond, C., Bergman, H., and Brown, P. (2007). Pathological synchronization in Parkinson's disease: networks, models and treatments. *Trends Neurosci.* 30, 357–364. doi: 10.1016/j.tins.2007.05.004

Herzog, J., Fietzek, U., Hamel, W., Morsnowski, A., Steigerwald, F., Schrader, B., et al. (2004). Most effective stimulation site in subthalamic deep brain stimulation for Parkinson's disease. *Mov. Disord.* 19, 1050–1054. doi: 10.1002/mds.20056

Hohlefeld, F. U., Huchzermeyer, C., Huebl, J., Schneider, G. H., Brücke, C., Schönecker, T., et al. (2014). Interhemispheric functional interactions between the subthalamic nuclei of patients with Parkinson's disease. *Eur. J. Neurosci.* 40, 3273–3283. doi: 10.1111/ejn.12686

Hohlefeld, F. U., Huchzermeyer, C., Huebl, J., Schneider, G. H., Nolte, G., Brücke, C., et al. (2013). Functional and effective connectivity in subthalamic local field potential recordings of patients with Parkinson's disease. *Neuroscience* 250, 320–332. doi: 10.1016/j.neuroscience.2013.07.028

Holdefer, R. N., Cohen, B. A., and Greene, K. A. (2010). Intraoperative local field recording for deep brain stimulation in Parkinson's disease and essential tremor. *Mov. Disord.* 25, 2067–2075. doi: 10.1002/mds.23232

Huerta, P. T., and Lisman, J. E. (1993). Heightened synaptic plasticity of hippocampal CA1 neurons during a cholinergically induced rhythmic state. *Nature* 364, 723–725. doi: 10.1038/364723a0

Huerta, P. T., and Lisman, J. E. (1995). Bidirectional synaptic plasticity induced by a single burst during cholinergic theta oscillation in CA1 *in vitro*. *Neuron* 15, 1053–1063. doi: 10.1016/0896-6273(95)90094-2

Kauer, J. A., and Malenka, R. C. (2007). Synaptic plasticity and addiction. *Nat. Rev. Neurosci.* 8, 844–858. doi: 10.1038/nrn2234

Kralemann, B., Cimponeriu, L., Rosenblum, M., Pikovsky, A., and Mrowka, R. (2007). Uncovering interaction of coupled oscillators from data. *Phys. Rev. E* 76, 055201. doi: 10.1103/PhysRevE.76.055201

Kralemann, B., Cimponeriu, L., Rosenblum, M., Pikovsky, A., and Mrowka, R. (2008). Phase dynamics of coupled oscillators reconstructed from data. *Phys. Rev. E* 77:066205. doi: 10.1103/PhysRevE.77.066205

Kralemann, B., Frühwirth, M., Pikovsky, A., Rosenblum, M., Kenner, T., Schaefer, J., et al. (2013). *In vivo* cardiac phase response curve elucidates human respiratory heart rate variability. *Nat. Commun.* 4:2418. doi: 10.1038/ncomms3418

Little, S., and Brown, P. (2012). What brain signals are suitable for feedback control of deep brain stimulation in Parkinson's disease? *Ann. N. Y. Acad. Sci.* 1265, 9–24. doi: 10.1111/j.1749-6632.2012.06650.x

Little, S., and Brown, P. (2014). Focusing brain therapeutic interventions in space and time for Parkinson's disease. *Curr. Biol.* 24, R898–R909. doi: 10.1016/j.cub.2014.08.002

Little S., Pogosyan A., Neal S., Zavala B., Zrinzo L., Hariz M., et al. (2013). Adaptive deep brain stimulation in advanced Parkinson disease. *Ann. Neurol.* 74, 449–457. doi: 10.1002/ana.23951

Machado, A., Rezai, A. R., Kopell, B. H., Gross, R. E., Sharan, A. D., and Benabid, A.-L. (2006). Deep brain stimulation for Parkinson's disease: surgical technique and perioperative management. *Mov. Disord.* 21, S247–S258. doi: 10.1002/mds.20959

Martin, S. J., Grimwood, P. D., and Morris, R. G. M. (2000). Synaptic plasticity and memory: an evaluation of the hypothesis. *Annu. Rev. Neurosci.* 23, 649–711. doi: 10.1146/annurev.neuro.23.1.649

Mitra, P. P., and Pesaran, B. (1999). Analysis of dynamic brain imaging data. *Biophys. J.* 76, 691–708. doi: 10.1016/S0006-3495(99)77236-X

Moro, E., Poon, Y. W., Lozano, A. M., Saint-Cyr, J. A., and Lang, A. E. (2006). Subthalamic nucleus stimulation: improvements in outcome with reprogramming. *Arch. Neurol.* 63, 1266–1272. doi: 10.1001/archneur.63.9.1266

Mure, H., Hirano, S., Tang, C. C., Isaias, I. U., Antonini, A., Ma, Y., et al. (2011). Parkinson's disease tremor-related metabolic network: characterization, progression, and treatment effects. *NeuroImage* 54, 1244–1253. doi: 10.1016/j.neuroimage.2010.09.028

Nolte, G., Bai, O., Wheaton, L., Mari, Z., Vorbach, S., and Hallett, M. (2004). Identifying true brain interaction from EEG data using the imaginary part of coherency. *Clin. Neurophysiol.* 115, 2292–2307. doi: 10.1016/j.clinph.2004.04.029

Novak, P., Przybyszewski, A. W., Barborica, A., Ravin, P., Margolin, L., and Pilitsis, J. G. (2011). Localization of the subthalamic nucleus in Parkinson disease using multiunit activity. *J. Neurol. Sci.* 310, 44–49. doi: 10.1016/j.jns.2011.07.027

Oostenveld, R., Fries, P., Maris, E., and Schoffelen, J.-M. (2011). FieldTrip: open source software for advanced analysis of MEG, EEG, and invasive electrophysiological data. *Intell. Neurosci.* 2011, 1–9. doi: 10.1155/2011/156869

Pavlides, C., Greenstein, Y. J., Grudman, M., and Winson, J. (1988). Long-term potentiation in the dentate gyrus is induced preferentially on the positive phase of θ-rhythm. *Brain Res.* 439, 383–387. doi: 10.1016/0006-8993(88)91499-0

Pfister, J.-P., and Tass, P. (2010). STDP in oscillatory recurrent networks: theoretical conditions for desynchronization and applications to deep-brain stimulation. *Front. Comput. Neurosci.* 4:22. doi: 10.3389/fncom.2010.00022

Pikovsky, A., Rosenblum, M., and Kurths, J. (2001). *Synchronization: A Universal Concept in Nonlinear Sciences*. Cambridge: Cambridge University Press.

Pogosyan, A., Yoshida, F., Chen, C. C., Martinez-Torres, I., Foltynie, T., Limousin, P., et al. (2010). Parkinsonian impairment correlates with spatially extensive subthalamic oscillatory synchronization. *Neuroscience* 171, 245–257. doi: 10.1016/j.neuroscience.2010.08.068

Raz, A., Eimerl, D., Zaidel, A., Bergman, H., and Israel, Z. (2010). Propofol decreases neuronal population spiking activity in the subthalamic nucleus of parkinsonian patients. *Anesth. Anal.* 111, 1285–1289. doi: 10.1213/ANE.0b013e3181f565f2

Rosenblum, M. G., and Pikovsky, A. S. (2001). Detecting direction of coupling in interacting oscillators. *Phys. Rev. E* 64:045202. doi: 10.1103/PhysRevE.64.045202

Rosin, B., Slovik, M., Mitelman, R., Rivlin-Etzion, M., Haber, S. N., Israel, Z., et al. (2011). Closed-loop deep brain stimulation is superior in ameliorating parkinsonism. *Neuron* 72, 370–384. doi: 10.1016/j.neuron.2011.08.023

Schlaier, J., Hanson, C., Janzen, A., Fellner, C., Hochreiter, A., Proescholdt, M., et al. (2014). Deep brain stimulation in Parkinson's disease: motor effects relative to the MRI-defined STN. *Neurosurg. Rev.* 37, 461–471. doi: 10.1007/s10143-014-0521-2

Schuepbach, W. M. M., Rau, J., Knudsen, K., Volkmann, J., Krack, P., Timmermann, L., et al. (2013). Neurostimulation for Parkinson's disease with early motor complications. *N. Eng. J. Med.* 368, 610–622. doi: 10.1056/NEJMoa1205158

Smeal, R. M., Ermentrout, G. B., and White, J. A. (2010). Phase-response curves and synchronized neural networks. *Philos. Trans. R. Soc. Lond. B Biol. Sci.* 365, 2407–2422. doi: 10.1098/rstb.2009.0292

Vidailhet, M., Vercueil, L., Houeto, J.-L., Krystkowiak, P., Benabid, A.-L., Cornu, P., et al. (2005). Bilateral deep-brain stimulation of the globus pallidus in primary generalized dystonia. *N. Eng. J. Med.* 352, 459–467. doi: 10.1056/NEJMoa042187

Vinck, M., Oostenveld, R., van Wingerden, M., Battaglia, F., and Pennartz, C. M. A. (2011). An improved index of phase-synchronization for electrophysiological data in the presence of volume-conduction, noise and sample-size bias. *NeuroImage* 55, 1548–1565. doi: 10.1016/j.neuroimage.2011.01.055

Wang, X.-J. (2010). Neurophysiological and computational principles of cortical rhythms in cognition. *Physiol. Rev.* 90, 1195–1268. doi: 10.1152/physrev.00035.2008

Witt, A., Palmigiano, A., Neef, A., El Hady, A., Wolf, F., and Battaglia, D. (2013). Controlling the oscillation phase through precisely timed closed-loop optogenetic stimulation: a computational study. *Front. Neural Circuits* 7:49. doi: 10.3389/fncir.2013.00049

Yokoyama, T., Ando, N., Sugiyama, K., Akamine, S., and Namba, H. (2006). Relationship of stimulation site location within the subthalamic nucleus region to clinical effects on parkinsonian symptoms. *Stereotact. Funct. Neurosurg.* 84, 170–175. doi: 10.1159/000094956

Yoshida, F., Martinez-Torres, I., Pogosyan, A., Holl, E., Petersen, E., Chen, C. C., et al. (2010). Value of subthalamic nucleus local field potentials recordings in predicting stimulation parameters for deep brain stimulation in Parkinson's disease. *J. Neurol. Neurosurg. Psychiatry* 81, 885–889. doi: 10.1136/jnnp.2009.190918

Zaidel, A., Spivak, A., Grieb, B., Bergman, H., and Israel, Z. (2010). Subthalamic span of β oscillations predicts deep brain stimulation efficacy for patients with Parkinson's disease. *Brain* 133(Pt 7), 2007–2021. doi: 10.1093/brain/awq144

Zhu, Y., Hsieh, Y.-H., Dhingra, R. R., Dick, T. E., Jacono, F. J., and Galán, R. F. (2013). Quantifying interactions between real oscillators with information theory and phase models: application to cardiorespiratory coupling. *Phys. Rev. E* 87:022709. doi: 10.1103/PhysRevE.87.022709

Conflict of Interest Statement: The authors declare that the research was conducted in the absence of any commercial or financial relationships that could be construed as a potential conflict of interest.

Received: 29 October 2014; accepted: 09 February 2015; published online: 26 February 2015.

*Citation: Azodi-Avval R and Gharabaghi A (2015) Phase-dependent modulation as a novel approach for therapeutic brain stimulation. Front. Comput. Neurosci. **9**:26. doi: 10.3389/fncom.2015.00026*

This article was submitted to the journal Frontiers in Computational Neuroscience.